A MODEL OF THE KRAFT RECOVERY FURNACE

A thesis submitted by

Andrew K. Jones

B.A.Sc., June, 1984, The University of Toronto

M.A.Sc. November 1985, The University of Toronto

in partial fulfillment of the requirements
of The Institute of Paper Chemistry
for the degree of Doctor of Philosophy
from Lawrence University,
Appleton, Wisconsin

January, 1989

FOREWORD

This thesis is part of a project that included three PhD theses. To gain a full understanding of every part of the FLUENT/RFM model it is necessary to consult the theses of Allan Walsh and Dan Sumnicht. Instructions on running a simulation using FLUENT/RFM can be obtained by consulting the Users Manual.

TABLE OF CONTENTS

ABSTRACT

This thesis describes a fundamental, three-dimensional model of the kraft recovery furnace that was developed based on a finite volume solution of the governing equations for mass, momentum, energy, and species concentration for the gas phase. Bed burning and in-flight burning of liquor drops are included and affect the gas phase through source and sink terms. The model is constructed around a commercially available computational fluid dynamics code (FLUENT), with appropriate modifications to incorporate the critical features of kraft recovery furnaces.

FLUENT was selected as the underlying code because of its versatility, applicability, and the availability of the source code for modification. Model development included writing original code and modifying the base code to provide for five chemical species (fuel, water, oxygen, carbon dioxide, and carbon monoxide), a revised combustion model, and the source and sink terms needed to communicate with the bed and in-flight burning models. The code development in this thesis was combined with the models developed by Sumnicht and Walsh to produce the final code called FLUENT/RFM (Recovery Furnace Model).

A converged solution of a recovery furnace simulation using all the features present in FLUENT/RFM was obtained. Convergence involved a certain amount of operator interaction as it proceeded and required 3500 iterations and some twelve trillion math operations.

The recovery furnace simulation (Base Case) gave results which were reasonable and consistent with experience. A large central core of hot, oxygen-deficient, high-upward velocity gas was a dominant feature of the flow pattern. This central core is formed by the collision of the primary and secondary jets in the center of the lower furnace. The tertiary air was not effective in breaking up the central core. A substantial amount of in-flight liquor burning occurs and the solids reaching the bed tend to arrive around the perimeter of the furnace. The simulation provides a great deal of insight into recovery furnace processes.

The gas flow pattern for the full Base Case simulation was quite similar to that in a simulation using the same geometry and an temperature equal to the average temperature in the Base Case but without black liquor and combustion. This suggests that gas flows in a recovery furnace are primarily a function of furnace geometry and the details of air introduction and are only weakly affected by the combustion processes.

Full validation of the FLUENT/RFM code was not possible because detailed data on flow variables in actual recovery boilers were not available. However, the basic FLUENT code was validated by comparing the results of a cold flow simulation with experimental flow data from recovery furnace scale model tests. The agreement was quite reasonable.

OBJECTIVES

The main objectives of this thesis were as follows: 1. To develop a three-dimensional, fundamental, mathematical model of the kraft recovery furnace; 2. To ensure that the deficiencies present in earlier recovery furnace models are avoided; 3. To validate the model when possible; and 4. To converge a simulation that makes use of all the aspects of the computer code developed. The remainder of this section will examine these objectives in more detail.

The primary objective of this thesis was the development of a three-dimensional, fundamental, mathematical model of the kraft recovery furnace. Models of the kraft recovery furnace have been constructed before, but the model developed in this PhD thesis has some unique and highly desirable properties absent in earlier models. The model is three-dimensional, allowing for an accurate description of furnace geometry. Empiricism is avoided whenever possible by the use of recently acquired experimental data. The zonal approach taken in earlier models is replaced by state-of-the-art computational fluid flow techniques that eliminate the need to specify the sites at which physical and chemical processes take place; additionally, solution of fundamental mass, energy, and momentum balances allow for almost unlimited flexibility in the geometry of the furnace being simulated.

A problem of some earlier models was the lack of closure in the energy and mass balances; the code that was developed satisfies mass continuity and energy conservation and shows this to the user. Some previous models have suffered from poor graphics for viewing results. High quality full color graphics are provided in order to interpret the large amount of data a three-dimensional model produces.

Validation was addressed when possible. Limited data is available concerning the gas flow patterns obtained by cold flow modelling of the kraft recovery furnace. Cold flow is the gas pattern that derives directly from the geometry and method of air introduction, without the influence of in-flight and bed

burning. Additional data is available for comparison of aspects of the energy balance and some of the properties of the gas at the furnace outlet.

Convergence of a simulation using all the aspects of the recovery furnace model developed was accomplished. In the process of obtaining this converged result, the techniques necessary for convergence of a simulation were determined.

Two further objectives concern the optimization of the model. Methods for reducing the convergence time are investigated. In addition, suggestions concerning the software and hardware enhancements that will be necessary in the future are included.

INTRODUCTION

Before describing a model of the kraft recovery furnace it is first necessary to describe what a recovery furnace does, what it is physically, and how it operates. An understanding of these topics will illustrate the need for analytical modelling as a means to investigate alternative operating methods and furnace geometries.

A DESCRIPTION OF THE KRAFT RECOVERY FURNACE

The kraft recovery furnace is a large combustion unit which has three main functions: 1. The recovery of the inorganic pulping chemical as smelt; 2. The generation of steam by the burning of the organic material in the black liquor; and 3. The elimination of pollutants (i.e. H_2S and CO) by combustion. Figure 1 shows the geometry of a kraft recovery furnace.

Kraft recovery furnaces can be up to 60 meters high, with a cross-sectional area in excess of 100 square meters. The walls of the furnace are composed of tubes that are kept cool by circulating boiling water through them. The tubes that make up this "water-wall" are insulated on the outside. The furnace cavity is box-shaped, with a square or rectangular cross-section. The top of the furnace is usually partially blocked-off by the bullnose in order to direct the flow of gas over the superheater. The bullnose side of the furnace is referred to as the back of the furnace. The combustion cavity of interest in this work extends from the bullnose to the furnace floor.

Air is introduced into the furnace at two or three different levels. Three levels is standard in furnaces of recent construction, two levels were used on some older units. The primary air enters at the bottom of the furnace, typically on all four walls. Secondary air, when it is used, is introduced just below the liquor guns on two or four walls. About ten meters above the furnace floor is the usual injection site for tertiary air, tertiary air ports are usually located on just the front and back walls.

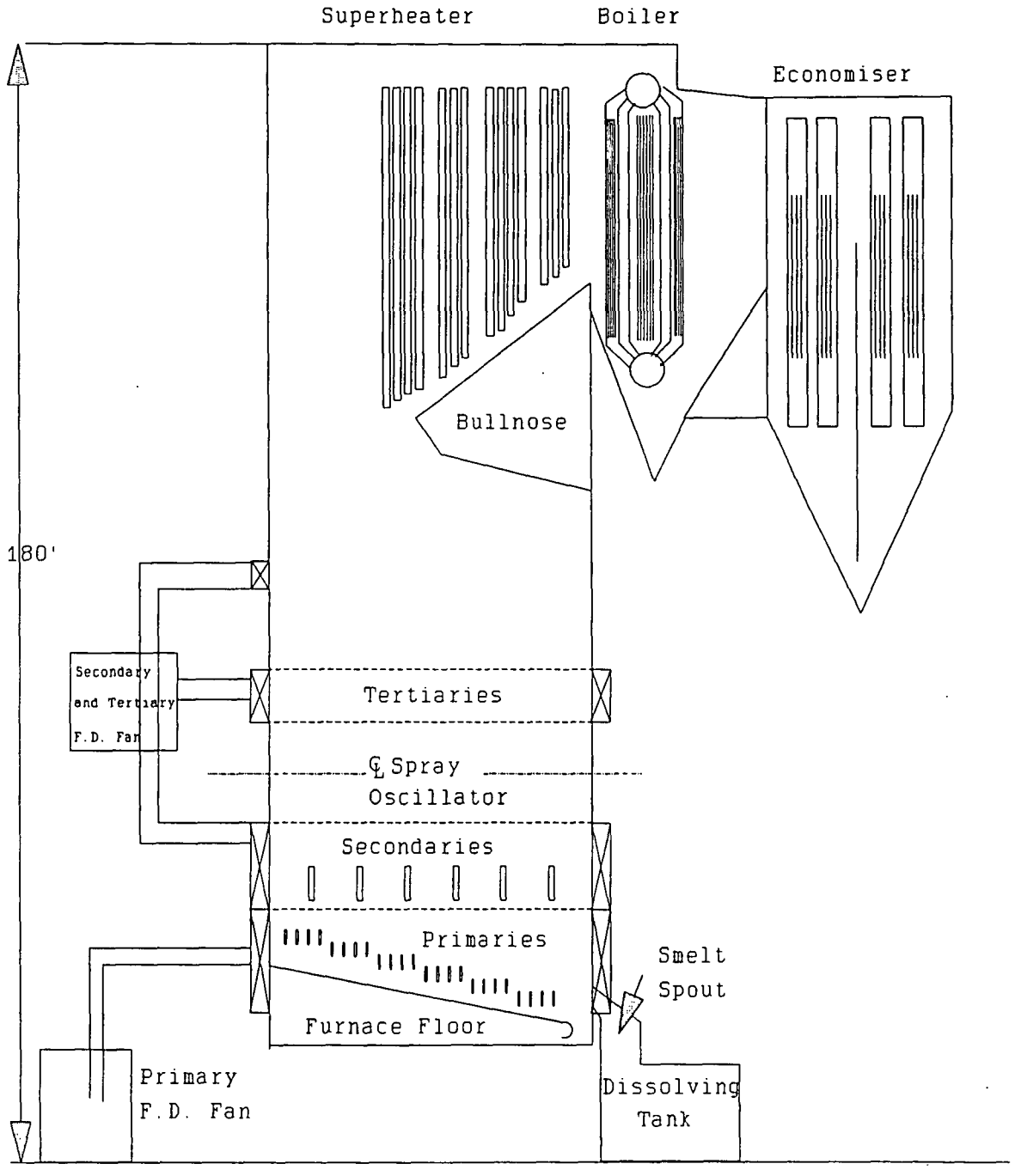

Figure 1 - Geometry of a Recovery Furnace (B&W Design)

In a 1000 ton per day furnace (a typical size), about 50 kilograms of air per second is introduced into the furnace. If three levels of air are used then about 40% of the air enters through the primaries, 40% through the secondaries, and 20% through the tertiaries. When two levels of air are used, then about 65% enters as primary air, and about 35% as tertiary air.[1] The inlet velocities of the air jets are approximately 40 meters per second for both the primaries and the secondaries (if present), and about 70 meters per second for the tertiaries. The pressure drop necessary for gas flow is created by the ID and FD fans. The ID or induced draft fan applies a negative pressure drop to aid in the removal of combustion gases. The FD or forced draft fan applies a positive pressure drop necessary to develop the inlet gas jets. The furnace cavity itself is at approximately atmospheric pressure.

The material fired in the kraft recovery furnace is called black liquor, a by-product of the pulping process. It contains mostly lignin, degraded carbohydrates, and spent pulping chemicals. Dilute black liquor is recovered during the washing of pulp. Concentration of this dilute stream to approximately 65% solids is accomplished by the use of evaporators. In a 1000 ton per day furnace about 15 kilograms of black liquor per second is sprayed into the furnace. The solid portion is composed of approximately half organic material and half inorganic material. The black liquor is introduced into the furnace via liquor guns that are located on the walls of the furnace about three or four meters above the furnace floor. The liquor is sprayed into the furnace as drops that are from one to four millimeters in diameter.

The black liquor undergoes a number of steps during combustion.[2,3] These steps usually occur in sequence, although with larger drops some overlap of stages may occur. First the drop dries; following this step the drop begins to pyrolyze, releasing combustible gases. Next is a step referred to as char burning: the fixed carbon that remains after combustion is burned, leaving an inorganic smelt drop. The smelt drop is in a reduced condition following char combustion, and reoxidation can then take place.

All drops will not necessarily undergo all these combustion steps, as they may exit the furnace entrained in the gas stream, or hit the wall or the char bed in any stage of combustion. Drops that hit the walls and the bed with some residual carbon contribute to the mass of the char bed.

The char bed is a mound of inorganic smelt and carbon that forms in the bottom of the furnace cavity. It is supplied with air by the primary and secondary air ports located on the walls of the furnace. In the bed, chemical reactions take place that result in the combustion of carbon and the formation of a smelt that is primarily a mixture of sodium carbonate and sodium sulfide. This smelt exits the furnace via smelt spouts located at base of the furnace walls (see Figure 1). The active layer of the bed is only a few inches thick; it is in this surface layer that the bed reactions take place. Further into the bed the decreasing temperature and low oxygen concentration prevent further char reactions.

The heat transfer function of the recovery boiler is provided by the water walls of the furnace, and by the heat exchange devices downstream of the furnace outlet. The main mechanism of heat transfer in the furnace cavity is by radiation from the furnace gases to the walls. Once the furnace gases exit the furnace cavity they come in contact with the heat transfer sections: the superheater, followed by the boiler and then the economizer. Particulate is removed from the flue gas by an electrostatic precipitator. The flue gas is then sent to the stack.

Kraft recovery furnaces differ from other combustion units in a number of significant ways. Kraft recovery furnaces operate with diffusion type flames, as the fuel (black liquor) and oxygen are introduced separately. Pulverized coal-fired furnaces use premixed flames, where the pulverized coal and combustion air are mixed before entering the furnace. Stoker-fired furnaces for coal or wood use underfire and overfire air. Underfire air cannot be used in the recovery furnace due to the presence of liquid smelt over the entire floor of the furnace. One way in which recovery furnaces differ most from other combustion units is the low melting temperature of the ash formed as a result of combustion.

Another major difference is that the recovery furnace must produce a reduced smelt product, yet all organic carbon must be burned with minimal carryover.

CURRENT LIMITATIONS AND PROBLEMS WITH THE KRAFT RECOVERY FURNACE

The requirements of burning a variable fuel, maintaining a stable char bed, along with additional operating constraints makes the operation of a recovery boiler at or near an optimal level a complex task. Furnace operation involves the manipulation of quantities such as air distribution, nozzle pressure, the angle of the nozzle, and firing rate. The black liquor properties vary considerably with time depending on the wood species being pulped and the pulping process parameters. In addition, a variable and often unknown amount of dust collected from the flue gas is recycled back to the fired black liquor. Operators try to maintain stable operation of the recovery boiler without knowledge of the changing properties of the incoming black liquor. In addition, the operator has limited feedback concerning the effect of any changes made in operating variables.

From a production standpoint, the recovery furnace is often a "bottle-neck", with the production of the entire mill limited by the amount of black liquor that can be burned in the recovery furnace. Recovery furnaces often operate at or above design levels, essentially pushed to the limit. The throughput is frequently limited by excessive amounts of carryover. Carryover results from overloading or incorrect operation of the furnace and consists of partially burned black liquor or smelt drops that exit the furnace cavity and building up on the heat exchanger surfaces.[5] This can cause an increase in the pressure drop, leading to higher demands being placed on the ID fan. Eventually a furnace shutdown is necessary in order to prevent complete blockage of the gas flow passages. It is advantageous to increase the capacity of the existing furnace, rather than purchasing a larger furnace as the recovery furnace is the single most expensive unit in the pulp mill.

Another operational problem that plagues recovery furnaces is corrosion. The recovery furnace is subject to corrosion, especially in areas where carbon steel is exposed to high temperatures and

corrosive chemicals.[4] One location that is prone to corrosion is the wall tubes in the lower part of the furnace.

Smelt water explosions, which can occur when water comes in contact with smelt that exists in the bottom of the furnace, are a major concern. Failure of wall tubes and low solids in the incoming black liquor are two ways in which excessive water can enter the furnace cavity. Explosions of this type can be very destructive. Two or three explosions of this type occur every year in North America.[4] Two other types of explosions that are not unique to the recovery boiler can occur: pyrolysis gas explosions, where explosive concentrations of pyrolysis gases suddenly ignite; and auxiliary burner explosions (oil or gas burners are used during start-up and other transient situations).

If a recovery furnace is being operated incorrectly, large amounts of reduced sulfur species may be emitted. These gases (H_2S and mercaptans) can be detected by the human nose at very low concentrations, and give the kraft mill its characteristic "rotten eggs" odor. Other pollutants that are produced include sulfur dioxide and carbon monoxide. Elimination of partially combusted species in the furnace is accomplished by increasing mixing in the furnace cavity, or by increasing the amount of excess oxygen.

POSSIBLE WAYS OF SOLVING OPERATIONAL AND SAFETY PROBLEMS

Operational problems such as excessive carryover and regions of high temperature can be corrected by modifying the operating parameters such as air jet location and geometry, primary/secondary/tertiary flow ratios, liquor gun location, and black liquor spray characteristics. Some basis for these changes must be established. Usually this is simply done by trial and error; more rigorous methods are available. The purpose of this section is to evaluate the available techniques.

Actual furnace tests have been performed on many occasions. These involve the installation of instrumentation on an operating recovery furnace. Experiments are conducted by manipulating the inputs to the furnace, or by recording these inputs during normal operation of the furnace. The effects

of changes in these inputs on the variables measured by the installed instrumentation are then determined. The first of these techniques can lead to unstable and even dangerous conditions if care is not taken, the second restricts the range over which manipulated variables can be examined. The instrumentation that is necessary in order to obtain useful results is expensive, and difficult to maintain.

Scale modelling of the kraft recovery furnace is conducted by constructing a miniature model of the furnace of interest.[7] Simple scaling of all furnace dimensions is not possible, as the scaling criteria must be based on momentum balances which are not linearly related to the scaling factor. These scaling criteria are not exact, and often are impossible to satisfy. The gas flows that are found with this technique are "cold flows", that is, the effects of temperature distributions within the furnace are neglected; an average temperature is used throughout the furnace cavity. The temperature of the gases in the miniature furnace will be uniform, and usually at room temperature. The use of scaling parameters applied to the inlet velocities permits the simulation of higher temperatures. Tests of this type allow the visualization of gas flow patterns in the scale model, and are used to make decisions on port design and flow ratios in full scale furnaces.

Another method for evaluating operational problems and design modifications is computer simulation. Gas phase simulations are obtaining from a numerical solution of the Navier-Stokes equation (a fundamental description of fluid flow). A common technique uses the finite difference method. The flow region is divided up into computational cells. The properties of the flow within each cell are then calculated by the solution of an integrated form of the Navier-Stokes equation. An iterative approach must be taken, as neighboring cells will influence the cell currently being considered, and vice versa. A restriction on computer memory puts a limit on the number of discrete cells that can be used in the simulation. If enough cells are used then a good approximation of the exact solution of the Navier-Stokes equation can be obtained. The limit in computer speed restricts the size of a case as well: convergence of a flow field may require thousands of iterations. In order to be useful a simulation must converge in a reasonable amount of time. Solving for too many variables or too many cells results

in code that takes an excessive amount of time to converge. Computer modelling is not a stand-alone technique (experimental confirmation is necessary) but computer simulation has the capability to reduce the effort required to find solutions to a given operational problem.

CURRENT COMPUTER HARDWARE AND SOFTWARE LIMITATIONS

Two of the limitations involved in computer modelling discussed previously were computer memory and computer speed; however, the limits of these areas are being expanded continuously. Currently, such diverse areas as world-wide meteorological simulations and microscale turbulence have been modelled[40]. The computational requirements of the most complex simulations are very large, on the order of days of CPU time on a CRAY supercomputer computer (about 100 trillion calculations). Supercomputer time is expensive, with an hour on a commercial system costing in excess of $10,000. At the current time, emphasis should be placed on developing code that can describe the physical processes taking place. The computer capabilities should soon be available to economically perform these simulations involving 250,000 to a million nodes.

Currently, software is available that can solve both transient and steady state three-dimensional fluid flow simulations, but they are not sufficiently flexible as to be used without revision. Commercially available packages include FLUENT[8], PHOENICS[9], NEKTON[10] and FIDAP[11]. In order to simulate the processes in the recovery furnace it is necessary to have the source code. The description of the drop behavior and the bed burning is unique to the recovery furnace, and this must be added to the code.

OUTLINE OF MATERIAL TO BE PRESENTED

This thesis begins with a review of previously developed recovery furnace models, in order to illustrate the need for a three-dimensional model specific to the kraft recovery furnace. Coal burning

models are investigated next, as the coal burning processes is similar to that of black liquor and the models that have been developed may prove useful.

The model that was developed in this thesis is described in general terms. This discussion examines the structure of the model and how it was constructed. The fluid flow model used as a framework for this model (FLUENT) is examined next, and reasons for using an existing program are discussed along with justification for choosing FLUENT. A description of FLUENT/RFM (Recovery Furnace Model), the CFD code specific to the kraft recovery furnace, then follows. This description examines the code changes made, how the bed burning and in-flight models are incorporated into the code, how a simulation is converged, how to determine when convergence has been reached, and how to obtain results.

The remainder of the thesis is concerned with the simulations that were performed using the recovery furnace model. The first simulation to be performed was an investigation of jet penetration using FLUENT, in order to determine node requirements around the air ports. Next the cold flow in a recovery furnace was simulated; this was compared to existing experimental work. The cold flow work used the original version of FLUENT, and was a logical first step in the modelling effort. Code changes made to the combustion model in FLUENT were evaluated using a simple model of a gas combustion unit, the results of this work are presented next. The "Base Case" is then described. This is a model of a recovery furnace that was solved using FLUENT/RFM. A description of this case along with the results of the simulation are provided. The final simulation described employs the same geometry as the Base Case but uses a bulk average temperature. This was done in order to examine the effects that black liquor firing and bed burning have on the gas flows in the recovery furnace.

A REVIEW OF CURRENT MODELLING LITERATURE

The literature that has been reviewed can be classified into four categories: 1. Previously developed models of the kraft recovery furnace; 2. Models of coal combustion; 3. General combustion models; and 4. Auxiliary programs. The models in each of these categories were examined, with emphasis placed on determining their utility in the development of a three dimensional model of the kraft recovery furnace.

KRAFT RECOVERY FURNACE MODELS

At present, five kraft recovery furnace models have been developed, listed in chronological order as follows:

1. A model constructed by Bhanda, Lange, and Markant of B&W;[12]
2. The "Purdue" model, written by Williams and Galtung;[13]
3. The "ADL" model, written by Merriam;[14]
4. The "GEMS" model written by Shiang and Edwards;[15]
5. Shick's model which was based on the ADL model.[16]

The purpose of this section is to describe and critique each of these models.

The B&W Model

The first published description of a model of the kraft recovery furnace was given by Bhada et al in 1972.[12] The model was used to determine the effect of operating variables on gaseous and particle emissions.

The model was based on material and energy balances along with thermodynamic equilibrium and kinetic calculations for a series of zones in the furnace. Figure 2 illustrates the zones that were assumed to exist in the recovery furnace. This zonal approach was taken throughout the model. The model is one dimensional, meaning that each zone is treated as a batch reactor, with the physical

processes taking place being homogenous throughout the zone. The zones modelled are from bottom to top: the gasification section, where partially combusted gas and smelt are produced according to thermodynamic equilibrium; the secondary combustion zone, where the further combustion of the pyrolysis gases takes place; the volatilization zone, where the volatile components of the black liquor are released; and the complete combustion zone, where the furnace gases are burned to a final fraction of completeness.

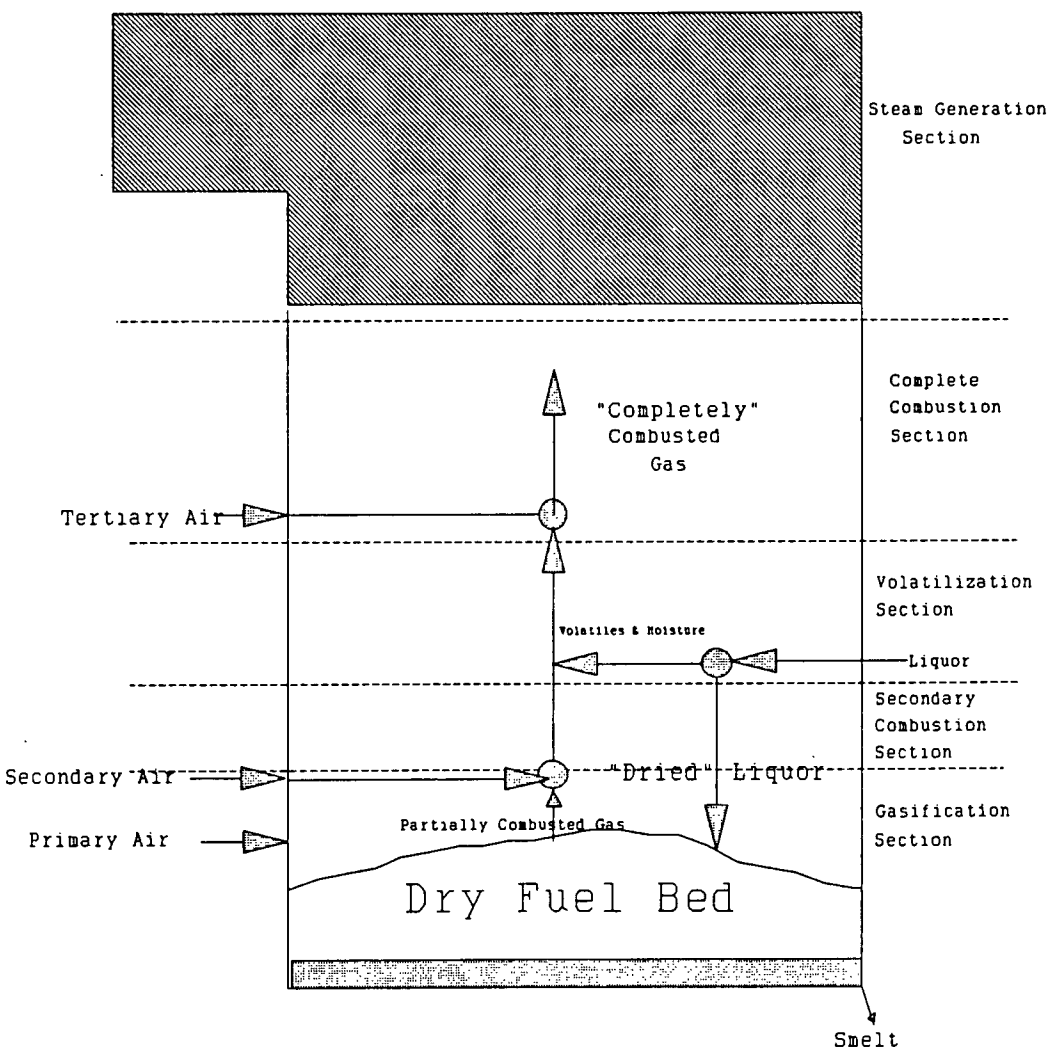

Figure 2 - Schematic of B&W Model

This early model has a number of flaws. One example is the assumption of thermodynamic equilibrium in the char bed. The zonal approach assumes that the specified physical processes take place in a predetermined location (i.e. pyrolysis of the liquor drops in the volatilization zone); there is no justification for this approach other than reduction of the computational effort. The "completely" combusted gas, is not completely combusted; the name of this zone is misleading. The amount of excess air used and the degree of turbulence in this zone determines the extent of combustion. The gas leaving this zone could contain some fraction of reduced gases (e.g. H_2S). If the gas leaving was always completely combusted then this model would be useless in predicting the emission of reduced gaseous species.

The Purdue Model

The Purdue model was developed as an aid in the design of recovery boiler control systems. This was the first attempt to one-dimensionally model the entire recovery furnace including the heat transfer sections, cascade evaporator, and precipitator.[13] The model was developed on the basis of material and energy balances, kinetics, and thermodynamic equilibrium, relying on assumptions and empiricism when the required information was unavailable. Unfortunately, a number of the assumptions were questionable; this was due mainly to the lack of existing data at the time the model was constructed.

The model was written specifically for a Combustion Engineering type kraft recovery furnace. The model concerned itself with the entire furnace unit; namely, the furnace cavity, the heat exchanger region, the salt cake makeup, the cascade evaporator, and the precipitator. The furnace cavity was divided up into three zones: the char bed, the primary zone (char bed to secondary air ports), and the secondary zone (primary zone to screen tubes). A block diagram showing the various zones used and the flows that exist between these zones is shown in Figure 3. Only those zones within the recovery furnace will be evaluated, as this thesis is concerned only with the furnace cavity.

Liquor Spray

The liquor spray was assumed to consist of three size groups:

1. The volume fraction of spray due to drops < 10 μm. These drops are assumed to account for the fine sodium particles that are found in the precipitator; this is wrong, as the fine particles are formed as a result of fuming processes of burning particles in-flight and on the char bed;

2. The volume fraction of spray due to drops > 500 μm. These drops are assumed to never become entrained. 500μm is too low a cutoff, (drops of 1mm would have been a better size limit). Better yet, no cutoff should have been used;

3. The volume fraction of spray due to drops between 10 and 500 μm. These drops are entrained as a linear function of the upward gas velocity in the primary zone.

The ratio of drops in each of these groups is taken to be a function of liquor temperature. As the temperature increases, the number of small drops increases. This is an empirical description of drop formation that provides a link between spray temperature, load and carryover. The effect of nozzle geometry is neglected, this plays a important role in drop size distribution.

The effects of liquor drop swelling are ignored. The drops that reach the bed are assumed to arrive there still wet, with no in-flight evaporation taking place. This assumption was made due to the lack of experimental data available on liquor drying in a furnace environment. In addition, the model does not account for any pyrolysis or combustion of the drops that reach the bed.

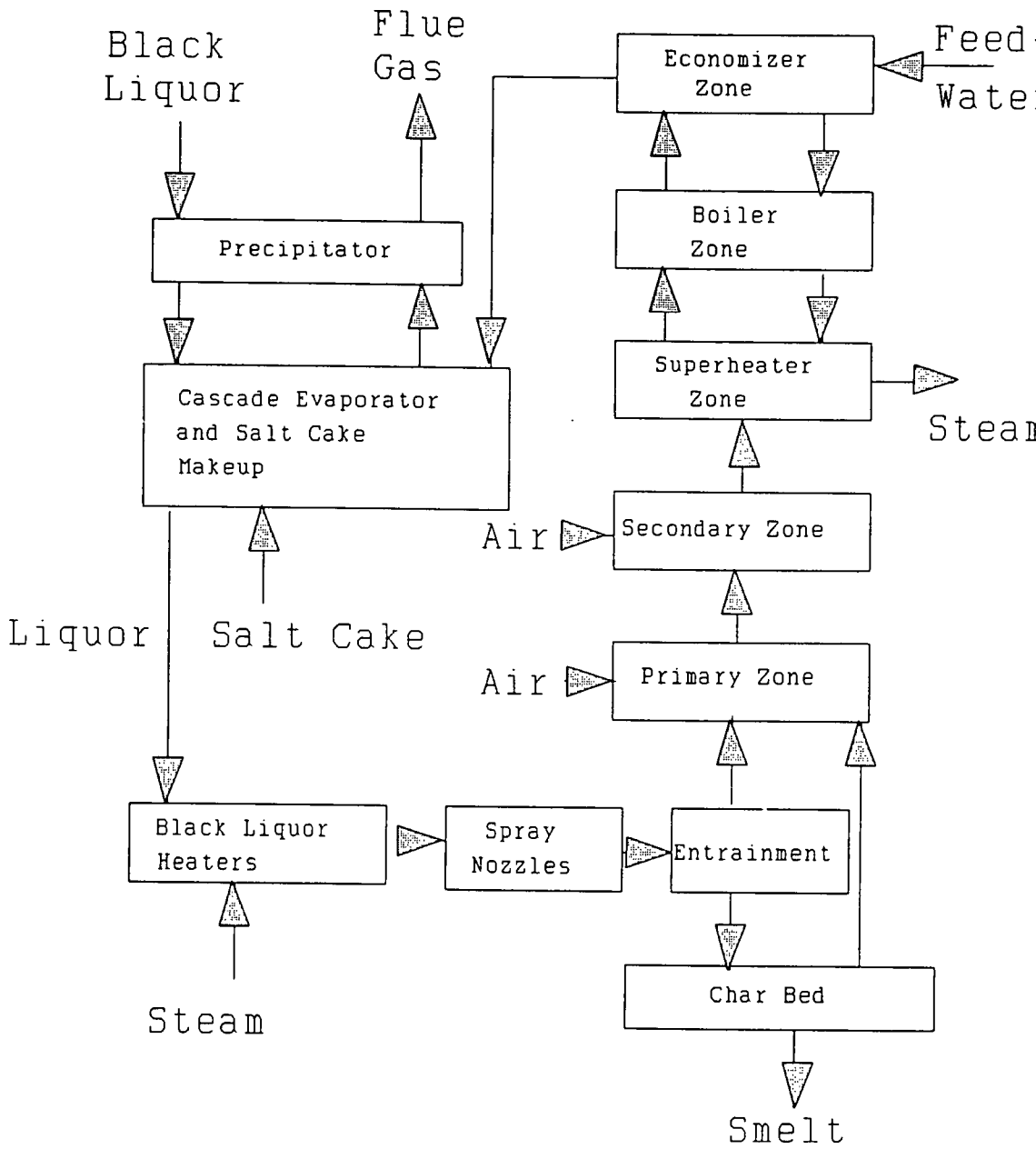

Figure 3 - Schematic of Purdue Model

Char Bed

The water entering the bed with the liquor drop is assumed to evaporate immediately. All sodium and sulfur that enters the bed with the drop is assumed to exit with the smelt. This is a poor assumption, as considerable sodium is lost as a result of bed fuming, and sulfur is lost as reduced sulfur gases and SO_2.

The rate of reaction of the char bed solids is proportional to the mass fraction of carbon in the bed and to an Arrhenius term. The reduction efficiency is calculated based on equilibrium, which is incorrect. The reduction of sulphate and the burning of char is now known to proceed via the sulfate-sulfide cycle, which is controlled by oxygen mass transfer[3]. The oxygen deficiency in the bed is set equal to the theoretical oxygen deficiency immediately above the bed, which is determined on the basis of thermodynamic equilibrium. The temperature used for the bed is that of the surface layer.

Primary Zone

All the water from the entrained spray is assumed to evaporate in the primary zone. No combustion takes place; this is an invalid assumption as pyrolysis gases from the black liquor and black liquor drops will be burning in this region. The only source of sodium and sulfur is the entrained spray; this is incorrect, as the char bed will contribute sulfur and sodium as well.

Secondary Zone

Conditions in the secondary zone are assumed to determine the final composition of the entrained particles and the combustion gas, a reasonable assumption if the gas temperatures are low enough, preventing further reaction.

The formation of SO_2, H_2S, and CO is determined by the excess O_2 and by the degree of turbulence due to the injection of secondary air; this relationship is determined empirically.

H_2S and SO_2 formation is determined based on the amount of excess oxygen and the degree of turbulence. The total sulfur minus the sulfur used in the formation of H_2S and SO_2 is assumed to react with the sodium carbonate in the fine drops to form sodium sulfate. Any remaining sulfur is then reacted with the larger entrained drops (> 10 μm). The sodium remaining forms sodium carbonate, the oxygen and nitrogen pass through unchanged, and the carbon forms carbon dioxide.

Energy Balances

The total heat of combustion is taken to be the heating value of the black liquor less the heat of reduction of sulfur and the heat of formation of water. The combustion energy released in the primary zone and char bed is assumed to be proportional to the fraction of oxygen present in these two zones, divided by the total oxygen requirement.

The heat transfer between burning gases in the primary and the secondary zones with the char bed is neglected; this could create considerable error in the overall temperature distribution. A steady state solution to the gas phase energy balance in both the primary and secondary zones is used, as the dynamics of the gas phase should be rapid.

In general, the Purdue model has been criticized as being cumbersome and difficult to apply. Many of the assumptions used have now been shown to be incorrect. It was never widely accepted by the pulp and paper industry.

The Arthur D. Little (ADL) Model

The Arthur D. Little model was concerned with the chemical, mass transfer and energy exchange processes taking place in the lower furnace.[14] The original reason for developing the model was to determine the firing conditions required to maintain low bed height while still achieving good reduction efficiency. Such process conditions would minimize bed cooling times and potential lower furnace

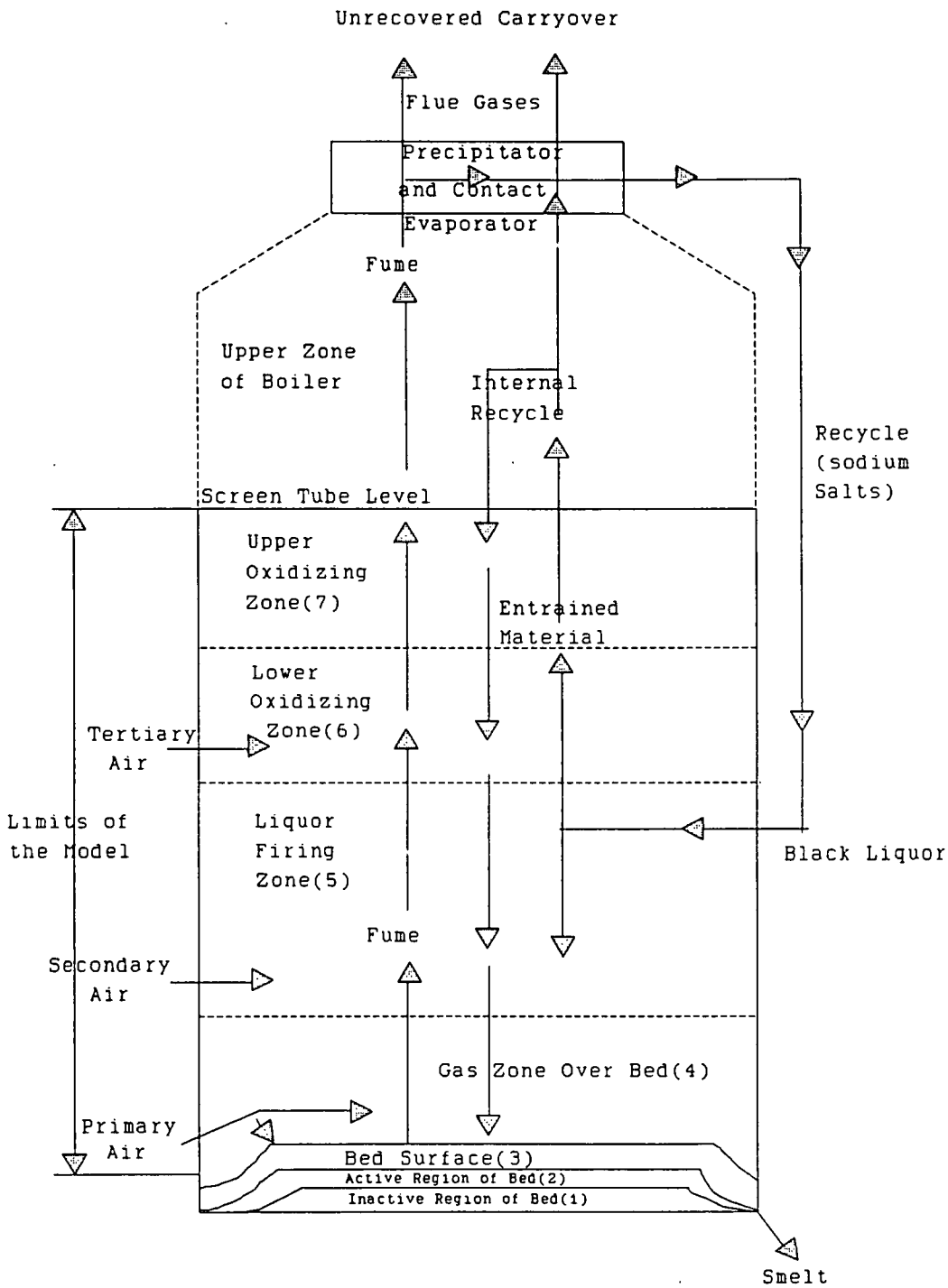

Figure 4 - Schematic of ADL Model

problems during unstable periods. In its final form the model went well beyond the original goals, simulating the entire furnace cavity.

The model is adaptable to both CE and B&W type furnaces, and uses a one-dimensional vertical description that takes into account the horizontal dimensions when calculating the radiative heat flux between the flue gases and the walls. The furnace is divided into seven zones, as shown in Figure 4. The zones designate areas of the furnace that have specific chemical and physical properties. Zone 1 is a model of the subsurface of the char bed where no reactions take place. Heat flow to the walls is by conduction and radiation. The active region of the bed is designated by zone 2; smelt reduction takes place in this region. In zone 3, the bed surface, oxygen is transferred into this zone and reaction products of the bed are transferred out. The primary air enters zone 4 and partially oxidizes the gases leaving the bed. The black liquor is introduced in zone 5. Zone 6 is the site of tertiary air introduction. Combustion is completed in zone 7.

The major assumptions of the model:

1. Overall - The furnace operation is steady state, except for the char bed which is pseudo-steady state, furnace conditions determine the rate at which mass is accumulating or being depleted from the bed. Each zone is uniform in temperature and composition;

2. Chemical - The furnace gases are in equilibrium in each zone. The bed surface is in equilibrium except for fume generation which is kinetically controlled. The reduction of sulphate and CO_2 in the active region of the bed is kinetically controlled;

3. Mass and Energy - Mass flows are in the vertical direction only. The partially dried and pyrolyzed spray is assumed to be distributed uniformly over the surface of the bed. The flow of oxygen to the bed is limited by mass diffusion and is controlled by the film thickness (a user specified parameter). The heat transfer between zones is by radiation only.

The main contributions of this model are the description of the black liquor spray and the bed processes. Aspects of the black liquor spray model include a characterization of the drop distribution and initial velocities, and a description of the steps in black liquor burning (drying, pyrolysis, and char burning). Correlations were developed for the spray patterns produced by both splash plate and hollow cone type spray nozzles. The drop distributions for these nozzles were determined from published correlations. The spray trajectories are determined from a fundamental force balance. The drops were injected into a simple gas flow pattern; the fate of the drop was determined and this information was then used as input to the overall one-dimensional model.

Considerable detail was involved in the description of black liquor combustion. Heat transfer to the drop was assumed to take place by radiation and conduction. Drying was modelled by the shrinking core model; wall drying was treated empirically. Pyrolysis was described by a number of parallel reactions, including swelling. The char combustion stage was modelled as three reactions between carbon and oxygen, carbon dioxide, and steam, respectively.

The bed burning model includes kinetic effects (a more realistic model of bed burning than those found in earlier models), fume formation, conduction of heat, and the flow of smelt. The kinetic reactions that were considered included the formation of sodium fume, the reduction of sodium sulphate, and formation of carbon dioxide. Thermodynamic equilibrium determines the final concentration of all other chemical species in the char bed.

The main inputs to the model are furnace geometry, wall temperature, percent recycle of salt cake, furnace type (CE or B&W), liquor properties, spray geometry, liquor chemistry, and incoming air distribution. The main outputs are drop trajectories, conditions of solids reaching the bed, smelt properties, and composition and temperature of flue gases.

Additional experimental data was deemed necessary for developing the relationship between drop size distributions and operating parameters in the furnace. Information on black liquor pyrolysis was also found to be insufficient.

In general, this model has received criticism due to errors in the code that resulted in mass and energy balances that did not converge. The model suffers from a lack of valid data in a number of areas, such as liquor drop size distributions and pyrolysis. The inclusion of kinetically controlled reactions in the bed was an improvement on previous models, but is in disagreement with current experimental results that suggest bed burning is oxygen mass transfer limited.

The GEMS Model

The GEMS model of the recovery boiler is a modular, steady-state, one-dimensional model which takes into account horizontal dimensions when determining radiative heat transfer.[15] The model of the recovery boiler is designed to be incorporated into a mill-wide simulation package. The approach taken is similar to that of the ADL model, the main difference being that the zones specified can be linked together by the user and included in a simulation of the entire kraft pulp mill. A schematic diagram of the modules that make up the recovery furnace simulation are shown in Figure 5.

The main outputs of the model are vertical gas temperature profiles, pressure drops, and the composition of the flue gas and smelt. It uses a kinetic approach to bed burning (based on Grace, et. al[3]), but does not describe the drying, pyrolysis and burning of the black liquor in flight.

A variety of different modules can be used to build up the recovery furnace simulation:

FURN - this module calculates the radiative heat transfer between the flue gases and the water walls;

COMB - this module performs a free energy minimization of the input chemical species to determine the flue gas composition in a given zone;

Revised COMB - allows for the kinetically-limited processes taking place in the smelt bed;

HSMEL - simulates the removal of heat from the smelt by the floor tubes and the wall tubes surrounding the smelt.

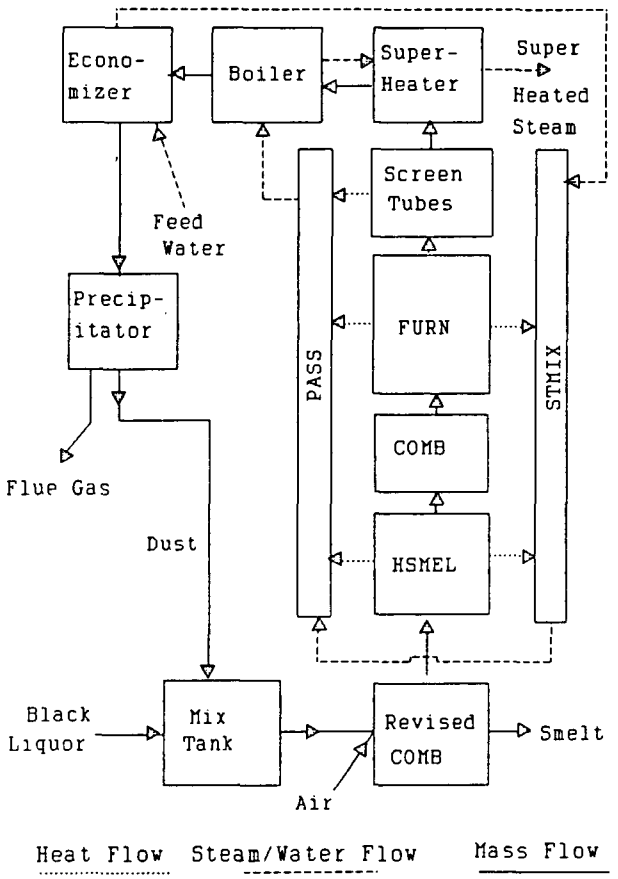

Figure 5 - Schematic of GEMS Model

Other blocks are used to determine the heat transfer to the screen tubes, superheater, boiler and economizer. The wall tubes are represented by downflowing (STMIX) and upflowing (PASS) sections which exchange energy with the FURN and HSMEL blocks.

The modules require user inputs; for example, the fraction of entrained black liquor falling back to the hearth is required by the COMB block. The other inputs to the model include furnace geometry (e.g. air port location), heat transfer surface area, tube emissivity, air distribution, black liquor flow rate heating value and composition, reduction of smelt, excess air, and incoming air temperature. The main outputs are heat fluxes to the walls, gas temperature and composition in each zone, and smelt flow rate.

The model has been shown to accurately reproduce the temperature as a function of height and reduction efficiencies in existing furnaces[15]. It can be used to predict the effect of changing a parameter (for example, liquor firing rate), once a base case has been established and validated.

Major unknown factors include the ash build-up on tubes, the degree of mixing, and the effective wall tube emissivity.

The application of this model is in predicting the effect of changes in the input parameters for an existing furnace, once a base case has been established. The unknown factors discussed in the previous paragraph must be adjusted so that the heat fluxes and emissions in the base case agree with those found in the actual furnace. The model is not sufficiently flexible to predict the effects of design changes.

Shick's Model

The main purpose of Shick's model was to use computer graphics to illustrate the in-flight behavior of black liquor drops in a recovery furnace.[16] The paths taken by individual black liquor drops are shown in three dimensions. This was the first model to calculate drop trajectories with variable gas flows. The region modelled lies between the tertiary air ports and the surface of the bed.

A wide variety of parameters can be specified by the users, including furnace geometry, degree of turbulence, amount of recirculation in the gas flow, temperature distribution, and oxygen concentration. In addition, properties of the black liquor spray are specified, including initial velocity, composition and temperature. Graphical output of the model depicts the path taken by the individual drops and the their physical state (i.e drying, pyrolyzing, burning, or burnt out) by using a variety of colors.

Each of the steps of black liquor combustion are modelled using many of the same equations as the ADL model, although a number of recent experimental findings were incorporated into the model. Examples of improvements are the inclusion of oxygen mass transfer controlled char combustion and swelling characteristics.

Shick recognized the limitations of this model: individual air ports are not modelled, gas flow patterns are imposed rather than calculated, the interaction between the liquor spray and the furnace gases is not modelled, and an average oxygen concentration is used.

Summary of Information on Existing Kraft Recovery Furnace Models

Model	Purpose	Main Contribution	Main Flaws	Dimensionality
B&W 1972	To determine furnace emissions.	First model, demonstrated zonal approach.	Thermo. equil. in bed, lack of data on black liquor burning.	1 for all calculations
Purdue 1972	To assist in control system design	Modelled entire recovery furnace, kinetics in bed.	Bad assumptions on drop behavior, difficult to use.	1 for all calculations
ADL 1980	To determine optimum firing conditions.	Detailed spray and bed models.	Mass and energy balances didn't converge, computational errors. Equilibrium in bed.	1 except for radiation and drop calculations which are 2.
GEMS 1984	To fit into mill-wide simulation.	Modular flexible approach, validated on actual furnaces.	Requires a number of user supplied parameters.	1 except for radiation which is 3.
Shick 1985	To visualize black liquor behavior.	Three-dimensional model of furnace flows and black liquor trajectory.	Gas flows imposed, coupling between spray and gas not included.	3

Limitations of Previous Models

The main limitations of previous models lie in their one-dimensional, rigid structure. These models do not deal with the three-dimensional nature of the gas flow patterns, temperature, and species concentration. No attempt has been made to couple the behavior of the black liquor spray and the gas flow. The zonal approach used biases the results obtained by specifying the location of combustion processes prior to the solution of a simulation.

These models can also be improved by incorporating the knowledge gained at IPC and elsewhere, in the last few years. The combustion behavior of black liquor is better understood, along with the

characterization of the spray. It is now possible to eliminate much of the empiricism needed to construct the earlier models.

COAL COMBUSTION MODELS

Coal combustion has many similarities to black liquor combustion. Much can be learned from the coal combustion models that have been developed, especially considering that development of coal combustion models has been ongoing for many years. The coal combustion models that have been developed use a continuum approach. The velocities, temperatures, and species concentrations are determined from the finite-difference solution of the fundamental governing equations. The kraft recovery furnace models discussed earlier used a zonal approach.

There are also some major differences, including the geometry of the furnace, and the means by which the fuels are introduced into the furnace. In pulverized coal combustion the fuel (coal) and air are premixed and introduced as a primary stream; a secondary air stream is swirled around the primary stream. The flame that forms in coal combustion is classified as a premixed flame, rather than the diffusion flame that is present during black liquor firing.

The fuels are similar in chemical composition, consisting of water, volatile materials, carbon, and inorganics. The relative amounts of these substituents differ, with coal containing 6 to 10 percent volatiles, compared to black liquor which contains about 25 percent. The moisture level of most coal is lower than black liquor (10%, vs 25 to 40% for black liquor). These differences result in the coal flame being hotter and more efficient than the combustion occurring during black liquor firing.

Despite these differences a coal furnace and a kraft recovery furnace can be modelled similarly. There are three common aspects of both furnaces:

1. The series of reactions that both black liquor and coal undergo: drying, pyrolysis, and char burning.

2. The reactions of the gas phase, including oxidation of the pyrolysis gas and the production of pollutants.

3. Radiation as the dominant means of heat transfer.

Thus coal combustion models provide useful techniques for examining radiative heat transfer, gas phase combustion and the modelling of black liquor combustion.

1-DICOG Model

Smith and Smoot have developed a one-dimensional model for pulverized coal combustion called 1-DICOG (1-DImensional Combustion Or Gasification).[17] The coal particle undergoes a number of physical, thermal and chemical processes; namely, the moisture vaporization, coal devolatilization, heterogeneous char oxidation, gas-particle interchange, radiation, gas phase oxidation, primary and secondary stream mixing, and heat losses.

The model uses the macroscopic form of the general conservation equations (conservation of momentum, energy, and mass continuity) and solves these differential equations by the use of a predictor-corrector solution technique. The differential equations used are steady-state and one-dimensional; this means the model is unable to predict local mean or fluctuating properties. Other limitations of the model: 1. jet mixing and recirculation are inputs rather than being generated variables; 2. kinetic parameters in the coal reaction equations are not well known; and 3. simplification of some of the processes taking place has been performed in order to save computer time.

PCGC-2 - A 2 Dimensional Coal Burning Model

PCGC-2 is a two-dimensional model of pulverized coal burning developed by Smith, Smoot, and Fletcher, of Brigham Young University as an extension of the 1-DICOG model.[18] Variations in flow properties are considered in the radial and axial directions, symmetry is assumed in the angular direction. The model predicts mean gas properties for axisymmetric, steady-state, turbulent diffusion

flames. Turbulence in the gas phase is modelled by breaking the variables into a constant and time varying component. The k-ϵ model is used to describe the turbulent behavior of the gases[41]. The radiation field is a multi-component, non-uniform, emitting, absorbing, scattering gas-particle system.

The physical and chemical behavior of the pulverized coal particles are modelled; this includes a description of particle trajectories, modelling of the steps involved in combustion, and transfer of material to the gas phase.

GENERAL COMBUSTION MODELS

A number of modelling packages have been developed for application to general combustion processes. With the addition of information on black liquor drying, pyrolysis and burning, it would be possible to apply some aspects of these models to the kraft recovery furnace.

The PSI-CELL Model

The PSI-CELL (Particle Source In CELL) model is specifically designed to predict the temperature and velocity history of a cloud of drops or particles in a given gas flow field.[19] The difficulty in modelling such a system lies in describing the coupling that exists between the gas flow field and the particles. In many simulations this is ignored, but the PSI-CELL model takes the coupling of these two phases into account.

There are three ways in which the gas phase and the particle phase are coupled:

1. Mass Coupling - for example, the evaporation of water from the drop will increase the mass of the gas phase;

2. Momentum Coupling - for example, the momentum of the gas phase will be reduced due to the drag of the liquor drops passing through the gas;

3. Thermal Energy Coupling - for example, the burning of black liquor drops is a source of energy for the gas phase.

In the gas phase information is required concerning the velocity, pressure and temperature. In the condensed phase (for example the black liquor spray) we require information on the trajectory, size and temperature history of the drop. In the case of the recovery furnace the chemical composition of both these streams is also important.

The PSI-CELL model solves for the desired properties of a combustion system by first dividing the flow field into discrete cells. Finite difference equations for mass, momentum, and energy conservation are developed and applied to the gas phase in each cell. The effect of the condensed phase is included as source and sink terms in the finite difference equations.

The general solution technique is as follows:

1. The gas flow field is solved in a stationary reference frame (Eulerian approach). The velocity, pressure and temperature of the gas field without the influence of the particles is then found;

2. The trajectories of the particles are with respect to a stationary reference frame. The state equations for the particles are in a reference frame that moves with the particle (Lagrangian approach). The condition of the particles as they cross the cell boundaries is recorded;

3. The source or sink terms due to the particles are incorporated into the gas flow finite difference equations. For example, the mass of a particle entering a given cell minus the mass of the particle when it exits that cell, is a source of mass for that cell;

4. The gas flow field is solved again to determine the effect of the condensed phase;

5. New particle trajectories, temperature histories and size can then be calculated and used to develop new source and sink terms;

6. This process is continued iteratively until the results converge.

CORA2 Model

The CORA2 (COmbustion and Radiation Analyzer 2 - Dimensional) model was produced by Markatos and Moult.[20] In its most general application it could be used to predict unsteady, turbulent, compressive flows without any single dominant flow direction; these flows could also include chemical reaction, significant radiation and swirling about an axis of symmetry.

This model cannot accomodate three-dimensional flows, except those with an axis of symmetry, nor multi-phase flows. These restrictions prevent the application to a kraft recovery furnace; significant velocity gradients exist in all three axes, and the flow has two distinct phases (black liquor and air).

The variables calculated on a time-averaged basis are the axial and radial velocity components, the swirl velocity, the pressure, the stagnation enthalpy, the temperature, the turbulent kinetic energy, the dissipation rate of turbulence, the mass fractions of all chemical species, and the radiation fluxes in both coordinate directions.

The turbulence model used the two-equation model of Harlow and Nakayana[41]. The chemical reaction model has two species (fuel and oxidant) reacting to form a product. Reactions in laminar flows are assumed to obey the Arrhenius-type relation; in turbulent flows the eddy-break-up model of Spalding is used. The radiation model used is a four flux type, with fluxes in both the positive and negative coordinate directions.

The system equations are solved by the use of a finite difference approach. The system area is divided into control volumes by intersecting lines. The intersection points are called nodes; all flow properties except velocity are evaluated at these nodes. The velocities are evaluated halfway between the nodes. The finite difference equations are developed by integrating the differential equations over a control volume surrounding the node.

Three Dimensional Furnace Simulation

Hjertager and Magnussen co-authored a paper entitled "Computer Simulation of Flow, Heat Transfer and Combustion in Three-Dimensional Furnaces", in which they discuss their model.[21] The model handles the coupled processes of flow, heat transfer, mass transfer, and combustion in three dimensions.[16]

The general aspects of the model:

1. Turbulent mass, energy and momentum balances;

2. Single step reactions from reactants to products; the species assumed present are fuel, nitrogen, oxygen, carbon dioxide, and water vapor;

3. Both premixed and diffusion flames can be handled;

4. A radiation model that assumes an angular distribution of the radiation intensity. The distribution is assumed to be a truncated Taylor expansion of the angular dependance;

5. Turbulent modelling using a 2-equation model, with a special wall function close to the wall to reduce the number of grids required.

The solution is obtained by finite-difference methods, similar to those used in the CORA2 model. The calculations for a typical case required 600-800 iterations to obtain converged solutions.

Two limitations of this program, when applied to a kraft recovery furnace, can be envisioned:

1. The chemical equilibrium and kinetics are not handled well;

2. The black liquor spray would have to be handled separately.

The utility of this model appears to be in describing the three dimensional behavior of the gas phase. To apply it to black liquor firing, it would be necessary to incorporate models of the other processes taking place.

AUXILIARY PROGRAMS

Developing a simulation of the recovery furnace involves the building of many small models to simulate various physical processes taking place in the furnace. Areas where auxiliary programs may be useful in an intact or modified form are: 1. radiative heat transfer; 2. chemical reaction and kinetics; 3. particle trajectory models.

Radiative Heat Flux Models

Radiative heat fluxes can be described almost exactly by zone or Monte-Carlo models, but these models require a large amount of computer time. A number of methods exist that make approximations resulting in an accurate and computationally efficient model.

A six-flux radiation model is described by Siddall and Selcuk.[22] The model is applicable to rectangularly shaped enclosures (for example, a furnace). The region surrounding an arbitrary point P is divided into six pyramid-shaped solid angles. The pyramid-shaped regions can be specified so that they correspond to the walls of the enclosure. The radiative intensity within each region is assumed to be constant; although, the fluxes will be different in each direction. The points used would correspond to the centers of the computational cells within the furnace. The radiative fluxes will vary from cell to cell. Using this simplifying assumption, the solution of the radiative flux is reduced to a much simpler system of equations then those found in Monte Carlo or zone models.

Chemical Reaction and Equilibrium

In order to model the combustion process in the kraft recovery boiler it is necessary to identify the chemical species formed and the amounts formed. The situation is further complicated by the presence

of kinetically limited reactions, especially those in the smelt bed. A number of computational techniques have been developed to solve the chemical reaction calculations.

The CREK (Computer Reaction and Kinetics) program was developed as a module for incorporation into larger fluid mechanic models.[23] It was developed specifically for combustion applications and has the ability to generate initial estimates of the species concentrations. The final state of a chemical system is found by the minimization of the Gibb's free energy, with the kineticially limited reactions entering as constraints.

A simplified version of CREK also exists; CREE (Combustion Reaction Equilibrium for Elements) only calculates the equilibrium of the chemical species and requires as input the local element numbers.

Additional programs designed to calculate chemical equilibrium include: NASA-CEC[24], Edwards Air Force Base Model[25], and SOLGASMIX[26]. It is difficult to incorporate these chemical reaction and equilibrium programs simply and efficiently into a large combustion model. The information that is gained does not justify the effort. In most cases the reactions can be considered to go to completion.

Particle Trajectory Models

The path or trajectory followed by a black liquor drop, from the time it enters the furnace until it either exits with the gas stream (entrained) or falls onto the surface of the bed, has an important influence on the operation of the recovery furnace. In addition, the prediction of the black liquor drop trajectories is an essential component of any model of the recovery furnace.

Two authors (Shick[16] and Merriam[14]) have attempted to model the flight of the black liquor drop. In general, the path followed by the drop can be determined from a balance of the inertial, gravitational and drag forces on the drop.

The drag is a function of the drag coefficient, which in turn is related to the projected area of the drop; this will change as a function of time. Drying and pyrolysis of black liquor in an oxygen limited

atmosphere can result in a six to seven fold increase in the diameter. Merriam takes into account the effect of swelling by assuming a volume increase of three times during drying and a final swollen volume after pyrolysis of six to seven times the initial diameter. Shick takes into account swelling by allowing a user specified swelling coefficient.

Neither of these approaches is completely satisfactory; ideally, the swelling should be determined from the composition of the black liquor and the conditions it is subjected to in the furnace. Unfortunately, the experimental information in this area is still lacking[42]. It seems likely that swelling is not a deterministic processes, and that the degree of swelling of a black liquor drop cannot be determined from the black liquor composition and furnace conditions.

Determining the path of the drop is more difficult than it appears, as there is coupling between the gas and the condensed phase and collisions between individual drops. In addition, many drops with different initial properties (velocity and diameter) will have to be injected into the furnace to accurately reflect the behavior of the black liquor sprays.

A DESCRIPTION OF THE MODEL

The purpose of this section is to describe the computer code developed in this thesis. The code is a mixture of previously developed computer code (FLUENT), and computer code written by the author of this thesis, Allan Walsh, and Dan Sumnicht. First a general description of the code will be given. Next, an account of the steps involved in choosing a framework for the model is provided, followed by a description of the code chosen, FLUENT. A discussion of the limitations of the FLUENT code and the code development undertaken in order to overcome these shortcomings will follow. The computational fluid flow code that is developed, FLUENT/RFM (Recovery Furnace Model) is then described, including information on how to use the code.

A GENERAL DESCRIPTION OF THE RECOVERY FURNACE MODEL

The computer code developed in this thesis was designed specifically for simulating the kraft recovery furnace. A finite difference approach is taken in the solution of all flow variables (i.e. velocity, temperature, species concentrations); a detailed explanation of the solution technique can be found in the next section. A steady state, three-dimensional solution of the flow variables is found. The gas flow patterns are solved for in three dimensions by solution of the Navier-Stokes equation. Included in the program are both turbulence and six-flux radiation models. The influence of the second phase (black liquor drop) on the first phase (gas phase) is modelled by the PSI-CELL approach, as discussed in the literature review. A combustion model is included along with a bed burning model. The computer code developed in this thesis makes use of FLUENT as a framework for subsequent code development; this framework provides a procedure for setting up a simulation, a solution algorithm, and utilities for viewing the results.

CHOOSING A FRAMEWORK FOR THE MODEL

The first task of this modelling effort was to decide if existing code should be used, and if so, which code should be chosen. A major consideration in this decision was the time involved in developing a

code from scratch. The amount of time required to develop comprehensive, three-dimensional fluid flow models is on the order of five man years. This would be equivalent to two PhD theses. This time would not include the development of code specific to the recovery furnace, nor would it include the time required to converge, evaluate, and document any recovery furnace simulations. Another time consuming task would involve the validation of the code against existing experimental fluid flows.

It was decided that the use of an existing code would result in a better final product. Time and effort could be spent on developing the code to meet our specific requirements, and converging and documenting a simulation of the recovery furnace.

The first computational fluid dynamics (CFD) code considered was PHOENICS, a package marketed by CHAM[9]. PHOENICS can simulate three-dimensional, turbulent, reacting flows. A three day course was attended, where the capabilities of the code and how to use it were demonstrated. The main drawbacks seen with this code were 1. The cost of a software license, about $1,200 per month; 2. No radiation model; 3. No allowances for a second phase; and 4. The source code was not available. It appeared that it was possible to write second phase and radiation models, but the means of doing this was never made clear by CHAM.

At about the same time another CFD package, FLUENT[8], had been obtained by Dr. Ted Farrington, for use at the Institute of Paper Chemistry. This code had a number of significant advantages over PHOENICS, including: 1. Radiation and second phase models; 2. No license fee; and 3. The source code was available. Additional codes were not investigated as this code had the majority of the components necessary for meeting the original objectives of this modelling effort. None of the other CFD codes (FIDAP[11], NEKTON[10], CORA2[20], PCGC-2[18]) discussed previously offered as many of the required features. We were confident that the deficiencies present in FLUENT could be eliminated by suitable source code development and revisions.

A DESCRIPTION OF FLUENT

FLUENT is a commercially-available, finite-difference, fluid flow modelling program. This section will examine the theoretical basis behind FLUENT, the published applications of FLUENT; and its limitations.

Theoretical Basis For FLUENT

The FLUENT manual provides a description of the theoretical basis for the various sub-models that appear in FLUENT[8]. This section will give a summary of those features that are used in the recovery furnace simulation.

Gas Flow Equations

The gas flow velocities are found by the solution of the mass conservation and momentum conservation equations. Before presenting these equation an explanation of the notation is necessary. The equations that follow are written in tensor notation. Tensor notation implies a summation over all coordinate directions when indices are repeated in a term. An equation written in tensor notation can be expanded to more conventional form by summation as follows:

$$\frac{\partial(u_i u_j)}{\partial x_i} = \sum_i \underline{u}_i \bullet (\sum_j u_j) = \frac{\partial u_1 \underline{u}_j}{\partial x_1} + \frac{\partial u_2 \underline{u}_j}{\partial x_2} + \frac{\partial u_3 \underline{u}_j}{\partial x_3}$$

Mass Conservation:

$$\frac{\partial}{\partial x_i}(\rho u_i) = 0 \qquad [1]$$

Where: i is coordinate direction x, y, or z
ρ is the density of the gas
u_i is the velocity component

Momentum Conservation:

$$\frac{\partial}{\partial x_i}(\rho u_i u_j) = \frac{\partial}{\partial x_i}(\mu[\frac{\partial u_i}{\partial x_i} + \frac{\partial u_j}{\partial x_i}]) - \frac{\partial p}{\partial x_i} + \rho g_j + F_j \qquad [2]$$

Where: μ is the viscosity of the gas
p is the pressure
g_j is the body forces (i.e. gravity)
F_j is the momentum exchange from second phase

In order to determine the gas flow field, the velocities in each of the three coordinate directions and the pressure are calculated.

If the flow is turbulent then time averaged velocities must be used and a turbulence model applied in order to obtain effective viscosities, conductivities and diffusivities. The approach used in FLUENT is to calculate the effective viscosity, which is the sum of the molecular viscosity and the turbulent viscosity. Diffusivities and conductivities are then found by use of the Prandtl and Schmidt numbers. The turbulent viscosity is determined from the k-ϵ model of turbulence. A set of four equations is used, these equations must be solved iteratively, due to coupling between the variables. k is the turbulent kinetic energy and ϵ is the kinetic energy dissipation rate.

Transport equation for k:

$$\frac{\partial}{\partial x_i}(\rho u_i k) = \frac{\partial}{\partial x_i}\left[\frac{\mu}{\sigma_k}\frac{\partial k}{\partial x_i}\right] + G_k - \rho\epsilon \qquad [3]$$

Transport equation for ϵ:

$$\frac{\partial}{\partial x_i}(\rho u_i \epsilon) = \frac{\partial}{\partial x_i}\left[\frac{\mu}{\sigma_\epsilon}\frac{\partial \epsilon}{\partial x_i}\right] + C_1\frac{\epsilon}{k}G_k - C_2\rho\frac{\epsilon^2}{k} \qquad [4]$$

The generation term of k is G_k and is defined as follows:

$$G_k = \mu_t\left(\frac{\partial u_j}{\partial x_i} + \frac{\partial u_i}{\partial x_j}\right)\frac{\partial u_j}{\partial x_i} \qquad [5]$$

The turbulent viscosity is then found from the following relationship:

$$\mu_t = C_\mu \frac{k^2}{\epsilon} \qquad [6]$$

The values of the constants in the k-ϵ equations are obtained by correlation with experimental data. The optimal values and the default used in FLUENT are[43]:

$$C_1 = 1.44,\ C_2 = 1.92,\ C_\mu = 0.09,\ \sigma_k = 1.0,\ \sigma_\epsilon = 1.3$$

When turbulent flow is modelled, the viscosity term appearing in an equation is replaced by the effective viscosity which is the sum of the turbulent viscosity μ_t and the laminar viscosity.

If temperature effects are included in a gas flow, then the enthalpy of each cell must be determined using the following equation for enthalpy:

$$\frac{\partial}{\partial x_i}(\rho u_i h) = \frac{\partial}{\partial x_i}\left[\frac{\mu}{\sigma_h}\frac{\partial h}{\partial x_i}\right] + S_h \qquad [7]$$

Where: S_h is a source term of enthalpy, and includes heat of reaction, radiation, and any interphase transport;
h is enthalpy;
σ_h is the turbulent Prandtl number for enthalpy;
μ is the viscosity.

Enthalpy is related to temperature through the specific heat capacity; a 0K reference temperature is used. The gas phase does not condense, thus the enthalpy of phase transition is not considered:

$$\text{grad } h = C_p(\text{grad } T) \qquad [8]$$

Where: C_p is the temperature dependent specific heat capacity.

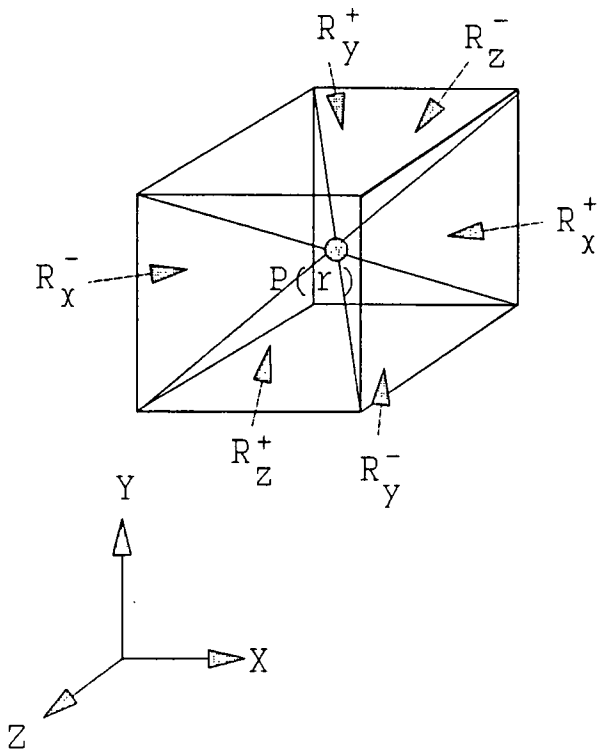

Figure 6 - Schematic of Six-Flux Radiation Model

The radiation fluxes are determined from a six flux radiation model, one flux in each of the positive and negative coordinate directions[22]. In a finite difference solution these fluxes are found for each cell and the net flux in a coordinate direction is solved for; this is equal to the flux in the positive coordinate direction minus the flux in the negative direction (see Figure 6):

$$\frac{d}{dx_i}\left[\left(\frac{1}{\alpha+s}\right)\frac{dR_i}{dx_i}\right] = \alpha(R_i - E) + \frac{s}{3}(2R_i - R_j - R_k) \qquad [9]$$

Where: R_i are the radiative heat fluxes;
E is the black body emissive power ($= \sigma T^4$);
α is the absorption coefficient;
s is the scattering coefficient;
i is the coordinate direction.

The enthalpy source term due to radiation is:

$$S_{rad} = 2\alpha[(R_x\text{-}E) + (R_y\text{-}E) + (R_z\text{-}E)] \qquad [10]$$

If chemical species calculations are to be performed, then the following equation must be solved for each species:

$$\frac{\partial}{\partial x_i}(\rho u_i f) = \frac{\partial}{\partial x_i}\left[\frac{\mu}{\sigma_f}\frac{\partial f}{\partial x_i}\right] + R_f + S_f \qquad [11]$$

Where: f is the mass fraction of the chemical species;
R_f is the mass rate of depletion/creation of the chemical species;
S_f is the mass rate of transfer from the second phase;
σ_f is the Prandtl number for the species.

The reaction model built into FLUENT allows for the reaction of a fuel with an oxidant, to form an oxidized product, three species in total.

The rate of chemical reaction is controlled by either the kinetic reaction rate, or by the degree of turbulent mixing. The reaction rate due to turbulent mixing R_f is given by the smaller of the following three equations (one for each reactant and one for the product):

$$R_f = -A\rho\frac{\epsilon}{k}m_f, \qquad R_f = -A\rho\frac{\epsilon}{k}m_o/S, \qquad R_f = \frac{A\rho\epsilon m_{prod}}{2\,k(1+S)} \qquad [12]$$

Where: S is the stoichiometric requirement of the oxidant species with the fuel species;
A is a constant, usually set to 4;
m_f is the mass fraction of fuel;
m_o is the mass fraction of oxidant;
m_{prod} is the mass fraction of the product species.

The smallest R_f is then compared to the kinetic reaction rate, and the smallest of these two quantities is then designated as the reaction rate. The heat of this reaction is added to the source term for enthalpy

The density of the flow is calculated from the ideal gas law, as follows:

$$\rho = \frac{P}{RT} \sum_j \frac{m_j}{M_j} \qquad [13]$$

Where: M_j is the molecular weight of species j;
m_j is the mass fraction of species j;
R is the gas constant.

Second Phase (Black Liquor) Equations

The existing model of the second phase was not applicable to black liquor

Bed Equations

No bed model existed in FLUENT.

Solution Technique

An important aspect of the theoretical description of FLUENT is a characterization of the solution technique. A system of partial differential equations as complex as those in FLUENT require special techniques, in order to obtain a converged solution. The first step is to rearrange the partial differential equations describing conservation of mass, momentum, energy, and chemical species, into a general form:

$$\frac{\partial}{\partial x_i} (\rho u_i \phi) = \frac{\partial}{\partial x_i} [\Gamma_\phi \frac{\partial \phi}{\partial x_i}] + S_\phi \qquad [14]$$

The left side of the equation is the convective portion of the transport equation, the first term on the right side is the diffusion term, and the second is the source term. Γ_ϕ is the diffusion coefficient for the process being considered. ϕ is used to represent a general variable (e.g. pressure).

The flow region is divided up into computational cells, by the use of lines in all three coordinate directions, as shown in Figure 7. The finite difference form of the equation is obtained by integrating this general equation over a computational cell. A nodal point is defined at the center of the computational cells; all physical properties and flow variables are calculated and stored at this location, with the exception of velocity. The velocities are calculated halfway between the nodal points (i.e. the upward velocity would be calculated at a point midway between a node and the node directly above it), in what is usually referred to as a "staggered grid"; this is done in order to promote computational stability.

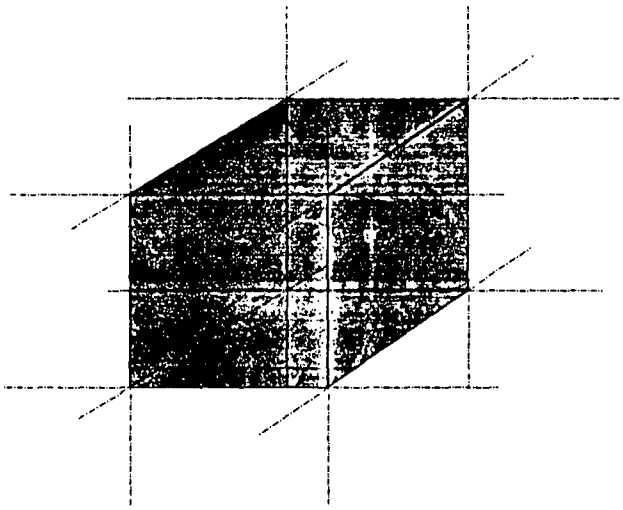

Figure 7 - Schematic of a Computational Cell

Once the integration procedure has been performed, the differential equations reduce to algebraic equations, as follows:

$$\phi_p \sum_i (a_i - S_p) = \sum_i a_i \phi_i - S_c \qquad [15]$$

Where: a_i is the finite difference coefficient;
i is N,S,E,W,U,D (north, south, east, west, up, down);
$S_\phi = S_c + S_p\phi_p$, where S_ϕ is the source of ϕ in cell p
thus the source of ϕ is expressed as a function of ϕ;

The summation of the terms in equation [15] occurs over all neighbor cells (six in a 3-D case). The subscript P refers to the current cell. This equation must be solved for all computational cells in the flow region. The convective and diffusive fluxes are contained in the coefficient a, which will vary depending on the quantity being considered (i.e. mass, momentum, energy, or chemical species).

The source of a flow quantity (i.e. S_ϕ) must be expressed as a linear function of the flow variable of which it is a source (i.e. ϕ_p). The resulting linear expression can be written as $S_\phi = S_c + S_p\phi_p$. This is necessary as non-linearities cannot be handled in the solution techniques used. Additionally, S_c must always be positive and S_p always negative in order to ensure convergence.

The "power law relationship" is used to interpolate between nodal values, and to calculate derivatives. This relationship is recommended by Patankar as it provides an accurate description of the variation in flow properties as a function of the Peclet number, with a minimum of computational effort.[27] Reducing the computational effort is important as this calculation will be performed six times for each variable at each nodal point. The power law relationship dictates the way in which neighboring cells affect the central cell. The influence of the neighbor cells is a function of the Peclet number:

$$P_e = \frac{\rho u L}{\Gamma} \qquad [16]$$

Where: L is the distance between the central node and the neighbor cell being considered;
Γ is the diffusion coefficient of the quantity being calculated.

This relationship can be rewritten as:

$$P_e = \frac{F}{D} \qquad [17]$$

Where: $F = \rho u A_f$
$D = \Gamma A_f / \delta x$
A_f is area of the cell face perpendicular to the direction of flow.

As an example, the power law relationship for the east neighbor (the adjacent cell in the positive X direction) as a function of Peclet number is given. D_e represents D for the east neighbor, and a_E is the finite difference coefficient for the east neighbor. A_f for the east cell would be $\Delta y \Delta z$. This technique is used to calculate a value of a_E (or a_i in general) as a function of the Peclet number in that cell:

For $P_e < -10$,

$$\frac{a_E}{D_e} = -P_e \qquad [18]$$

For $-10 \leq P_e < 0$,

$$\frac{a_E}{D_e} = (1 + 0.1P_e)^5 - P_e \qquad [19]$$

For $0 \leq P_e \leq 10$,

$$\frac{a_E}{D_e} = (1 - 0.1P_e)^5 \qquad [20]$$

For $P_e > 10$,

$$\frac{a_E}{D_e} = 0 \qquad [21]$$

The right side of the above equations is designated as $A(|P_e|)$. For example, suppose the Peclet number in a cell is -2, then $a_E = 0.83D_e$. This accounts for the diffusion flux. The convective flux is accounted for by adding the maximum of $-F_e$ or 0 (implying that convective transport F_e is only important if flow is from the east cell to the cell being considered) to a_E. Expressed in mathematical form:

$$a_E = D_e \bullet A(|P_e|) + \max\{-F_e, 0\} \qquad [22]$$

Equivalent expressions can be obtained for a_W, a_N, a_S, a_U, a_D.

The boundary conditions must be specified at all boundaries, due to the nature of the differential equations being solved. Boundary conditions at outlets are calculated by FLUENT, using overall continuity and assuming that the flow is fully developed at the outlet (i.e. no gradients in flow variables).

The solution proceeds by a semi-implicit scheme, starting with the boundary conditions, and an arbitrary internal flow field. A final converged solution is reached by successive iterations. The steps involved in a single iteration are:

1. The u, v, w momentum equations are solved with an assumed pressure field;

2. The pressure is then adjusted so that continuity is satisfied. This adjustment is made by solving a correction equation that is based on the continuity equation and a linearized form of the momentum equations;

3. The turbulence model is then determined by solving the differential equations for k and ϵ, which results in an updated viscosity field;

4. The auxiliary equations that govern the distribution of enthalpy, radiation, and chemical species are then solved using the updated values of the previously determined variables;

5. If the second phase is present, then a second phase calculation is performed. The generated source and sink terms are used to adjust the appropriate flow variables (this may not be done every iteration).

Iterations are performed until the flow variables change by less than a predetermined amount. Usually, in order to prevent unsteady and divergent behavior of the solution scheme, it is necessary to underrelax the flow variables. When a variable is underrelaxed, the newly determined value of the flow

variable is buffered by the previous value. Only about 20% of the implied change in the variable is normally applied.

Published Applications Of FLUENT

The FLUENT code has been used on a number of simulations similar to the kraft recovery furnace, including 1. Numerical Simulation of Flow and Combustion Phenomena in a Power Plant Boiler;[28] 2. Spray Combustor Modelling;[29] 3. Numerical Correlation of Gas Turbine Combustor Ignition.[30]

In addition, the FLUENT code has been used in a number of well known benchmark simulations, including the driven cavity flow and flow through a rectangular duct. Good agreement was found between the results of these benchmark cases and experimental results. The code changes discussed later in this thesis do not effect the validity of these benchmark tests as the calculation of pressure and the three velocity components are not modified.

Limitations Of Existing FLUENT Code

Although FLUENT was our choice as program for simulation of the kraft recovery boiler, it still has a number of limitations. This section will discuss these limitations.

Insufficient Species Available

The original FLUENT code solved for only three species (F,O,C). Species F is the fuel; species O is the oxidant; and species C is the combusted product. More species were required in order to realistically model the processes taking place in the recovery boiler.

Combustion Model

The combustion model in the original code assumed that the fuel reacted with the oxidant to form a combusted product. Incomplete combustion was not modelled, nor was a distinction made between carbon dioxide and water as the product of complete combustion.

Second Phase Model

The second phase model that was originally in FLUENT was not appropriate for black liquor. The main deficiencies that existed in the original code: 1. Evaporated water was given the same physical properties as combusted gases; 2. A description of the process of reoxidation of the entrained smelt drop was not possible; 3. Only 100 drops could be described, this description was severely limited; 4. A description of the phenomenon of wall drying was not possible; 5. Only one event (i.e drying, pyrolysis, char burning, or reoxidation), could take place for a given drop in a given cell; 6. The mass balance on the drop did not converge; and 7. It was not possible to describe wet drops if a description of all the other combustion events was desired.

Bed Burning

No allowance whatsoever was made for bed burning in the original FLUENT code, this section was developed entirely from scratch by Dan Sumnicht. The bed burning model required wall cells that could exchange mass; in addition, the temperature of these cells must be calculated rather than specified. Wall cells of this type were not available in the FLUENT code.

Output Capabilities

The existing output capabilities of the code were limited by the unavailability of a device driver, and by the inadequate facilities for viewing the cell-by-cell values of the flow variables. A device driver is a software package that performs simple plotting routines on an output device. The VR290 terminal we

were using is new; CREARE had yet to include a color device driver for it in the FLUENT program. We were able to generate only black and white plots on the screen with the FLUENT code as received.

Mass and Energy Balances

The mass balance is satisfied at all times by the code, but this was not explicitly shown by the program. A global energy balance was not calculated; this reduces a user's confidence in the degree of convergence and the accuracy of the code.

DEVELOPMENT OF FLUENT/RFM

The limitations of FLUENT discussed earlier were addressed by developing a new CFD code named FLUENT/RFM (Recovery Furnace Model). Development of this code involved revising the FLUENT source code and the generation of original code. Care was taken to ensure that all modifications were error-free, this was accomplished by double and triple checking between the three students working on the model. Many subroutines had to be revised in order to make the desired changes. The structure of FLUENT/RFM and how it is related to FLUENT is shown in Figure 8. It is important to note that the solver was not modified nor were the velocity and turbulent calculations altered. Thus, the validations discussed on Page 48 still apply.

All computer code was written in VAX FORTRAN. This section will discuss the code changes that were made, starting with a detailed description of the changes made by this author, followed by a brief summary of the changes made by the other two students involved in this project. More detail on the changes made by Allan Walsh and Dan Sumnicht can be found in their theses.

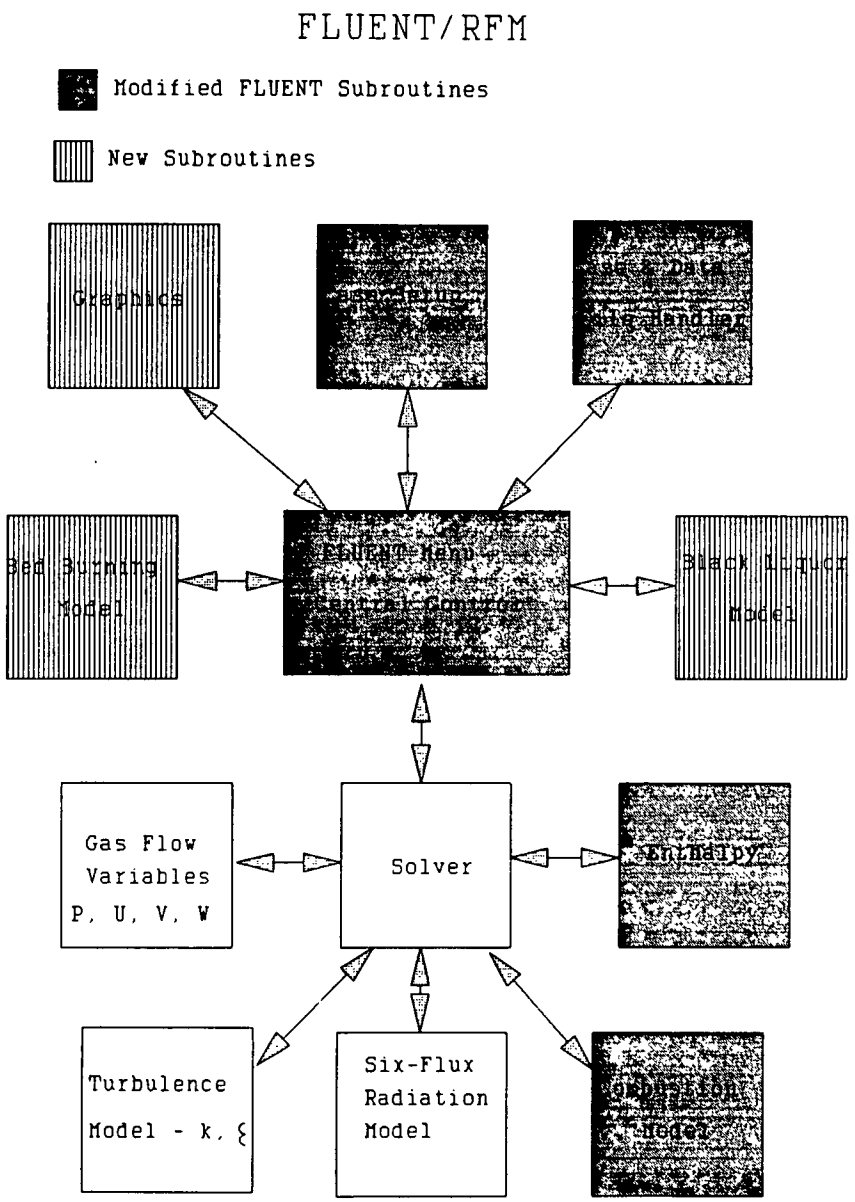

Figure 8 - Structure of FLUENT/RFM

Modified Combustion Model

The reasons for altering the combustion model found in FLUENT were discussed earlier. The main changes that were made were to allow for partial combustion, and to specify the relative mass fractions of the products of combustion. The fuel in a recovery furnace is the pyrolysis gas produced during the pyrolysis stage of black liquor combustion. The combustion of fuel was described by the following equation (note: equations written on a mass basis):

$$\text{Fuel} + S \bullet O_2 \Rightarrow (1+S)F_{CO} \bullet CO + (1+S)F_{CO2} \bullet CO_2 + (1+S)F_{H2O} \bullet H_2O \qquad [23]$$

Where: Fuel is pyrolysis gas in FLUENT/RFM;
S is the stoichiometric requirement of O_2 for complete combustion of the fuel;
F_{CO} is the mass fraction of CO formed;
F_{CO2} is the mass fraction of CO_2 formed;
F_{H2O} is the mass fraction of H_2O formed.

The fraction of each combustion product formed depends on the chemical composition assumed for the fuel, and on an assumed extent of combustion. All hydrogen forms water; this determines the amount of water formed. The CO/CO_2 ratio as specified by the user along with the amount of carbon in the fuel will then determine the amount of CO and CO_2 formed, along with the total O_2 requirement.

The second reaction that must be considered is the combustion of CO to form CO_2. The following reaction scheme (mass basis) was used:

$$CO + Q \bullet O_2 \Rightarrow (1+Q) \bullet CO_2 \qquad [24]$$

Where: Q is the stoichiometric requirement of O_2 for complete combustion of CO, (Q=0.571, (16g of O_2/28g of CO));

The combustion that takes place in the recovery furnace will usually involve a diffusion flame, rather than a pre-mixed flame. This allows us to make the assumption that all gas phase burning will be controlled by turbulent diffusion, rather than by kinetics. The assumption that the kinetics are fast has been made; in essence, this means that if fuel and oxidant meet then they will burn. The intensity of turbulence is used as a measure of the degree of mixing; the governing equations were discussed in the description of FLUENT presented earlier.

The amount of combustion occurring as a function of position in the furnace was added to the list of variables that could be viewed. The parameters describing both of these reactions can be specified in the S1 (setup phase 1) subroutine. Care must be taken by the users to ensure that the heat of reaction is consistent with the product mix specified. For example; if the $CO:(CO_2+CO)$ ratio is assumed to be 0.0 then the reaction shown in equation [23] will be more energetic than if the ratio was 1.0. The pre-exponential constant in the Arrhenius equation kinetic rate is made arbitrarily large, and the activation energy is set to zero, resulting in a very large rate, indicating control by turbulent mixing.

Additional Species

In order to use a more advanced combustion model is was necessary to add two new species, and to modify species C. The two species added were CO (Q), and H_2O (B). In order to add these two species the following source code changes were necessary:

1. Two new subroutines were added, QCALC and BCALC; these subroutines are used to update the values of these new species in each live cell of the flow field. They were copied from the existing subroutines OCALC, CCALC, and FCALC which were in the original FLUENT code.

2. The other subroutines used to calculate mass fraction of F, C, and O throughout the flow field were revised represent the new reaction schemes. Species C previously represented a generic combustion product; it was modified to represent CO_2;

3. Arrays for the new species were added to the common block, along with any parameters that described the behavior of these species (i.e. Prandtl number, heat capacity, molecular weight);

4. The newly declared variables associated with the new species were initialized, added to the subroutines that read and write the case and data files, added to the S1 subroutine so that they could be adjusted by the user, and were added to the list of variables that could be displayed if appropriate.

Newly developed source code appears in Appendix 3. Additional source code cannot be included due to copyright limitations.

Source and Sink Terms

Source and sink terms are used to transfer mass, energy, or momentum between the second phase (and the bed in FLUENT/RFM), and the gas phase. Due to the addition of the new species, and the addition of the bed, it was necessary to define three new arrays used for transferring mass between the second phase and the gas. One specially defined array is used for transferring mass and energy between the bed and the gas phase; this is discussed later.

The three new arrays created to handle the source of mass in the gas phase, from the second phase, were WMASEX, QMASEX, and OMASEX. WMASEX is used to record the amount of evaporation that takes place in a given cell; this quantity will increase the mass fraction of B in a cell. QMASEX is an array that keeps track of the amount of CO released in a cell; this quantity will increase the mass fraction of Q in a cell. OMASEX is used to record the amount of reoxidation that takes place in a cell. Reoxidation is the process by which Na_2S in a burned-out drop oxidizes to Na_2SO_4. Reoxidation reduces the oxygen mass fraction in a gas cell; in addition, this array is used to measure the amount of oxygen reaching the bed due to oxidized drops landing on the bed. Equation [11] is reproduced in order to show how the source term enters the calculation of mass fraction for a species. S_f is the source of species f in a given cell; for example, if the mass fraction of oxygen is being calculated then S_o

would equal OMASEX, the sink of oxygen due to smelt reoxidation. The source terms enter into the momentum and enthalpy calculations in the same manner.

$$\frac{\partial}{\partial x_i}(\rho u_i f) = \frac{\partial}{\partial x_i}\left[\frac{\mu}{\sigma_f}\frac{\partial f}{\partial x_i}\right] + R_f + S_f \qquad [11]$$

Where: f is the mass fraction of the chemical species;
R_f is the mass rate of depletion/creation of the chemical species;
S_f is the mass rate of transfer from the second phase;
σ_f is the Prandtl number for the species.

BEDCEL is the array used to transfer mass between the bed and the gas phase. This array is used to store a number of quantities in a given cell; this is accomplished by dividing up the array into small sections. Only a small fraction of the cells in the furnace are bed cells, thus only a small part of the BEDCEL array will be filled by a given variable. The quantities passed by this array to the gas phase are source of CO, source of CO_2, and a sink of O_2.

Species Dependent Heat Capacity

The existing FLUENT code calculated the heat capacity for an individual cell as a function of temperature only. If large amounts of water vapor are present, then this can lead to an overestimate of the actual temperature of a cell. The heat capacity of water vapor is substantially higher than that of the other high concentration gas species found in a recovery furnace.

The heat capacity for an individual cell is obtained by a summation of the heat capacity of each of the species present in that cell. Each of these individual heat capacities is found as a function of temperature. The species considered are H_2O, N_2, CO, CO_2, O_2, and pyrolysis gas. A simple linear model was used to determine the heat capacity of each species as a function of temperature. The equation used to calculate heat capacity was as follows:

$$C_p(I,J,K) = \Sigma \{m_i(I,J,K) \bullet [A_i + B_i \bullet T(I,J,K)]\} \qquad [25]$$

Where: $C_p(I,J,K)$ = the heat capacity for any cell;
$T(I,J,K)$ = the temperature of that cell;
$m_i(I,J,K)$ = the mass fraction of species i in the cell;
A_i = the intercept describing the heat capacity vs T;
B_i = the slope describing the heat capacity vs T;
i = CO, CO_2, N_2, H_2O, O_2, Fuel

Mass and Energy Balance

The original FLUENT code ensured that overall mass continuity was satisfied at all times. This was accomplished by performing a mass balance over the entire furnace, and then adjusting the exit velocity of the gas. The source code that was written showed this balance being satisfied, giving the user more confidence in the code. Serious errors in the simulation are present if the overall mass balance is not satisfied.

The next code addition was the inclusion an inert mass balance. The utility of this balance is in measuring the degree of convergence of a case. When a case is first set up, all the gas exiting the furnace is assumed to be inert. As the solution is developed by iterating the starting case, the species propagate through the furnace and eventually reach the exit. The inert mass balance will initially start at about 140-150%; at convergence, it should be equal to exactly 100%.

Expressed in mathematical form the inert balance is as follows:

$$I_{bal} = I_{out} \bullet 100/I_{in} \qquad [26]$$

Where: $I_{out} = M_{out} \bullet (1 - \Sigma m_i)$;
$I_{in} = M_{in} \bullet (1 - .231)$;
M_{out} is the mass of gas exiting the furnace;
M_{in} is the mass of gas entering the furnace;
m_i is the mass fraction of species i.

The energy balance was constructed for the same reason as the mass balance: to measure the approach to convergence, and to give the user assurance that the code is correct and the case specified appropriately. The elements of the energy balance are as follows:

1. Incoming Black Liquor - The sensible heat (273K reference) and heating value of the black liquor is calculated and included in the incoming energy; note that the latent heat of water is subtracted from the heating value;

2. Incoming Air - The incoming air sensible heat (273K reference) is calculated and added to the incoming energy;

3. Bed shrinkage - Some bed cells may be losing mass due to char burning in excess of the mass of char landing in that cell. The sensible heat and heat of combustion of the char are considered an energy input to the furnace. This is not double counting as any char or inorganic material reaching the bed is considered to have exited the boundaries of the model;

4. Exit Flue Gas - the sensible heat of the outgoing flue gas is added to the outgoing energy;

5. Carryover - the carryover that exits the furnace is added to the outgoing energy, both sensible heat, and heat of combustion remaining in the unburnt carbon;

6. Incompletely Combusted Gas - the incompletely combusted gases that exit the furnace (fuel and carbon dioxide) have their heat of combustion added to the outgoing energy;

7. Heat To Walls - the heat to the walls, both convective and radiative, is added to the outgoing energy, along with the radiation that goes out through the outlet of the furnace. The amount of heat necessary to evaporate the water in wet drops that reach the wall is subtracted from the heat to the walls;

8. Carbon Reaching Bed - the total carbon reaching the bed is calculated; the sensible heat and heat of combustion of this carbon is assumed to exit the control volume;

9. Inorganics Reaching Bed - the sensible heat of the inorganic materials reaching the bed is calculated and added to the total energy exiting the furnace.

The outgoing and incoming energy are then compared to determine the closure of the energy balance. If energy is being destroyed then the energy balance will be less than 100%, if energy is being created, then the energy balance will be greater than 100%. At the time a case is first started, the energy balance will be much less than 100%, as all energy is entering the furnace, but has not yet propagated through the furnace. At convergence the energy balance should be within a few percent of 100%. Exactly 100% closure is not possible as the temperature of the black liquor that reaches the bed or exits through the outlet is not available to the energy balance subroutine.

Black Liquor Trajectory and Combustion

The source code developed in order to model the black liquor trajectory and combustion calculations are documented in detail in Allan Walsh's thesis.[31] The technique used to determine the influence of the drop on the gas phase is the PSI-CELL approach described earlier. The black liquor model generates a number of source terms that enter into the gas phase mass, momentum, and energy equations as indicated in the section on the theoretical aspects of FLUENT.

Bed Calculations

The source code that was generated in order to model the bed involved the creation of a new type of cell, the bed cell. Bed cells behave like wall cells by acting as a barrier to flow, but unlike normal wall cells they can exchange mass and energy (normal wall cells exchange only energy). The bed is a sink of oxygen, which is obtained from the combustion air and from reoxidized smelt drops that land on the bed. The reactions that take place on the surface of the bed are assumed to follow the sulfate-sulfide cycle; thus, the burning of carbon is controlled by oxygen mass transfer to the bed. The reduction of sodium sulphate is kinetically controlled. Experimental work performed by Sumnicht established the parameters for the description of the kinetic rate of oxygen depletion (k_r) and combined this with an oxygen mass transfer model (k_m) to obtain the rate of oxygen depletion by the bed which is used in the bed burning model of FLUENT/RFM.[32]

$$S_{O2} = k_t \bullet Area \bullet [O_2] \qquad [27]$$

Where S_{O2} is the sink of oxygen due to bed burning;
$k_t = 1/k_r + 1/k_m$;
$k_m = D/d_m \bullet (2.0 + 0.6Re^{0.5}Sc^{0.33})$;
$k_r = 2.36 \bullet T \bullet Exp(-11022/T)$;
D is the diffusion coefficient of O_2;
d_m is the effective diameter of the char (=1.0);
T is temperature;
Re is the Reynolds number;
Sc is the Schmidt number.

Additional variables were added to the model to allow transfer of chemical species between the bed and those live cells adjacent to the bed. The temperature of the bed cells is determined by an enthalpy balance over the cell. The bed processes can be viewed using the graphic routines in FLUENT/RFM. Each time the bed model is called a short data file is written to disk, this file indicates average bed cell temperature, average oxygen concentration in cells adjacent to the bed cells, and net bed growth.

Output Viewing Facilities

The output viewing facilities were revised in order to assist in the interpretation of the results obtained. Two new device drivers were written, one for a VR290 terminal (written by Allan Walsh), and a second written for the HP 7475A plotter (written by the author of this thesis). The VR290 device driver permits the display of a number of plots at the same time, with as many as 16 colors. The HP 7475A device driver allows up to four plots to be plotted on the same page by the HP plotter, using six colors. The "View Alphanumerics" subroutine present in FLUENT was adapted so that the cell-by-cell values of any variable could be viewed in all three coordinate directions and in any region of the furnace. Previously, it was only possible to view the variables on z-direction planes, and the range of cells displayed could only be changed by use of the Expert option.

All newly defined variables were added to the list of variables that can be displayed. In addition, bed profiles can be viewed; this option permits the display of all bed cells on a single plane, making it

easier to observe the behavior of the bed. Bed profiles of quantities such as the sink of oxygen, the temperature of the bed surface and the amount of carbon landing on each bed cell can be displayed.

USING FLUENT/RFM

FLUENT has its own operating system, which was adapted and used in FLUENT/RFM. The modifications were performed so that the additional features of FLUENT/RFM could be used. This operating system provides a hierarchy of menus where options can be chosen by specifying the first two letters of the desired option. The "menu-driven" operating system prevents the user from entering incorrect data; for example, when setting up a case it prevents live cells (cells were in which the finite volume equations will be solved) from being placed on the boundaries of the flow. This would cause errors when the case is solved. The main menu appears when FLUENT/RFM is first activated, then sub-menus appear depending on the choice made in the main menu. Figure 8 illustrates the structure of FLUENT/RFM.

The steps involved in setting-up, running, and viewing a recovery boiler simulation would be as follows:

1. Run the case setup module (S1 option in main menu);

2. Save the case (SC option);

3. Call the solver (C1 option), which in turn solves the gas flow variables, the turbulence model, the radiation model, the combustion model (species concentrations), and determines the enthalpy;

4. Periodically (about every 10 calls to the solver) perform a calculation using the bed burning model and the black liquor spray model and bed burning model (C2 option);

5. Once the simulation has converged save the data (SD option), and view the results (VG option).

This is a simplified description (for more detail see the users manual in Appendix 4), but it provides a framework for further description of FLUENT/RFM.

When setting up a case the user can choose from a number of different types of cells. Wall cells are used to define solid surfaces on the boundaries of the flow, or internal surfaces. Boundaries through which gas can flow are specified by the use of inlet or outlet cells; the conditions at the inlets must be specified while the conditions at the outlets are calculated by FLUENT/RFM based on mass continuity. Symmetry cells can be used to reduce the number of computational cells if planes of symmetry exist in the flow region. The computation of flow variables takes place in live cells.

TABLE 1 - Cell types, their properties and uses

Cell Type	Flow Variables Solved	Barrier To Flow	Boundary Conditions Imposed	Use
Live Cells	All	No	None	Describe region where flow variables are solved.
Wall Cells	None	Yes	Temperature, velocity, emissivity.	Provide barriers to flow.
Bed Cells	Temperature, sink of O_2, source of CO/CO_2.	Yes	Velocity, emissivity.	Describe the bed surface.
Outlet Cells	All	No	Velocity to satisfy mass balance.	Provide site for flow to exit.
Inlet Cells	None	Yes	Velocity, temperature species concentration	Used to designate inlets to flow region.
Symmetry Cells	All	Yes, perpend. to symmetry plane	Velocity perpend. to symmetry plane=0	Reduces computational effort if planes of symmetry exist.

CONVERGENCE OF A RECOVERY FURNACE SIMULATION

The convergence of a kraft recovery boiler simulation involves a number of stages of solution, along with careful manipulation of the underrelaxation parameters. All the variables cannot be turned on at once with any hope of getting a converged or even a stable result. The best method found for convergence of a simulation is as follows:

1. Start with a solution of just the pressure and the three velocities, all other variables are turned off. The default underrelaxation parameters of 0.1 for the velocities and 0.25 for the pressure appear to be the largest value that can be used. Perform about 25 to 30 iterations (C1 calculations);

2. Next turn on the calculation of k and ϵ with the default underrelaxation of 0.2 for both, ensuring that the turbulent boundary conditions have been set. Perform an additional 150-200 iterations, until the normalized residuals for U, V, and W are below about 0.05. This should establish a velocity field;

3. The next step is to turn on the enthalpy calculations (H); the underrelaxation parameter for all variables should be turned down to 0.01, with the exception of pressure which should be set at 0.025, and temperature which can be set at 0.05. Ensure that all properties for the walls have been set (temperature and emissivity), then patch in a temperature of 1250K everywhere (the term patching refers to the technique of specifying the value of a variable, rather than calculating its value, and is accomplished using the PA option in the main menu of FLUENT/RFM); an additional 20 to 30 iterations should now be executed;

4. Black liquor firing can now begin, after making sure that the black liquor properties and the spray properties have been specified. Patch in an oxygen mass fraction of 0.04 everywhere in the furnace; one exception is those cells below the primary air jets and around the perimeter of the bed (J=2), the oxygen mass fraction should be patched in at a very small amount (1E-04 works). Problems occur in these cells due to the presence of oxygen, carbon monoxide (from the bed), and high

turbulence levels; this creates excessive amounts of CO_2, unless low oxygen levels are used. In addition, values for C and Q must be patched; a mass fraction of 0.01 for both is appropriate. Set the underrelaxation parameter for the drop equal to 0.2, and perform a C2 (second phase) calculation for every ten C1 calculations. The first C1 iteration following the first C2 calculation may result in the message "Rapid Divergence - Abort" being printed, ignore this message and continue with another C1 calculation, it shouldn't happen again. Keep the underrelaxation coefficients at the same level for the next 50 iterations, then slowly increase them;

The underrelaxation parameters should never be increased above 0.1 for U, V, W, H, D, E and viscosity. The maximum value used for pressure is 0.25, for the species F, O, C, B, and Q, a value of 0.3 has been successfully used. A value of 0.3 for the particle droplet calculation should be used, any larger value results in unstable bed growth and carryover.

The sweep direction can be specified, this determines the planes over which calculations are performed (e.g. sweep direction 2 solves the flow variables over the X-Z planes). Each slice or plane in a given direction is solved 1 or more times then the next plane in the sweep direction is considered. Either a sweep direction of 1 or 2 works, direction 3 does not. It may be best to alternate between direction 1 and 2, although this has not been determined. The number of sweeps can also be specified, this indicates the number of times the values of flow variables over a plane are calculated before moving onto the next plane in the specified sweep direction. A large number of sweeps is useful in cases that are difficult to converge, although more sweeps require more computer time. The best results found were using 10 sweeps for pressure and 5 sweeps for all the other variables.

Observations:

1. It appears that a uniform temperature field cannot be patched in without inducing unstable behavior of the simulation, after patching a temperature field very low values of the relaxation coefficients must be used;

2. Increasing the underrelaxation parameters above the recommended level causes rapid divergence;

3. Make frequent backups of the data file, so that if a simulation begins to diverge the user can back up and start again;

4. Do not change the ratio of the pressure and the velocity underrelaxation parameters; a ratio of 2.5 : 1 seems to work best.

DETERMINATION OF CONVERGENCE

Convergence of a simulation can be determined by a number of methods, the most dependable of which appears to be average temperature. The average temperature is determined in the "heat flux by zone" calculation while in the main FLUENT/RFM menu. Once the temperature remains steady over about 100 calculations then one may be reasonable sure that the simulation is converged. Another way of determining convergence is by examining the closure of the inert mass balance, which approaches 100% from above. The normalized residuals of a simulation can be used as another means of determining convergence, although numerical problems with the simulation restrict how low these residuals can go. The final method is by observing some characteristics of the flow (e.g. a isovelocity plot) before and after a reasonable number of iterations (50-100), if no significant changes occur, then convergence is likely.

LIMITATIONS OF FLUENT/RFM

FLUENT/RFM is not the final word in kraft recovery furnace modelling. In the future, code development will have to be undertaken in order to include new experimental results. In addition, refinements can be made to the existing description of the processes taking place in the recovery furnace as described by FLUENT/RFM.

Our goal at the beginning of this project was to develop a model of the recovery furnace that eliminated empiricism as much as possible; a few empiricisms were included. Empiricism exists in the

treatment of black liquor that lands on the wall rather than the bed. Fifty percent by weight of the pyrolysis gas and all the water that reaches the wall is assumed to escape before the black liquor on the wall falls to the bed. In addition, the $CO\text{-}CO_2$ ratio during char combustion is a user defined parameter. The k-ϵ model is an empirical correlation and may not be valid in areas of high shear. The absorption coefficient of the gas is not well defined. The bed burning model uses an oxygen limited mass transfer model, the mass transfer coefficient in this model has not been accurately defined. In all these cases experimental data is necessary in order to remove the empiricism that currently exists.

SIMULATIONS PERFORMED USING FLUENT/RFM

In previous sections a justification for a three-dimensional model utilizing the most recent experimental data has been provided. In addition, a description of the model FLUENT/RFM, constructed partly as a component of this thesis and the theses of Sumnicht and Walsh has been furnished. The purpose of this section is to describe the results of applying the model to a number of simulations that use various portions of the complete FLUENT/RFM program.

The simulations that were performed were intended to answer a series of questions concerning the utility of fluid modelling as applied to the kraft recovery furnace. These questions, in increasing order of complexity:

1. Can the penetration of air jets into the furnace cavity be accurately reproduced, given a restriction on the total number of nodes used?;

2. Can the cold flow patterns (those flow patterns that result from the geometry of the furnace and the method of air introduction alone) in a kraft recovery furnace be accurately predicted by analytically modelling?;

3. Does the combustion model used in FLUENT/RFM give rational results?;

4. Can a furnace simulation including all the aspects of FLUENT/RFM be converged, and how much computer time is required?;

5. Do the results of a comprehensive furnace simulation give realistic results? (note that validation is not sought as experimental data for comparison is limited);

6. What is the difference between the flow patterns generated in the comprehensive simulation, and those found in a "cold flow" simulation? This has implications on the utility of cold flow modelling.

The simulations that were performed in order to answer these questions:

1. A simple model of jet penetration, with a variety of node spacings. The results are compared to theoretical values;

2. A cold flow model of a recovery furnace that was investigated previously by other researchers using experimental scale modelling;

3. A series of simulations using a simple geometry that investigated the effect of a number of parameters on the combustion of pyrolysis gas;

4. A simulation of a representative recovery furnace, hereafter called the "Base Case". Two simulations were performed using this furnace: a flow in which the effect of black liquor burning is simply represented as a bulk average temperature, and a second where black liquor influences are simulated by the inclusion of Walsh's black liquor model and Sumnicht's bed burning model;

These simulations will be described in the order they were introduced above: explanations for the behavior observed will be given, and the questions posed at the start of this section will be addressed.

JET PENETRATION - COMPUTATIONAL AND THEORETICAL COMPARISON

One question that had to be resolved was: "Is the penetration of the jets in the model consistent with those expected theoretically?". The importance of this question lies in the relationship between jet penetration and the breakup of the core of high velocity gas found in the center of the furnace[33]. If the penetration distances are grossly over- or underestimated, then erroneous conclusions could be drawn. The variable that affects the accuracy of the jet model is the node spacing, both in the direction of flow and the directions normal to the direction of flow. The purpose of this investigation was to determine if the node spacing used in the recovery furnace model was effective in predicting accurate behavior of the jets.

Computer Simulation

A simple square jet was modelled entering a stagnant volume of air, all temperatures were kept at the default value of 273K. The velocity of the jet was set at 10 meters per second. A free jet was modelled by specifying one boundary of the flow region as a wall, and all the other boundaries as outlets (see Figure 9). The flow region was made large enough so that the jet could develop and decay before reaching the boundary of the flow (10 meters in each coordinate direction was used). Three cases were examined. In each case a Reynolds number of 73,000 was used, corresponding to fully turbulent flow. A total of 1000 cells were used in all three cases, 10 in each coordinate direction. Three nodes are used to describe the air port in each case, one at the midpoint of the jet and two nodes 0.1 meters either side of the central node.

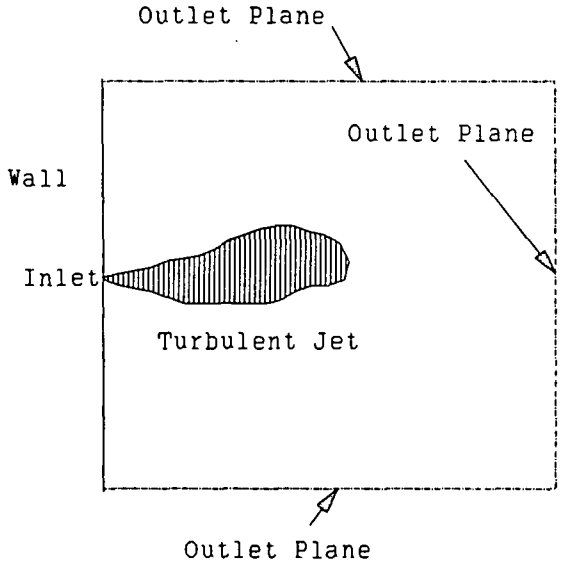

Figure 9 - Outline of Case Used to Test Jet Penetration

Case 1: Poor Node Spacing - The node spacing in the directions perpendicular to the direction of the jet were made deliberately poor; this was done by moving only the three nodes used to describe the air port.

Case 2: Good node spacing - The node spacing in the directions perpendicular to the jet were made as good as possible working with the 10 nodes available. Once the air port was described, the nodes adjacent to those used to describe the air port were moved so that the spacing between adjacent nodes increased as slowly as possible. The distance to be covered, and the total of ten nodes, constrained how gradual this increase could be.

Case 3: Node spacing used - The node spacing used was the same as that which was to be used in the recovery furnace model.

The computational cases required approximately 500 iterations to converge, the cases were deemed converged when the obtained velocities remained constant.

Theoretical Data

The theoretical results used for comparison were obtained from an article by Terry Adams in the 1988 Kraft Recovery Operations Seminar.[33]

Comparison of Theoretical and Computational Cases

A summary of the results of the computational and experimental cases is presented in Figure 10. The results demonstrate that node spacing in the directions perpendicular to the jet has a dramatic effect on the predicted penetration distance of the jet. The "poor node spacing" case significantly overpredicts the velocity of the jet at all locations. The "good node spacing" and "node spacing used" cases overpredict the jet velocity near the inlet, but are in good agreement as the jet penetrates deeper into the furnace. The "good node spacing" is slightly better than the "node spacing used" case.

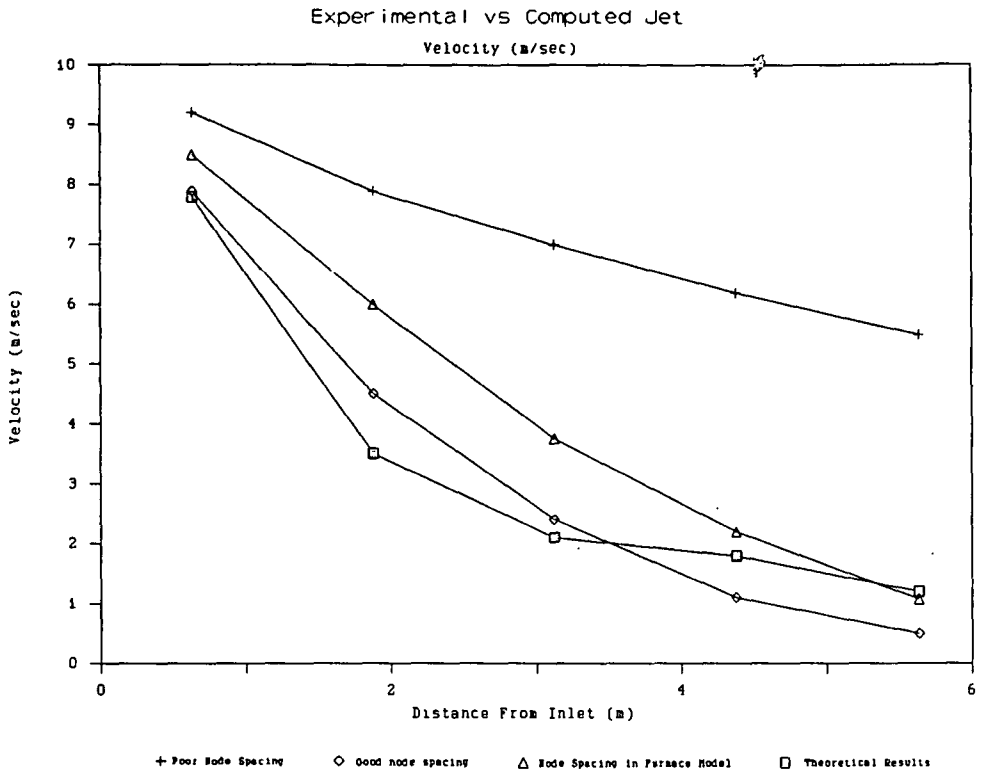

Figure 10 - Penetration of Turbulent Jets

This behavior is due to the reduced amount of entrainment of the jet that occurs when widely spaced nodes are used. The nodes describing the jet are unable to transfer momentum to the nodes located adjacent to the jet. The result is a jet that penetrates further than it should.

Conclusions

1. The importance of the node spacing perpendicular to a jet entering a furnace has been demonstrated. The spacing of the nodes adjacent to the inlet must be moved closer to the inlet in order to get an accurate description of jet entrainment and penetration. The node spacing along the

jet is not as important as the description of the inlet does not require moving nodal lines in this direction;

2. The node spacing used in the recovery furnace model should not lead to a significant error in predicting jet penetration despite the overestimate of jet velocity near the air port openings. The velocities of the jet predicted by the recovery furnace model overpredict the velocities by about 40% close to the inlets, while the velocities towards the middle of the furnace are accurate within about ±10%;

3. The limitation in the total number of computational cells (50,000) leads to an overprediction of the velocities near the inlets. The "good node spacing" used in this investigation would only be possible with two to three times the total number of computational cells.

THE COLD FLOW MODEL

The decision to simulate "cold flow" in the kraft recovery furnace was based on the following considerations:

1. Experimental work performed by B&W on a scale model of the Deridder furnace would serve as a comparison and a verification of the flows obtained analytically;[34]

2. Solving for the gas flows without including temperature effects and the influence of black liquor firing is a logical first step in the construction of a comprehensive model. From a standpoint of numerical stability, it is desirable to partially converge the gas flows before introducing thermal behavior;

3. None of the added features in FLUENT/RFM were used during this work. Familiarity with the original FLUENT source code was gained, along with confidence that a stable starting point for future code development existed.

The results of the cold flow modelling are presented in full in Appendix 1 in the form of a paper presented by this author at the 1988 TAPPI Engineering Conference. This section provides a summary of the paper.

Summary

A "cold flow" is the gas pattern that derives directly from the method of air introduction and furnace geometry, without complications from combustion, temperature distributions, and spray interactions. A three-dimensional description of the recovery furnace with 50,000 computational cells was used. Bilateral symmetry of the furnace was assumed to reduce the computational effort by a factor of two. The results of the computational model are compared with experimental data obtained on a 1/8th scale model of a recovery furnace.[34]

The main features of the contour plots of the T1 (lower traverse) are the upflow region in the center of the furnace and the downflow regions around the outside. The computational T1 traverse for both cases 1 and 2 show good agreement with the experimental results with respect to the general flow patterns, with the location of downflow regions and the maximum upward velocity corresponding to the experimental results. The average upward velocity is about 30% higher in the experimental case than in the computational cases. This is due to the use of a staggered bed, the air jets tend to be deflected upwards rather than following the surface of the bed. This reduces the intensity of the central core, as some of the gas is deflected upwards before it reaches the center of the furnace.

The velocities are highest in the center as all the secondary jets meet at this point and are forced to move upwards. The downflow regions around the perimeter of the furnace are created due to entrainment of gas by the secondary jets.

At the T2 traverse, a horizontal slice located above the tertiary jets, the velocity contours obtained experimentally have taken on a much different appearance. At the back of the furnace a region of recirculation is present. At the front of the furnace the upward velocities are large. The back of the furnace contains a large stagnant region, resulting in poor use of the furnace volume for combustion of the flue gases.

At the T2 traverse in case 1 the existence of a the large stagnant region seen experimentally is confirmed using FLUENT. The location of the maximum upward velocity is at the front wall in both cases. The average upward velocity in the experimental case is 1.50 m/sec, compared to 0.83 m/sec in the computational case. This is once again due to the numerical problems discussed earlier, persisting up to the T2 traverse.

Case 2 has much higher velocity tertiaries, which results in a better utilization of the furnace volume. The stagnant region at the back of the furnace has been eliminated.

The experimental T2 traverse in case 2 has no downflow, the computational results have only small areas of downflow against the side walls. The average upward velocity found experimentally and computationally are both 0.80 m/sec. The numerical problems are no longer a factor as the center core has been almost completely eliminated in both cases, and the average upward velocity should be just the total mass flow rate divided by, the cross sectional area times the density; which is the same in both cases.

Conclusions

The main conclusions drawn from this cold flow simulation:

1. FLUENT can be used effectively to simulate the flow patterns in the kraft recovery boiler;

2. Numerical problems are created due to the primary and secondary air jets impacting on the staggered bed. In subsequent simulations the bed will not extend above the level of the secondaries, which should result in a more realistic flow pattern.

3. The majority of the available nodes must be used in the lower furnace, especially in the regions around the bed; these are the areas of greatest variation in the flow variables.

TEST CASES USING THE REVISED COMBUSTION MODEL

Description

As a test of the combustion model written and added to FLUENT/RFM a small two-dimensional case was solved. The situation modelled was a burner with black liquor pyrolysis gas as the fuel. Two levels of air were used, above and below the location of the fuel inlet, see Figure 11. Six cases were examined:

1. A base case (Case 1) had the following properties: stoichiometric air; incoming turbulent intensity equal to 10% of the incoming jet kinetic energy; bone dry combustion air; and CO as the combustion product of fuel and oxygen.

2. In Case 2, the incoming air was increased to 150% of stoichiometric.

3. In Case 3, the base case was modified so that the incoming jets had a kinetic energy of turbulence equal to 20% of the total kinetic energy of the jet.

4. In Case 4, the base case was revised so that CO_2 was the combustion product of fuel and oxygen.

5. In Case 5, the combustion air was 20% water by weight.

6. In Case 6, the theoretical air was increased to 150% of stoichiometric by decreasing the fuel flow and CO_2 was the combustion product.

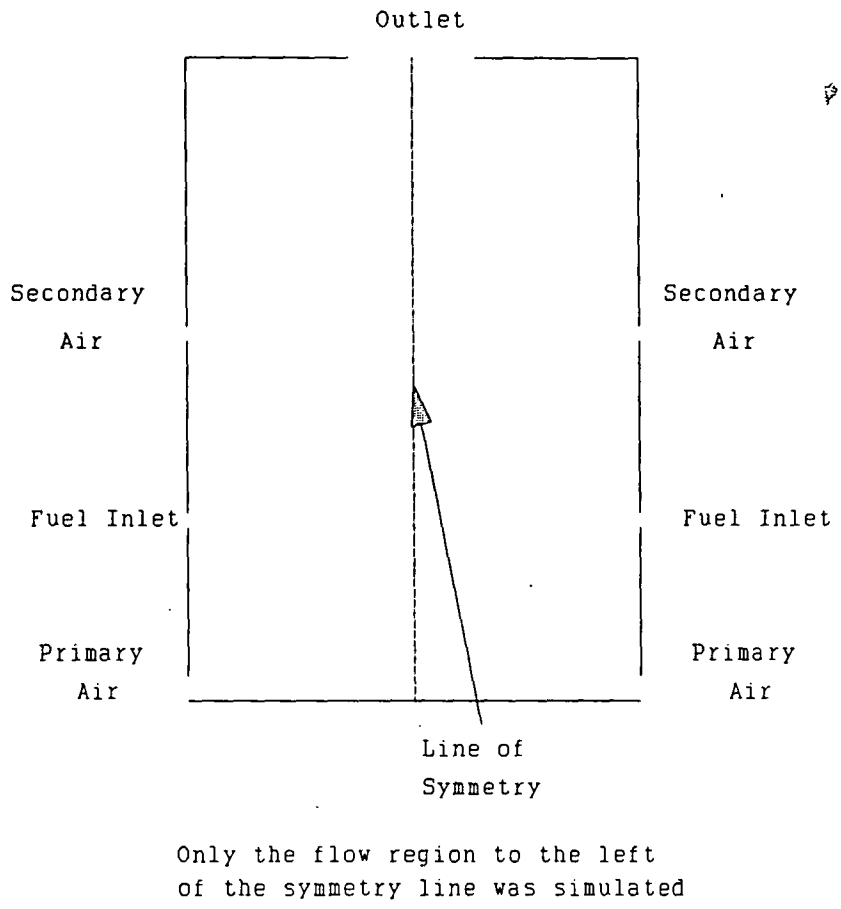

Figure 11 - Outline of Case Used to Test Combustion Model

Results

The cases described above were set up and solved using FLUENT/RFM. The results obtained were satisfying as they made logical sense, and the mass balances converged to within a fraction of a percent in all cases (see Table 1). An energy balance was not included in FLUENT/RFM when these test cases were run.

The following tables provide a comparison between the five cases examined.

Table 1 - Mass balances and exit mass fraction

Case	Mass Balance	Exit Mass Fractions				
	(% closure)	O_2	CO_2	H_2O	Fuel	CO
1	99.93	0.0081	0.119	0.0767	0.00096	0.00142
2	99.95	0.0485	0.0966	0.0615	0.00006	0.00026
3	99.94	0.0077	0.119	0.0769	0.00071	0.00106
4	99.99	0.0073	0.120	0.0764	0.00175	0.00000
5	99.94	0.0006	0.121	0.1930	0.00432	0.00170
6	100.10	0.0433	0.0845	0.0536	0.00004	0.00000

Table 2 - Maximum temperatures and maximum mass fractions

Case	Maximum Temp	Maximum Mass Fractions		
	(K)	CO_2	H_2O	CO
1	1489.1	0.1245	0.0798	0.0113
2	1569.8	0.1110	0.0763	0.0139
3	1515.9	0.1246	0.0798	0.0194
4	1507.5	0.1246	0.0790	0.0
5	1481.2	0.1222	0.200	0.0089
6	1453.4	0.0960	0.0536	0.0

The results are shown graphically in Figures 12 through 17. These figures show the distribution of temperature, and the five species that were simulated. The case, as stated earlier, is two-dimensional; therefore, only one plot is required to show the entire flow region for a given variable in each case.

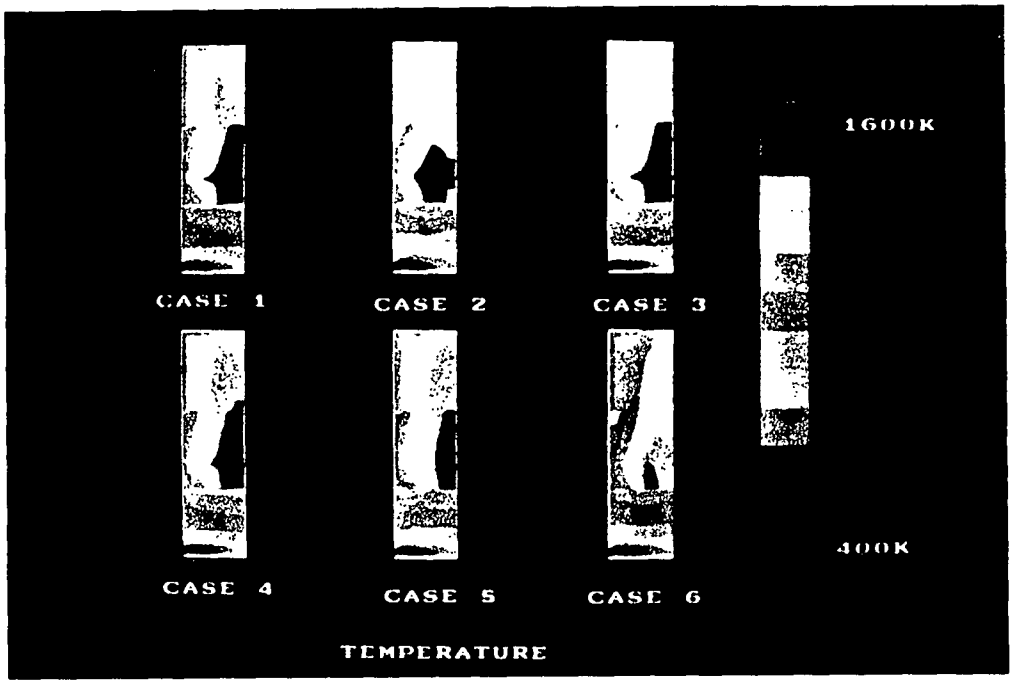

Figure 12 - Color Raster Plot of Temperature in Combustion Cases

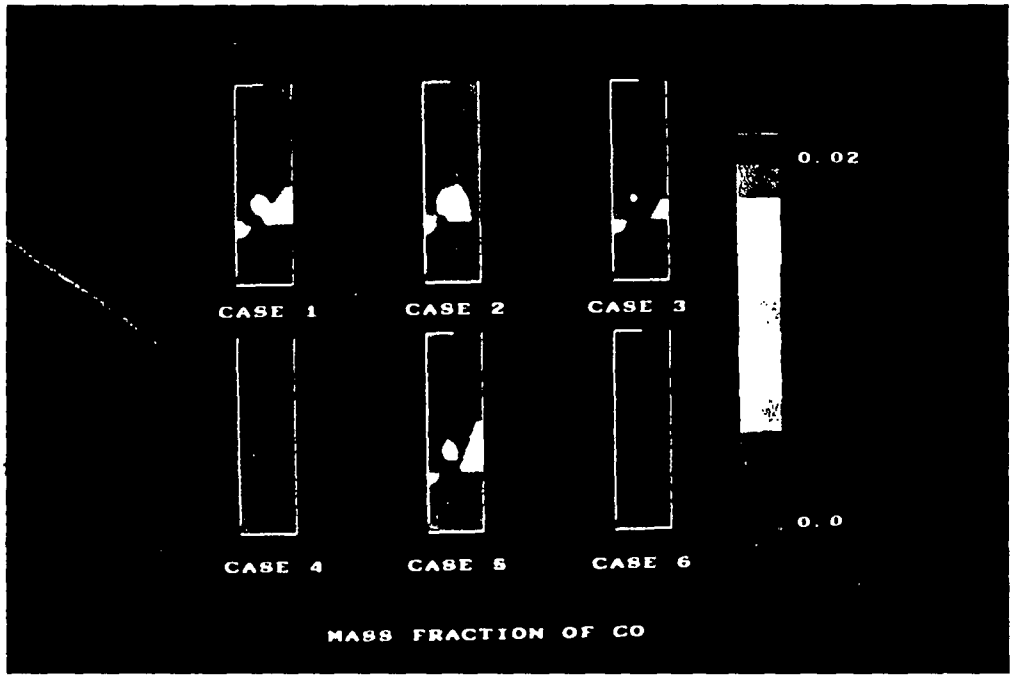

Figure 13 - Color Raster Plot of the Mass Fraction of CO in Combustion Cases

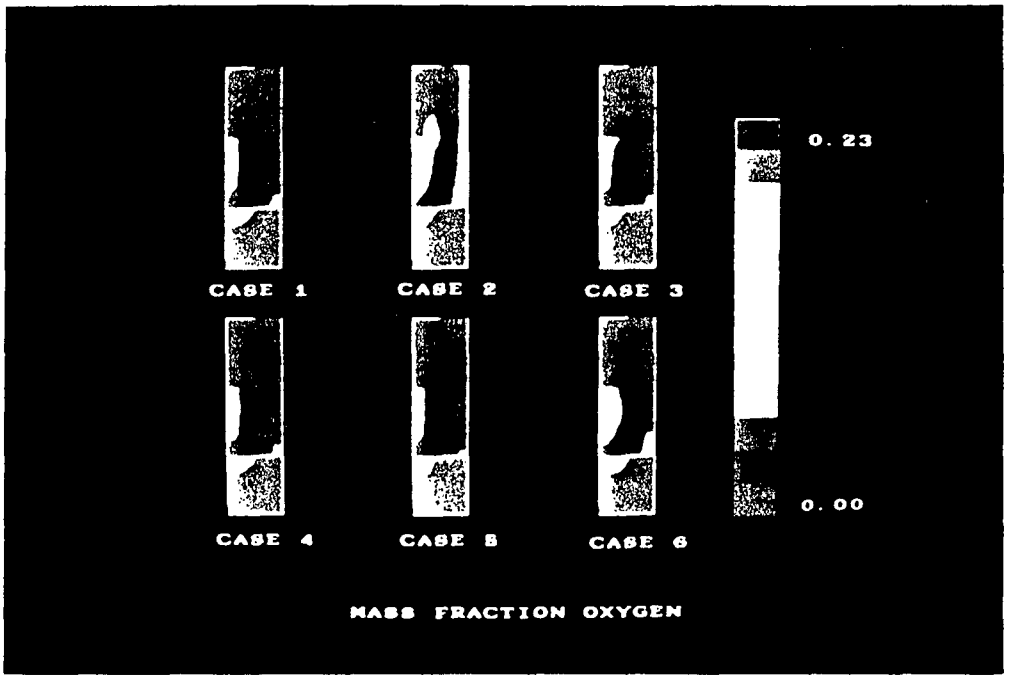

Figure 14 - Color Raster Plot of the Mass Fraction of O_2 in Combustion Cases

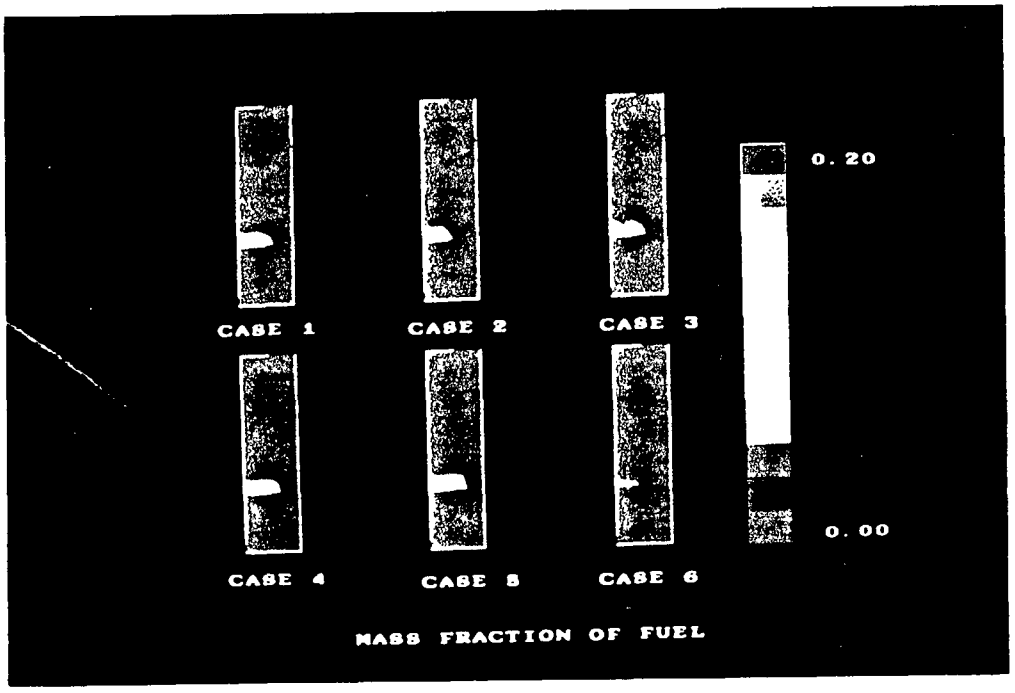

Figure 15 - Color Raster Plot of the Mass Fraction of Fuel in Combustion Cases

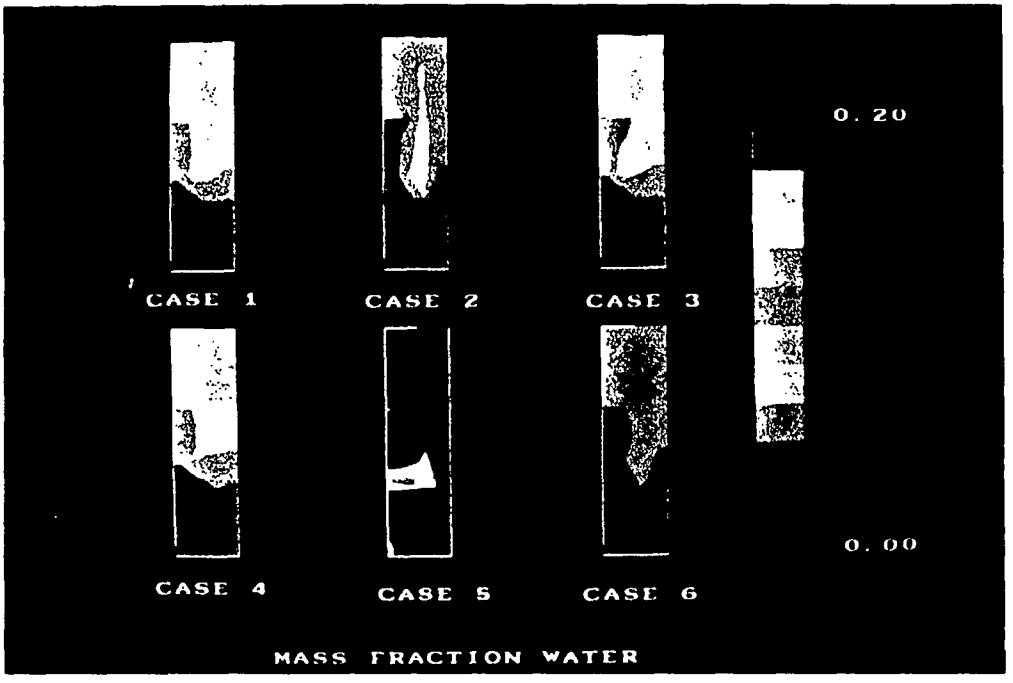

Figure 16 - Color Raster Plot of the Mass Fraction of H_2O in Combustion Cases

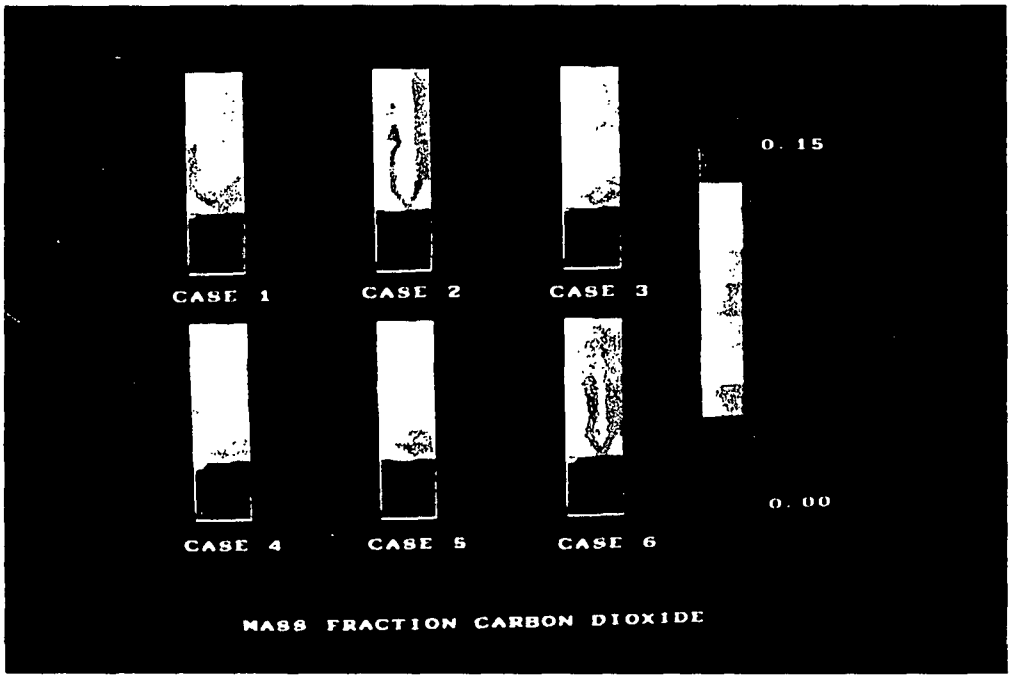

Figure 17 - Color Raster Plot of the Mass Fraction of CO_2 in Combustion Cases

The effect of increasing the amount of stoichiometric air can be seen by comparing Case 1 and Case 2, as shown in Figure 12. The main effects are more complete combustion and a higher peak temperature. If the mixing was perfect then the stoichiometric amount of air would be sufficient, but it is not perfect; thus, excess air is required to obtain complete combustion and the resulting higher temperature.

By increasing the turbulent intensity from 10% to 20% in the incoming jets it was possible to obtain a higher peak temperature and more complete combustion with the same air supply (Case 1 vs Case 3). The peak CO concentration was higher, as the reaction to form CO increased more rapidly than the combustion of CO, see Figure 13.

With CO_2 as the combustion product of fuel and oxygen the peak temperature was increased; this is as expected, as the heat release is more localized when the combustion process is single rather than multi-staged (Figure 12). More fuel is present in the exiting gas, due to the relatively higher oxygen concentrations necessary to react the fuel directly to carbon dioxide.

The addition of water to the incoming air had two major effects: the increased mass fraction of air resulted in a high heat capacity in a given cell, and thus a lower temperature (Figure 12); in addition, the dilution effect of the water vapor decreased the mass fractions of the other species present.

The results of case 6, where the air supply was increased to 150% of theoretical and no CO was formed, were similar to case 2 with the exception of the peak temperature, this is expected, as the total amount of fuel was decreased (Figure 12). The peak temperature was more than 100K lower in case 6 than in case 2.

Case 1 was rerun following addition of the inert balance discussed previously; an inert balance within 0.1% was obtained, following 500 iterations, further demonstrating that the combustion model is consistent.

Conclusions

1. The mass and inert balances are satisfied;

2. In each of the cases examined, changes in the input parameters resulted in a simulation that behaved in a predictable manner;

THE BASE CASE

This section will examine a simulation of a "Base Case". Included in this section are a discussion of why we chose to model this particular furnace design, a description of the Base Case, and the results of the simulation.

Reason For Modelling This Particular Furnace Design

The Base Case had the same geometry as the high velocity tertiary simulated in the cold flow work, with two exceptions. The results of the cold flow work demonstrated that the secondaries should not impinge directly on the side of the bed as this results in numerical problems. The secondary jets usually limit the bed height. In the Base Case the bed height was lowered so that the secondary jets could pass over the top of the bed. The second change made was to use a sloping bullnose. This particular geometry was chosen as the cold flow work demonstrated the desirable flow patterns produced (i.e. no stagnant region under the bullnose and no core of high-upward-velocity gas).

Other furnace designs were not considered for the following reasons: 1. There is very limited data available for any specific furnace; thus, there was no point in trying to describe exactly an existing furnace; 2. The goal of this work was to construct a model and to obtain a converged result, not to try to match experimental results; and 3. A geometry that had a plane of symmetry was required, which eliminated CE type furnaces, and units with two-wall interlaced secondaries.

Description of the Base Case

The Base Case simulation is of a B&W type furnace design; a schematic of this case is shown on the following page. Only half of the furnace is modelled, as 50,000 cells (the maximum number of cells that can be used on the MicroVAX computer) is not enough to accurately describe the air ports and bed surface for the entire furnace. The use of this symmetry plane causes some numerical problems, but these problems were not as severe as those created by using inadequate nodes around the surface of the

bed and around the air ports. In the remainder of this section, when the furnace is referred to, assume that only the half simulated is being described. The furnace is 10 meters deep, 5 meters wide and 30 meters high. The bullnose, located on the back of the furnace, is sloped downward towards the back of the furnace, and occupies about half of the cross-sectional area of the furnace. The base case simulation uses 50,000 nodes, 40 in the Y (vertical) direction, 25 in the Z direction, and 50 in the X direction.

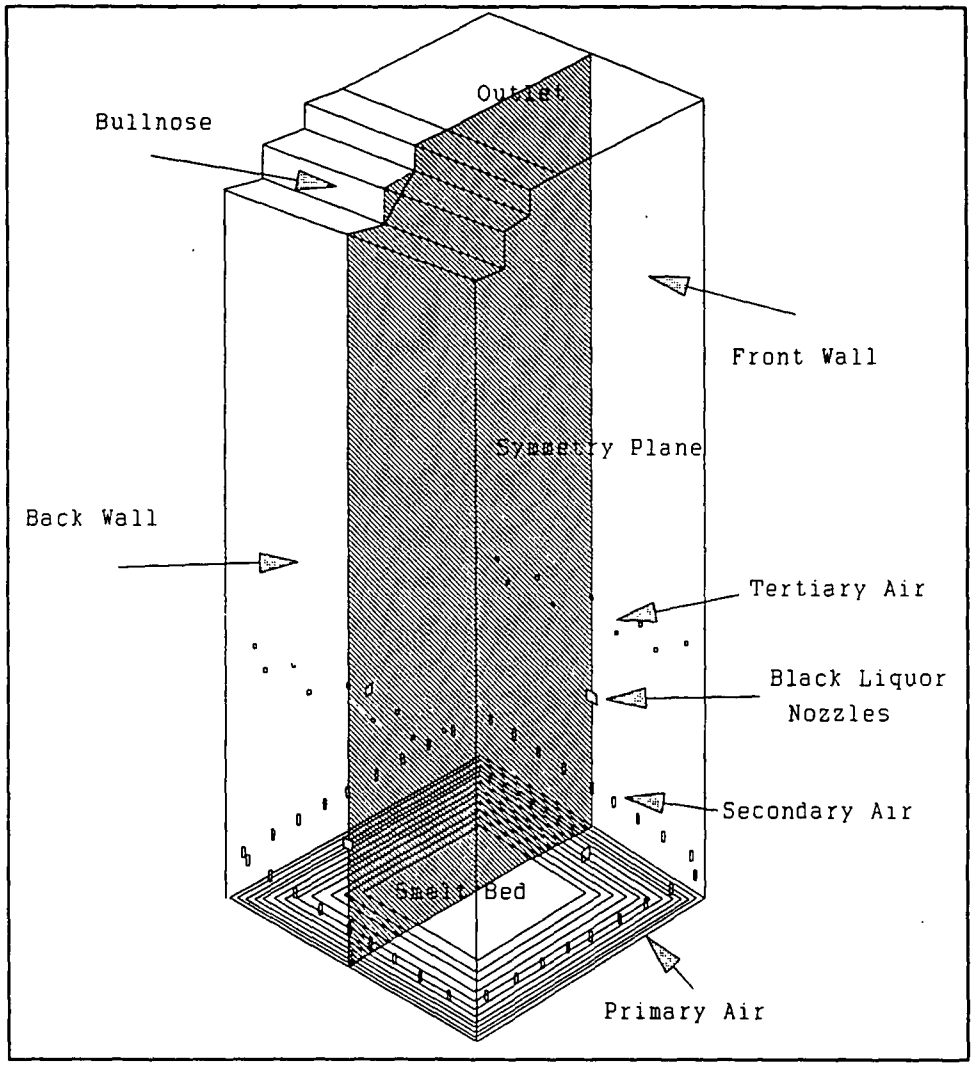

Figure 18 - Schematic of Base Case

At the bottom of the furnace is a char bed. The bed in this case does not extend as high as in the cold flow cases, due to the numerical problems experienced in the cold flow modelling. This earlier work indicated that if the bed extended above the level of the secondaries, then the secondary jets were directed upwards rather than following the surface of the bed. The side of the bed is constructed of steps; a step will approximate a diagonal surface, if enough nodes are used.

The total black liquor entering the furnace was 17.2 kg/sec, which corresponds to about 2.75 lbs of black liquor solids per ft^2 per minute. The combustion air that entered the furnace came in at three levels, primary, secondary, and tertiary. The mass flow rate of air was 52.7 kg/sec, about 10% excess air (48.0 kg/sec is stoichiometric). The high heating value of the black liquor was 6600 Btu/lb. When combined with the firing rate this results in a high loading.

Primary air

The primary air entered at 53 m/sec and made up 45% of the total air. Restrictions in the total number of nodes used meant that individual primary air jets could not be described. Instead, the primary jets are modelled as slot jets. The primary jets are located at the base of the walls, they extend along the entire length of the wall, and are 0.026 m high.

Secondary air

The secondary air jets had a velocity of 53 m/sec and made up 38% of the total air. Individual air ports were described. The ports were located two meters above the primary jets on all the walls. A total of 18 secondary air ports appeared in the simulation (36 in the full furnace), at a spacing of one meter. The jets were set up in an opposing fashion, rather than being interlaced. The dimensions of an individual port were 0.114 m wide by 0.214 m high (4.5" x 8.5").

Tertiary air

Tertiary air made up the remaining 17% of the air, and entered the furnace at 93 m/sec. Individual tertiary ports were described on the front and back walls. A total of 9 ports were modelled with dimensions of 0.114 m wide by 0.111 m high (4.5" x 4.4"). The width of the tertiary and secondary air ports were kept the same in order to reduce the number of nodes used.

Boundary Conditions

Boundary conditions have to be specified for the walls and the incoming air streams; output boundary conditions are calculated by FLUENT using mass continuity. All air streams were assumed to be at 400K, and to have 23.6 mass percent oxygen, with the remaining mass assumed to be nitrogen. The velocities of these air streams have already been indicated. A remaining boundary condition that must be specified is the turbulent kinetic energy; typically, a turbulent kinetic energy equal to 10% of the incoming kinetic energy is assumed (this guideline was followed).

Two conditions must be specified for the walls, the temperature and the radiative adsorption coefficient. The adsorption coefficient was assumed to be 0.8 for all walls. The temperature of the water walls was taken to be 900K, the radical deformation point of the molten slag that would be present on the walls. The bed surface temperature is solved for by the bed burning model and cannot be specified.

Physical Properties of the Gas Phase

The physical properties of the gas phase were chosen based on the best available information, and were as follows:

1. Thermal conductivity of the gas phase assumed to be that of nitrogen, described by a third order polynomial as a function of temperature;

2. Radiation adsorption coefficient of 0.4, with a scattering coefficient of 0.01;

3. Viscosity of the furnace gases assumed to be that of air, once again described by a third order polynomial as a function of temperature;

4. Density at standard temperature and pressure of 1.12 kg/m^3 (that of air), with the ideal gas law used to find density as a function of temperature;

5. The heat capacity equation of the gas was found as a function of temperature and mass fraction, based on equation [25], described earlier;

6. The following molecular weights were used: O_2(O) = 32, pyrolysis gas (F) = 27.8, CO_2 (C) = 44, CO (Q) = 28, H_2O = 18 (B);

7. The heat of reaction for the combustion of pyrolysis gas was assumed to be 25,100 kJ/kg of fuel[31], the heat of combustion of CO was specified as 10,100 kJ/kg of CO. The stoichiometric requirement for air was 0.948 kg/kg of F, and 0.571 kg/kg of CO. All of the carbon in the pyrolysis gas was assumed to form CO.

Drop Properties

The properties of the black liquor and of the spray must be specified. The following physical properties were used:

1. Black Liquor Composition - 65% solids, 30% of solids form pyrolysis gas, 20% of solids form char carbon, remaining solids form reduced smelt.

2. Black Liquor Physical Properties - density = 1400 kg/m^3, latent heat of vaporization for water = 2200 kJ/kg, swelling during drying = 150% of original diameter, solids at ignition = 90%, swelling during pyrolysis = 250% of original diameter, CO/(CO+CO_2) ratio of 0.9 during char combustion,

smelt stoichiometric ratio = 0.82 (ratio of oxygen required to oxidize Na_2S divided by mass of Na_2S, 64g/78g), heat of reaction of char = 32,860 kJ/kg, and a heat capacity of particles = 1000 J/kg-K;

3. Spray Locations - three spray guns were used, one on each wall (note that only three walls are present due to the use of the symmetry plane), one liquor gun was located in the middle of the side wall, and a half a liquor gun was located on the symmetry plane on both the front and back walls (the other half of these guns would appear on the other side of the symmetry plane, see Figure 19);

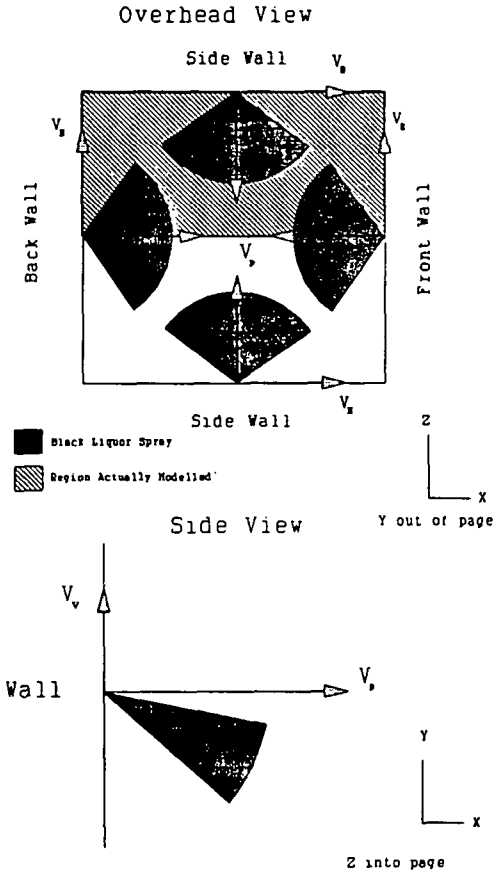

Figure 19 - Illustration of Black Liquor Spray

4. Drop Distribution - 10,000 total drops must be specified; this allows for a variation in the diameter of the drop and in their initial trajectories. A log-normal distribution of drop diameters was used (for justification of this see Allan Walsh's thesis)[31]. In addition, the three velocity

components of the drops (V_H, V_v, V_p) were varied so that they described the spray produced by a black liquor gun; see Figure 19.

Char Bed Properties

The only property of the bed that can be specified is the ratio of CO to (CO + CO_2) that is formed by the bed; a ratio of 1.0 was used implying that all CO formed.

Convergence Behavior of the Base Case

Convergence of the Base Case requires in excess of 3500 iterations and 4 months of computer time. A converged case was obtained (approximately 12 trillion calculations). The purpose of this section is to describe the way in which this case approached convergence. The variables chosen in order to follow convergence, and the reasons for choosing them are given below:

1. The inert balance, which is a measure of the convergence of the chemical species calculations (see equation [26]);

2. The normalized v-velocity (upward velocity) residual is a measure of the overall gas flow convergence. A residual is the difference between the value of a flow variable and the calculated value of the variable at the current iteration, normalization involves the division of the residual by the current value of the flow variable summed over the entire flow region;

3. The maximum v-velocity residual, an indication of the poorest convergence over the whole flow field;

4. The amount of inorganic carryover, an indication of the convergence of the second phase.

The energy balance is not a good measure of the approach to convergence as it is always within ±10% of closure. An initial guess of the global temperature is used at the start of the simulation, which ensures that the energy balance starts within a few percent of 100%.

The inert balance in the "converged" case was decreasing very slowly and was just under 102% after 3500 iterations. The inorganic carryover fluctuated between 0.26 and 0.29 lbs. In Figure 20 the normalized v-velocity residual and the maximum v-velocity residuals are shown over 20 iterations for the converged case. The largest v-velocity residual is about 0.25 m/sec. Thus the largest error in the prediction of upward velocity throughout the furnace cavity is 0.25 m/sec. Given the restrictions on computer time and the accuracy of the inputs to the model it was felt that this case could be deemed converged at this point.

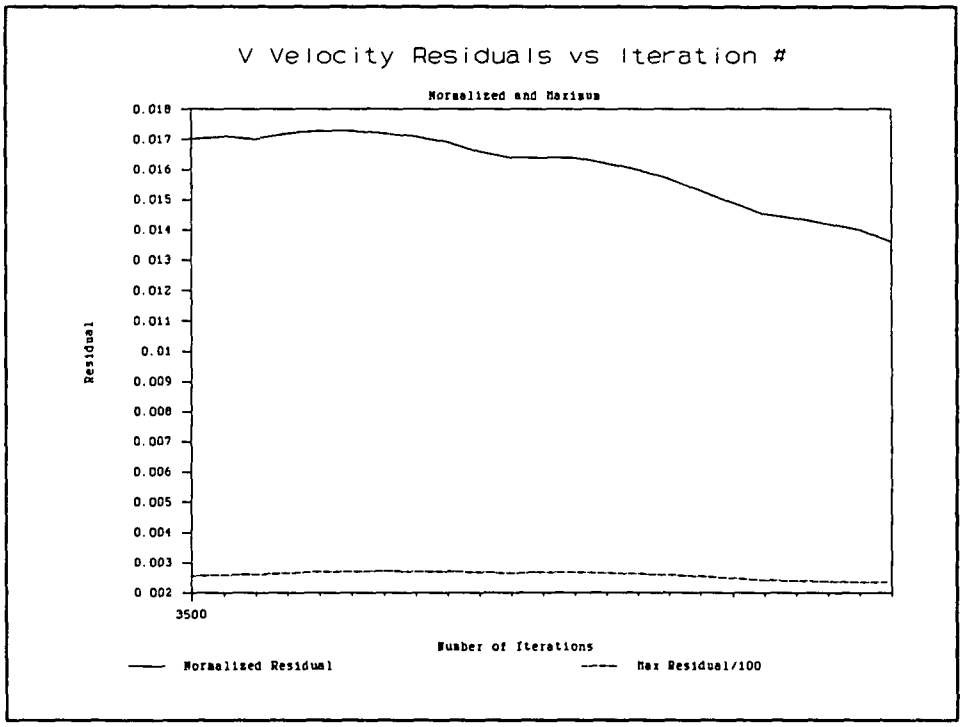

Figure 20 - V-Velocity Residuals of Converged Case

The results presented in the following three Figures were from a case that was run following convergence of the first case. Figure 21 shows the behavior of the inert balance, which decreases monotonically with the number of iterations. Figure 22 illustrates the behavior of the normalized v-velocity residual and the maximum v-velocity residual; note the cyclic nature of both. The actual flow fluctuated between upflow and downflow, with the maximum v-velocity residuals occurring at the extreme upflow and downflow conditions. In Figure 23 the inorganic carryover is shown, it follows the same cyclic behavior, due to the strong coupling between the gas flow patterns and the amount of carryover. Maximums and minimums in the amount of carryover as a function of iteration number correspond to the maximums in the v-velocity residual curve.

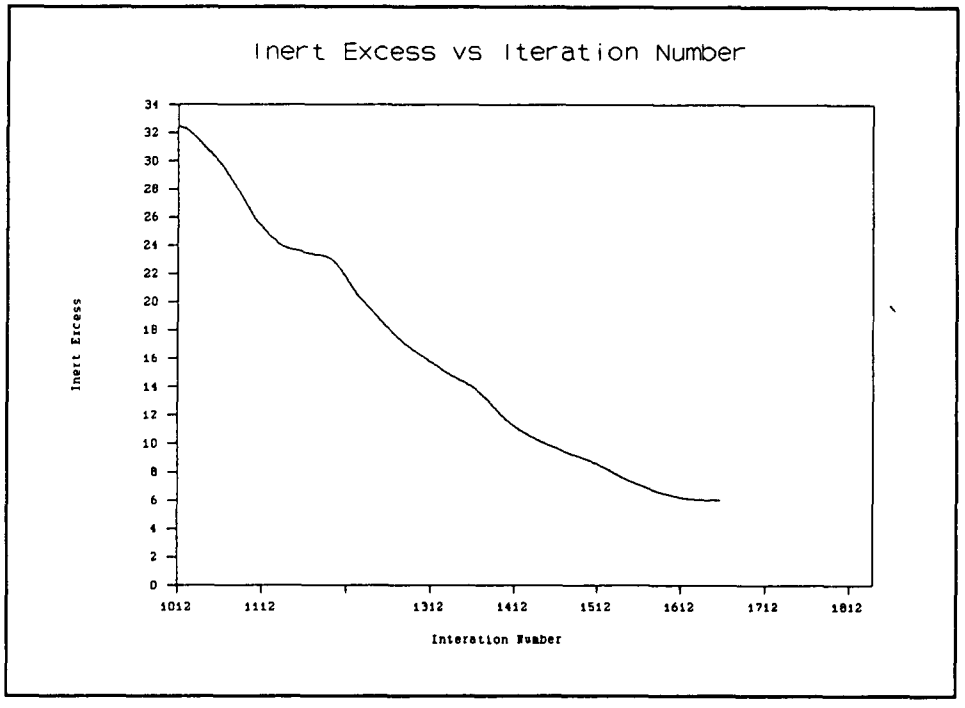

Figure 21 - Inert Excess vs Iteration Number

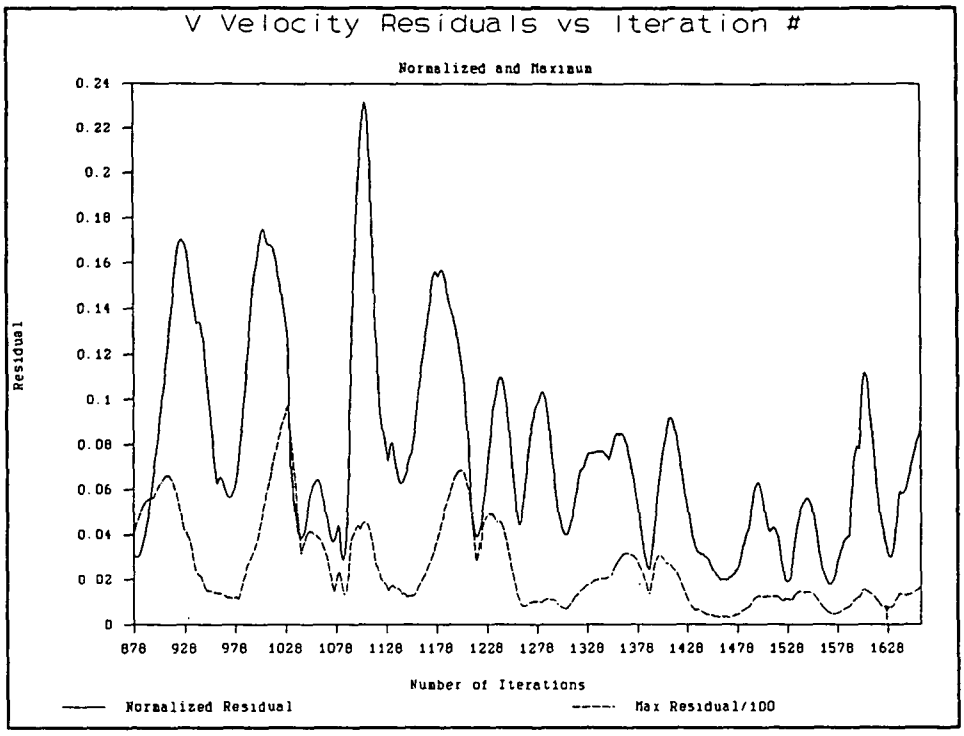

Figure 22 - V Velocity Residuals vs Iteration Number

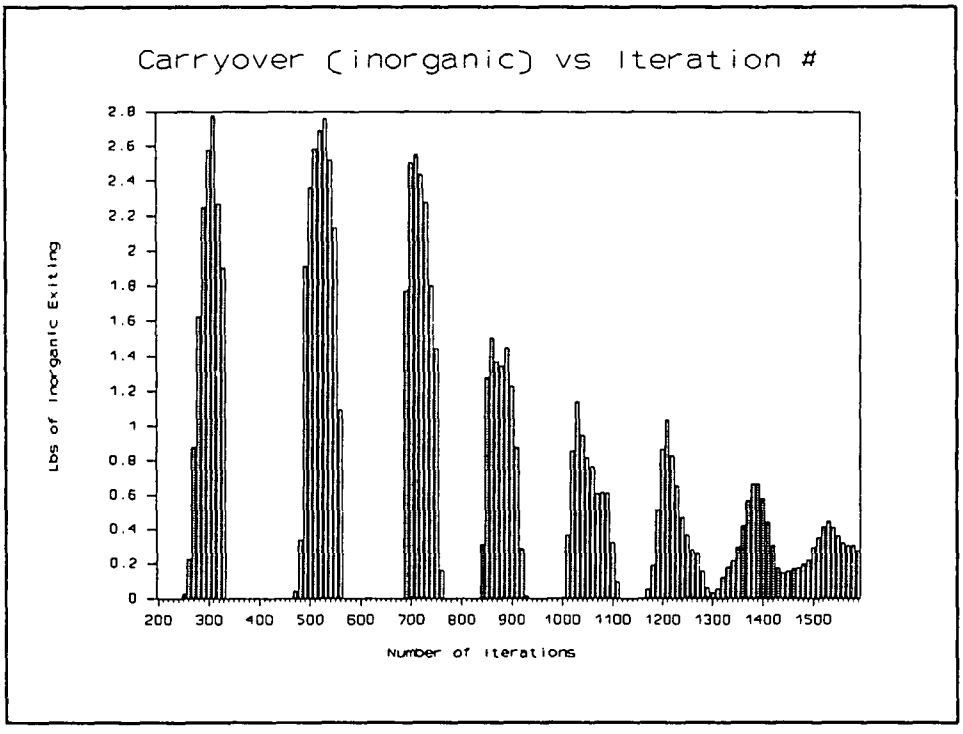

Figure 23 - Inorganic Carryover vs Iteration Number

Results of the Base Case Simulation

The purpose of this section is to describe the results of the converged Base Case simulation. The number of different flow quantities that could be presented is enormous, the number of ways in which they could be presented is equally immense. A data file for the Base Case contains over 6 million bytes of information. A difficult part of this work is determining which variables should be presented and in what manner; this problem of displaying the results was alleviated somewhat by the color device driver that was written by Allan Walsh. The results will usually be presented as color raster plots on planar slices of the recovery furnace.

The variables that were examined were chosen based on two criteria: first, their influence on the operation of the recovery furnace; and second, the availability of data for comparison. The main operational problems discussed in the introduction to this thesis were corrosion, pollutant formation, and carryover; each of these can be evaluated in the Base Case furnace by the selection of appropriate flow variables. Data is available for comparison in some isolated cases, but detailed data examining the three-dimensional distribution of velocity, temperature, or the mass fractions of gas species is unavailable. Data of this detail would be necessary for verification of the model.

General Flow Patterns

The flow patterns that exist in the furnace are illustrated by the use of vector plots of the velocity in Figures 24 through 39. The dominant characteristic of the flow is the large center core of high velocity gas; around the perimeter of the furnace is a region of downflow. This general flow pattern has been described by Adams[33]. The regions of downflow are formed due to entrainment of the furnace gases by the primary, secondary, and tertiary jets, as shown in Figures 33, 36 and 37.

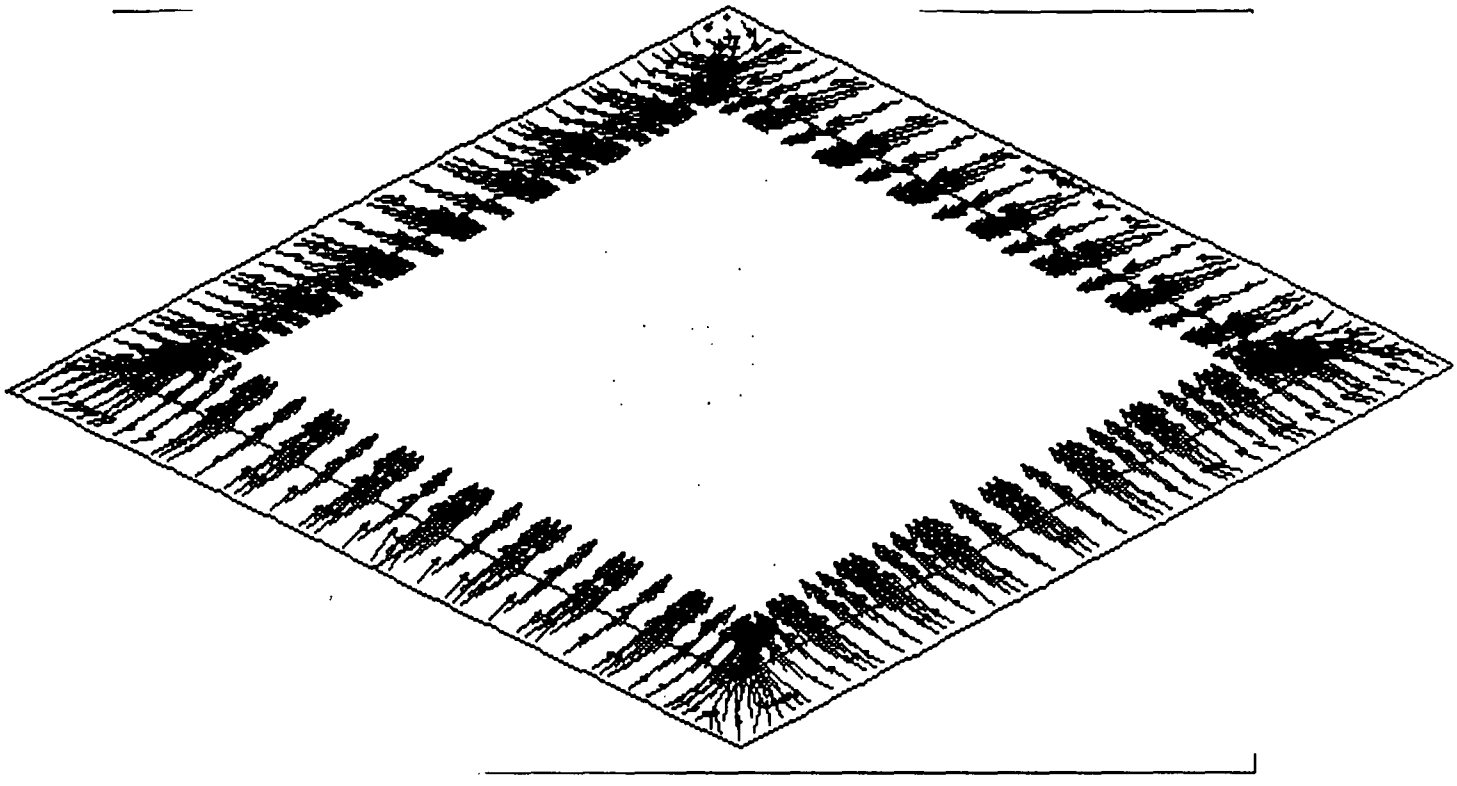

Figure 24 - Primary Air Jets Entering the Furnace

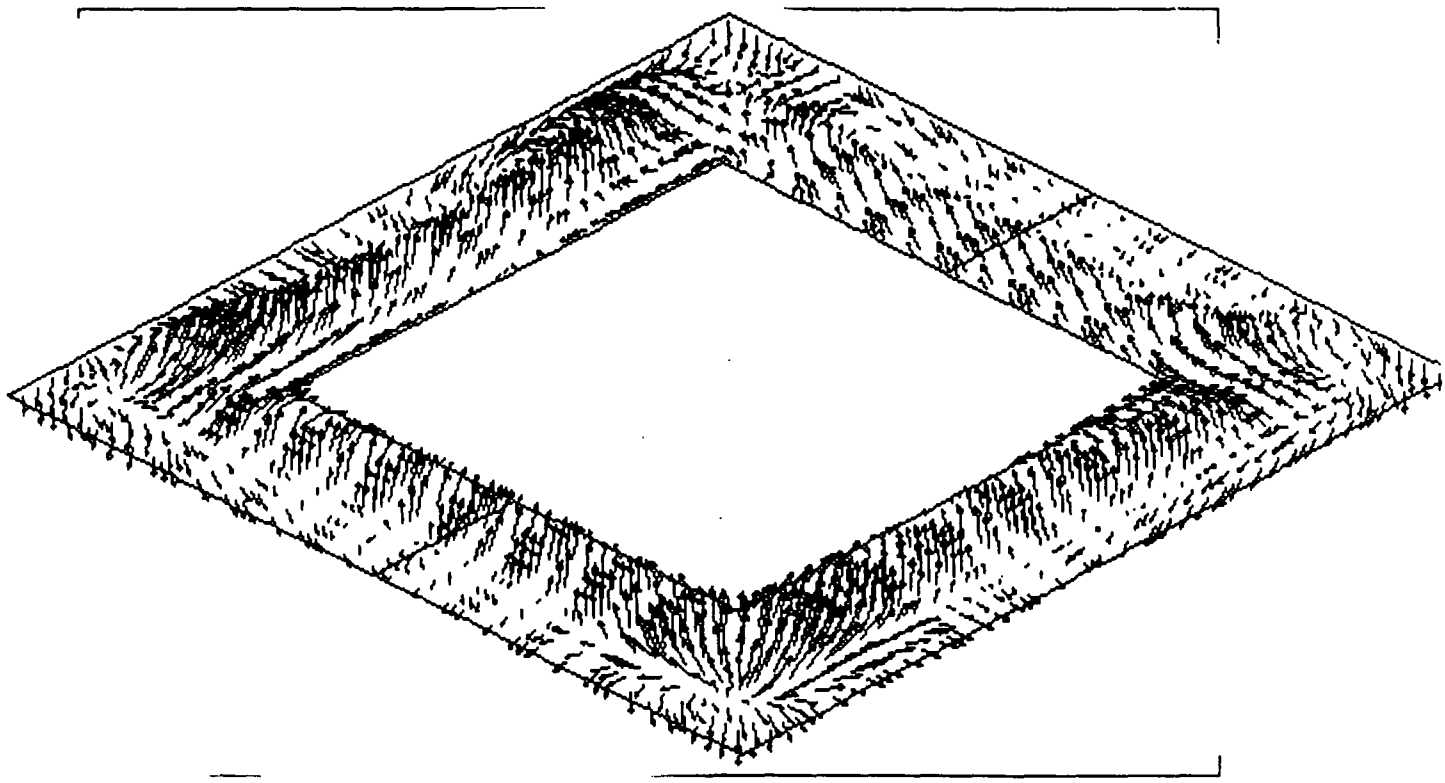

Figure 25 - Horizontal Slice of Furnace Between Primary and Secondary Air Levels

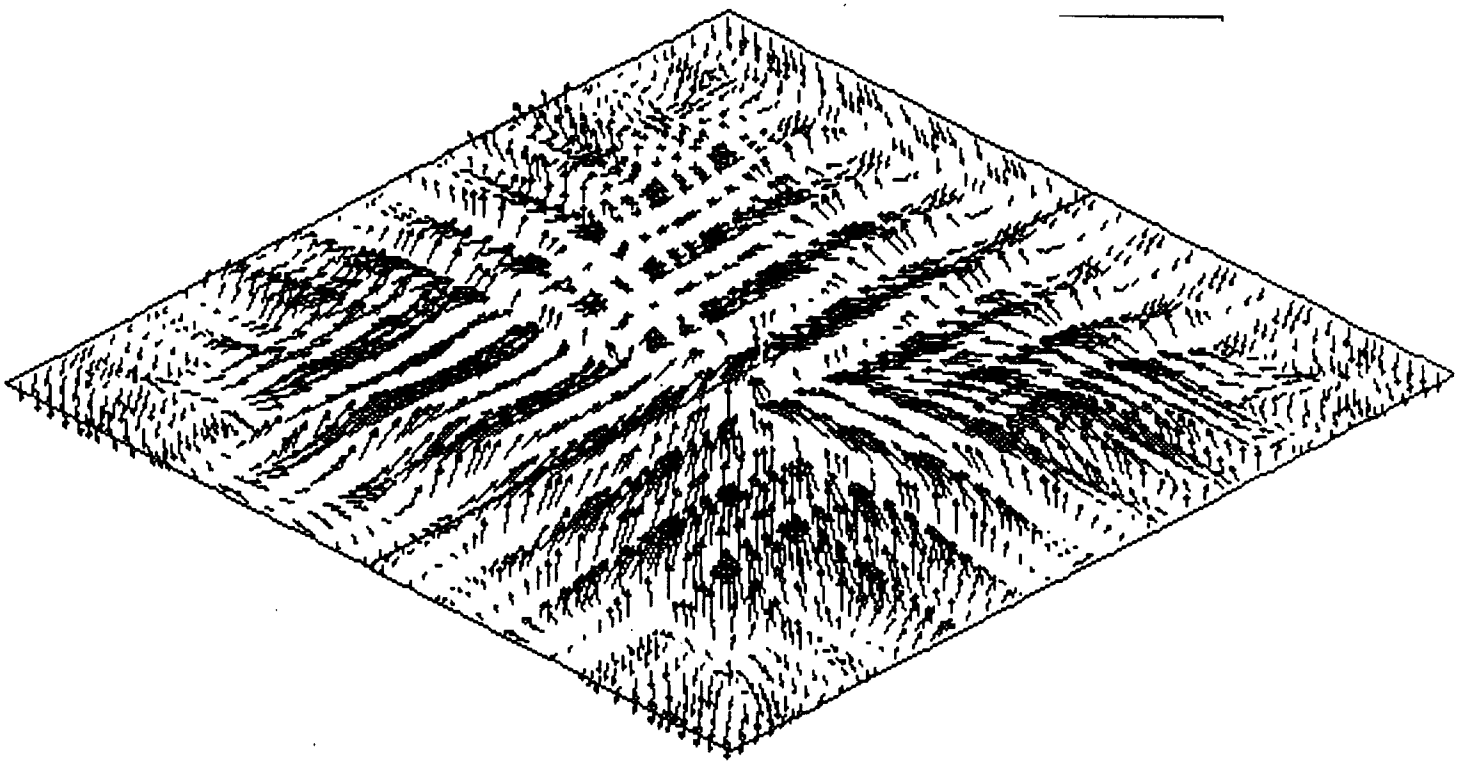

Figure 26 - Horizontal Slice Above Secondary Inlet

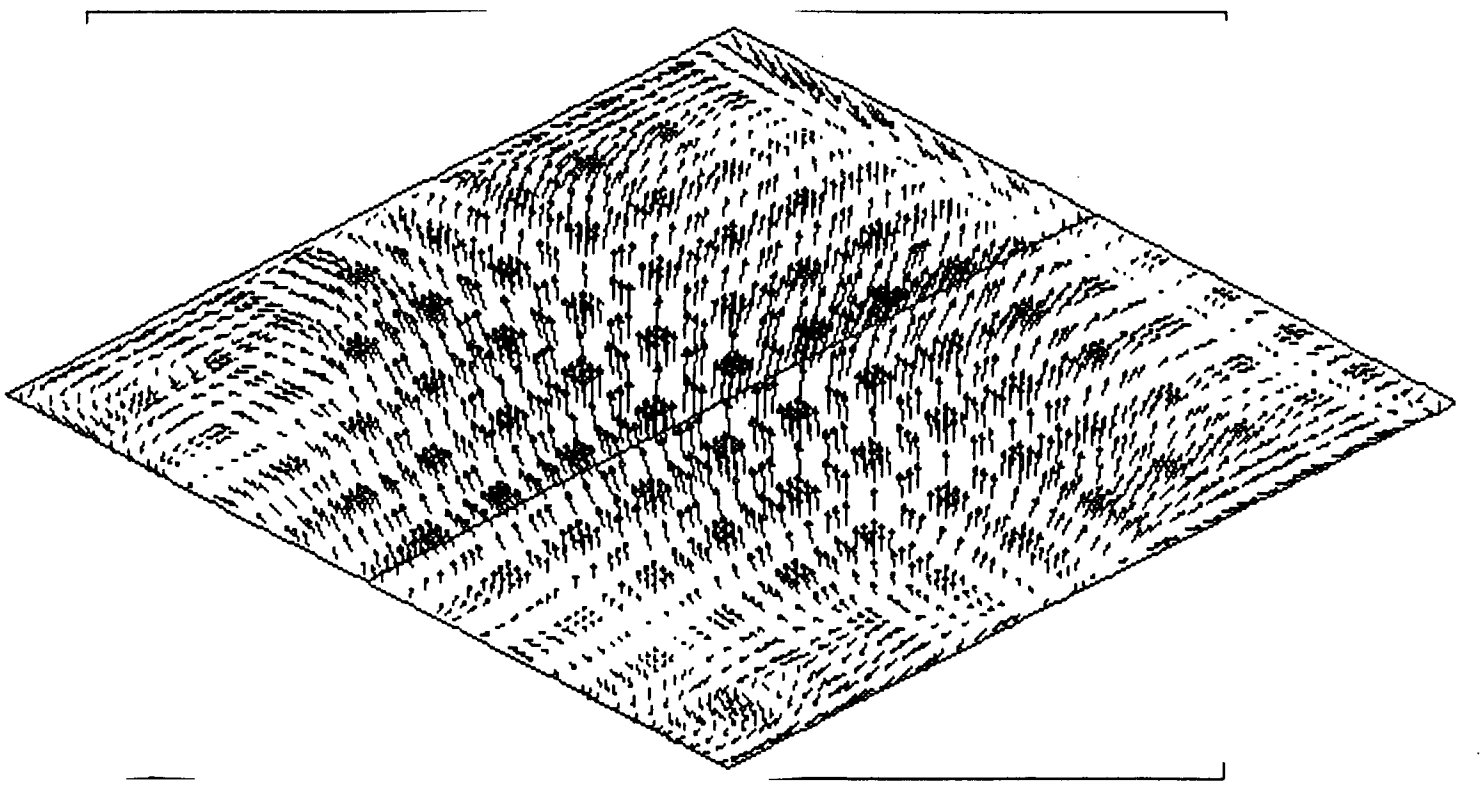

Figure 27 - Horizontal Slice Between Secondary and Tertiary Air Levels

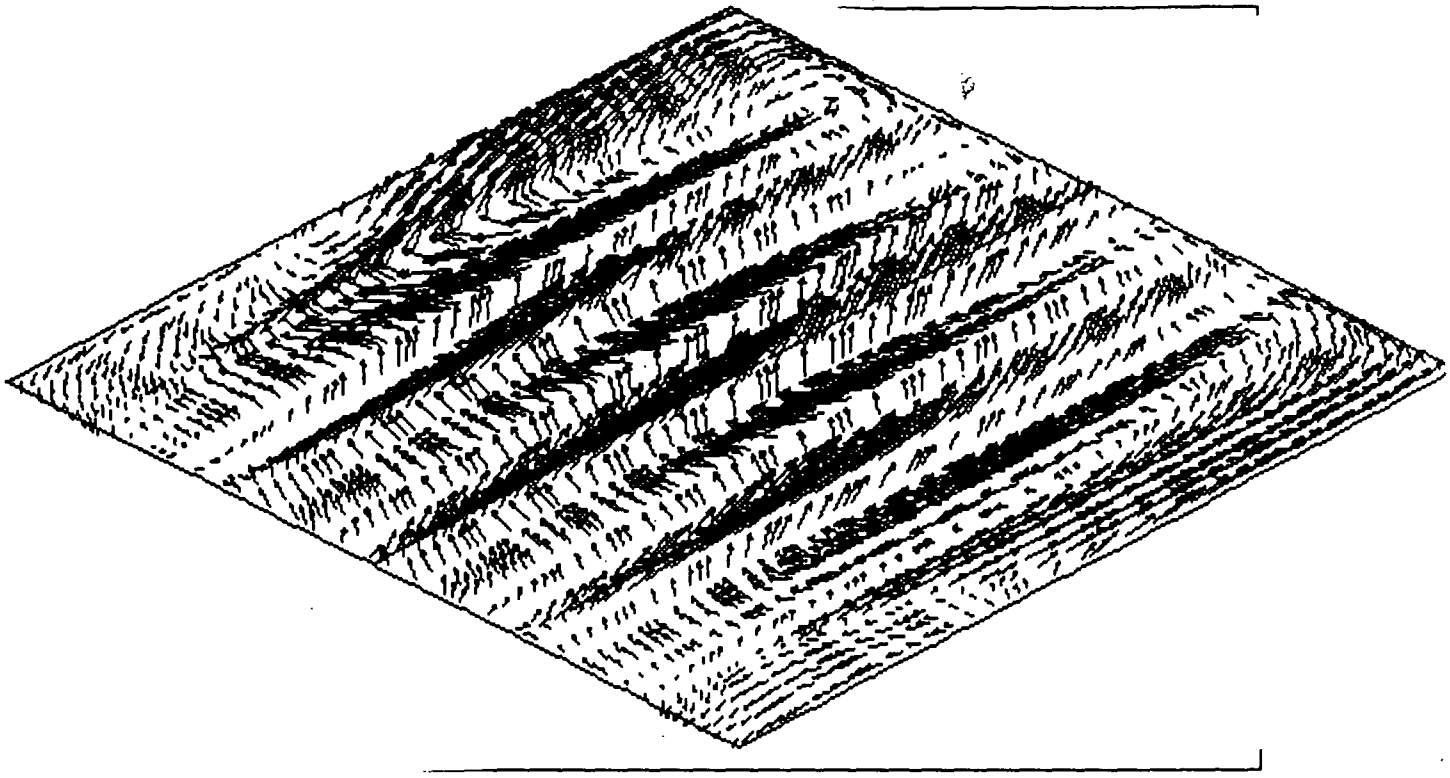

Figure 28 - Horizontal Slice at the Lower Tertiary Air Level

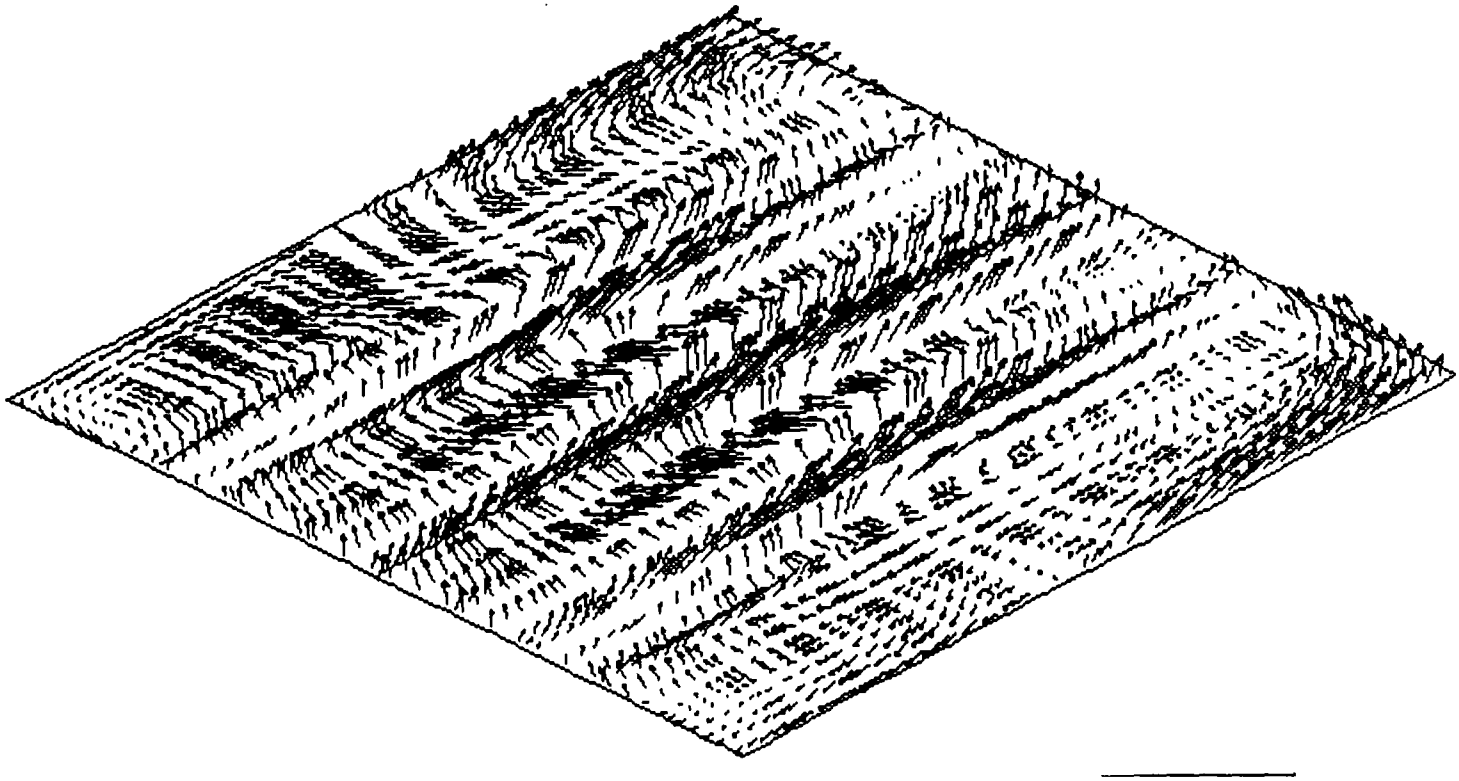

Figure 29 - Horizontal Slice Between Tertiary Air Levels

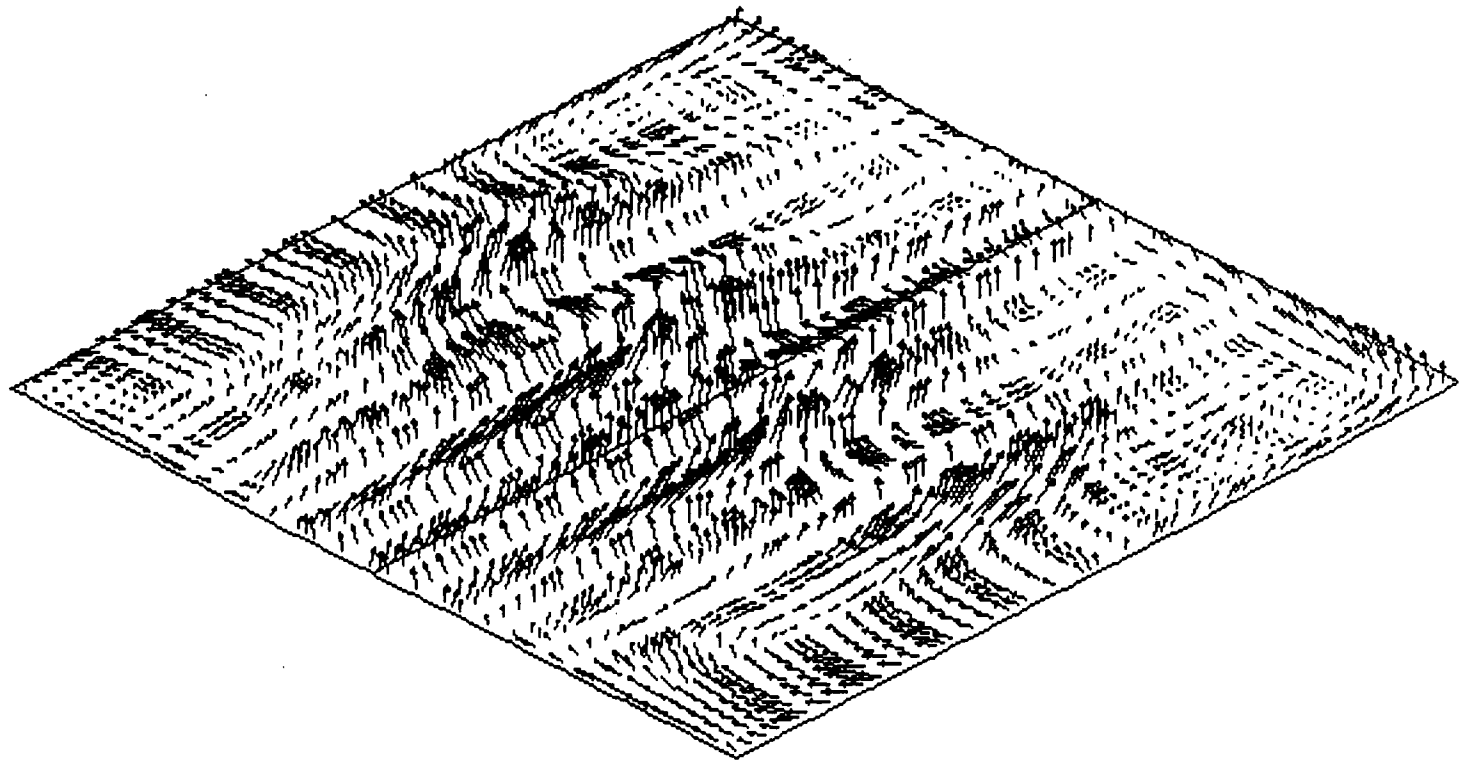

Figure 30 - Horizontal Slice Just Above Tertiary Air Level

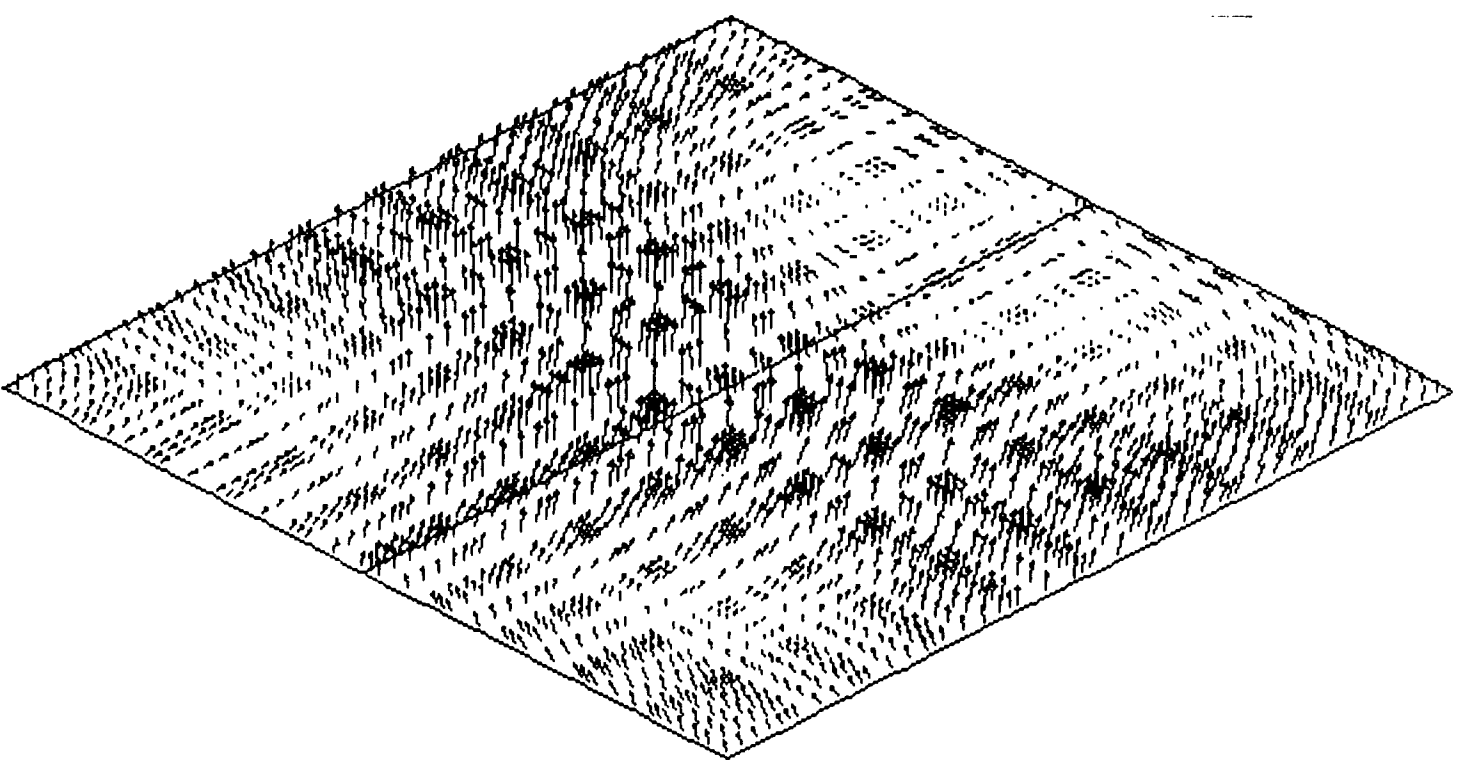

Figure 31 - Horizontal Slice Between Tertiary Level and Furnace Exit

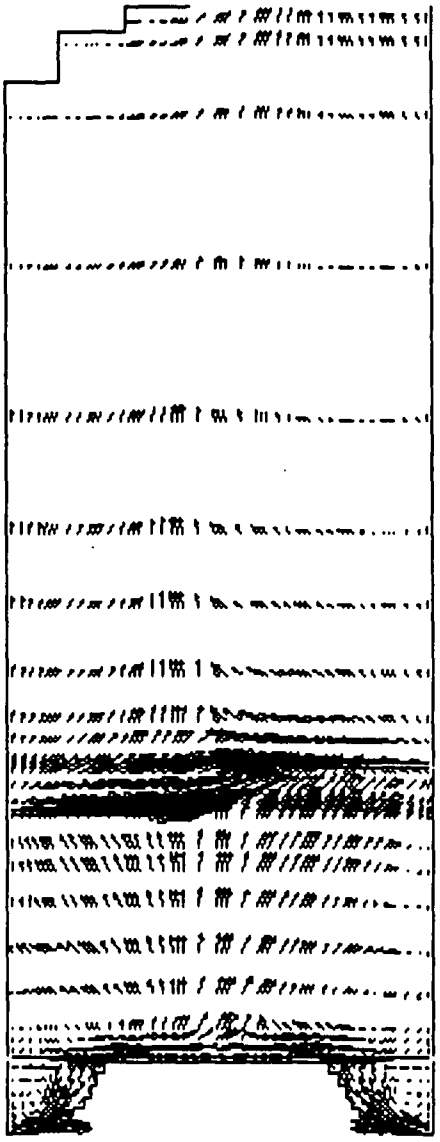

Figure 32 - Vertical Slice of Furnace at Centerline

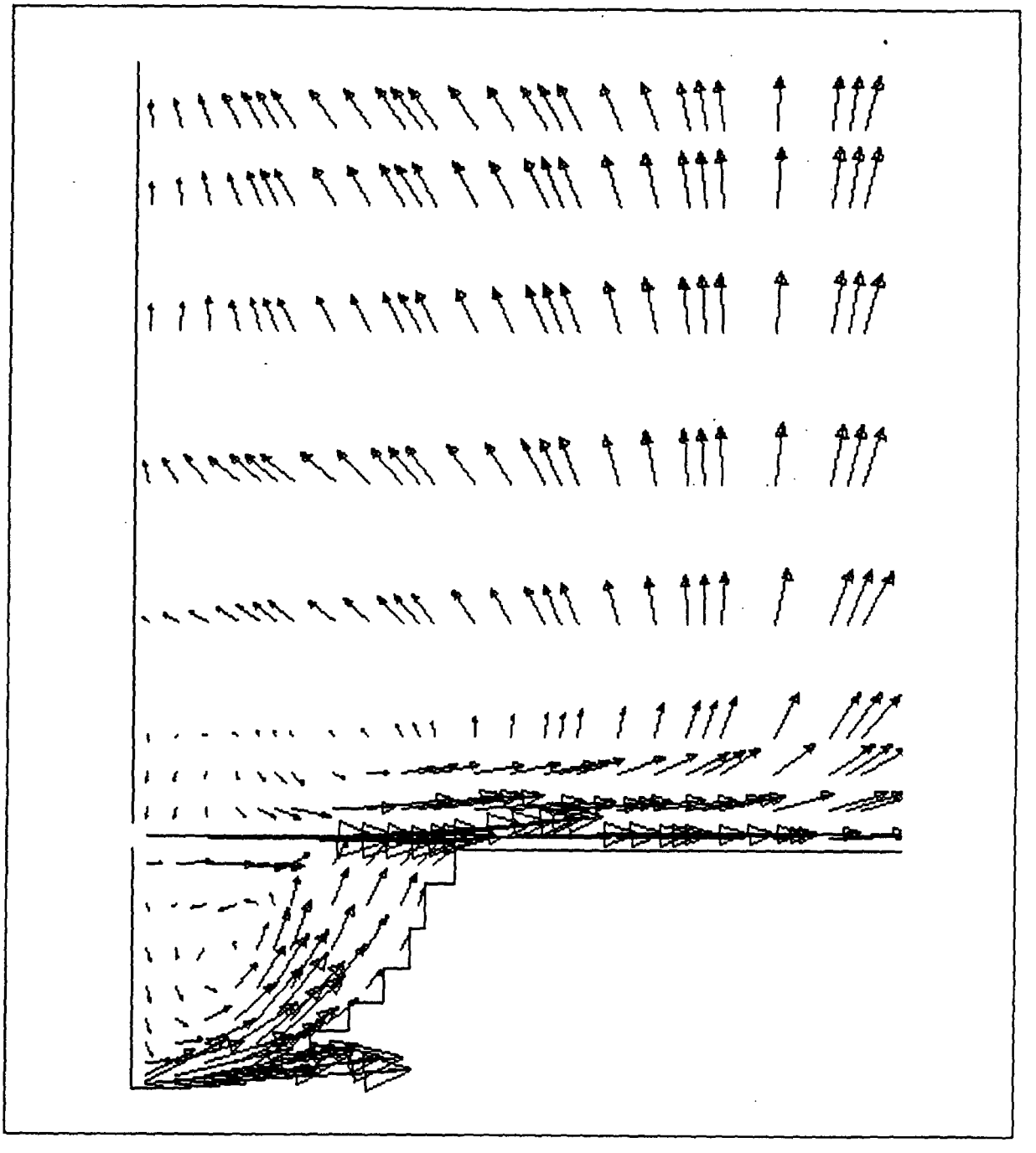

Figure 33 - Zoom of Lower Left Corner of Figure 31

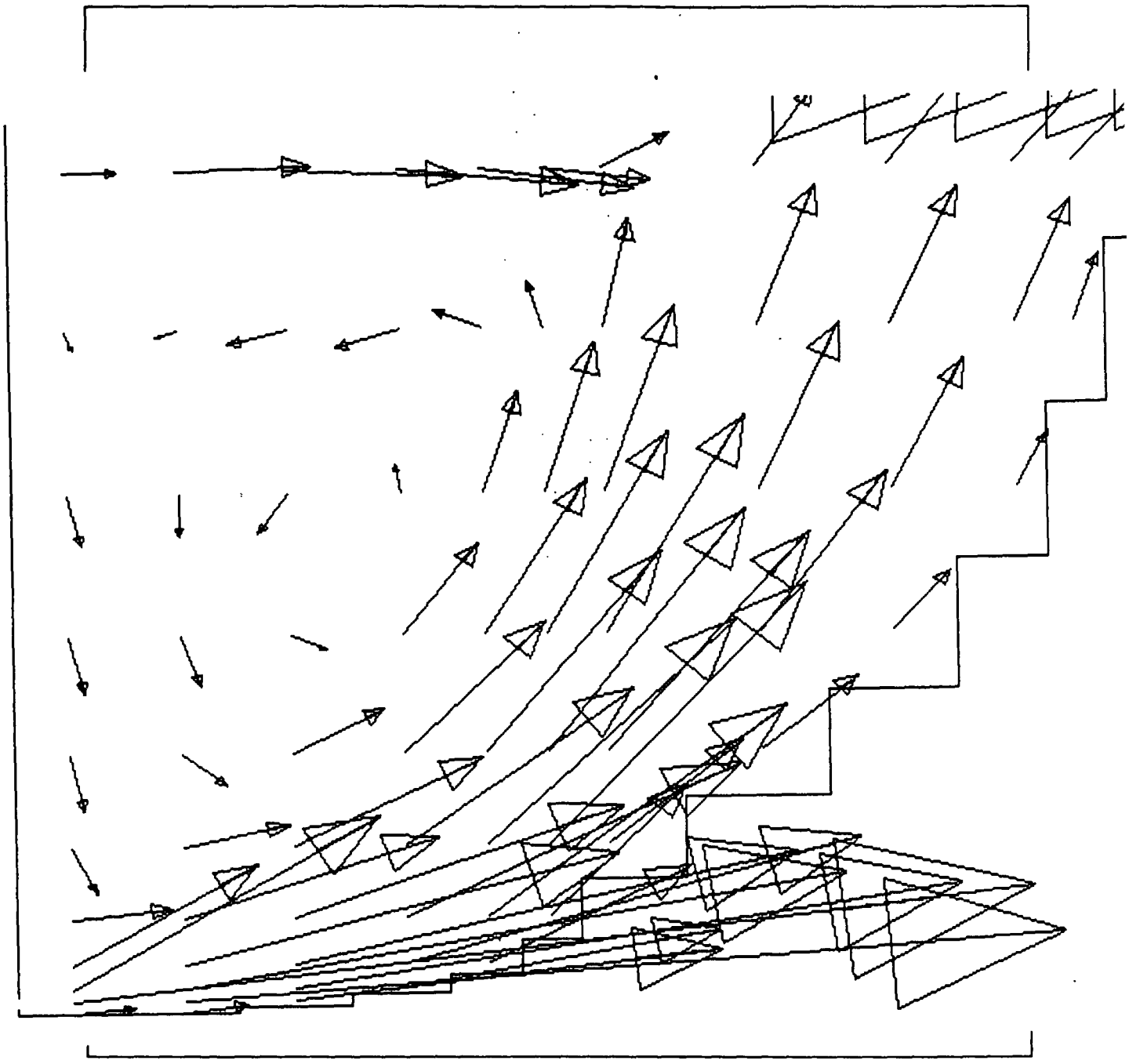

Figure 34 - Further Zoom of Lower Left Corner of Figure 31

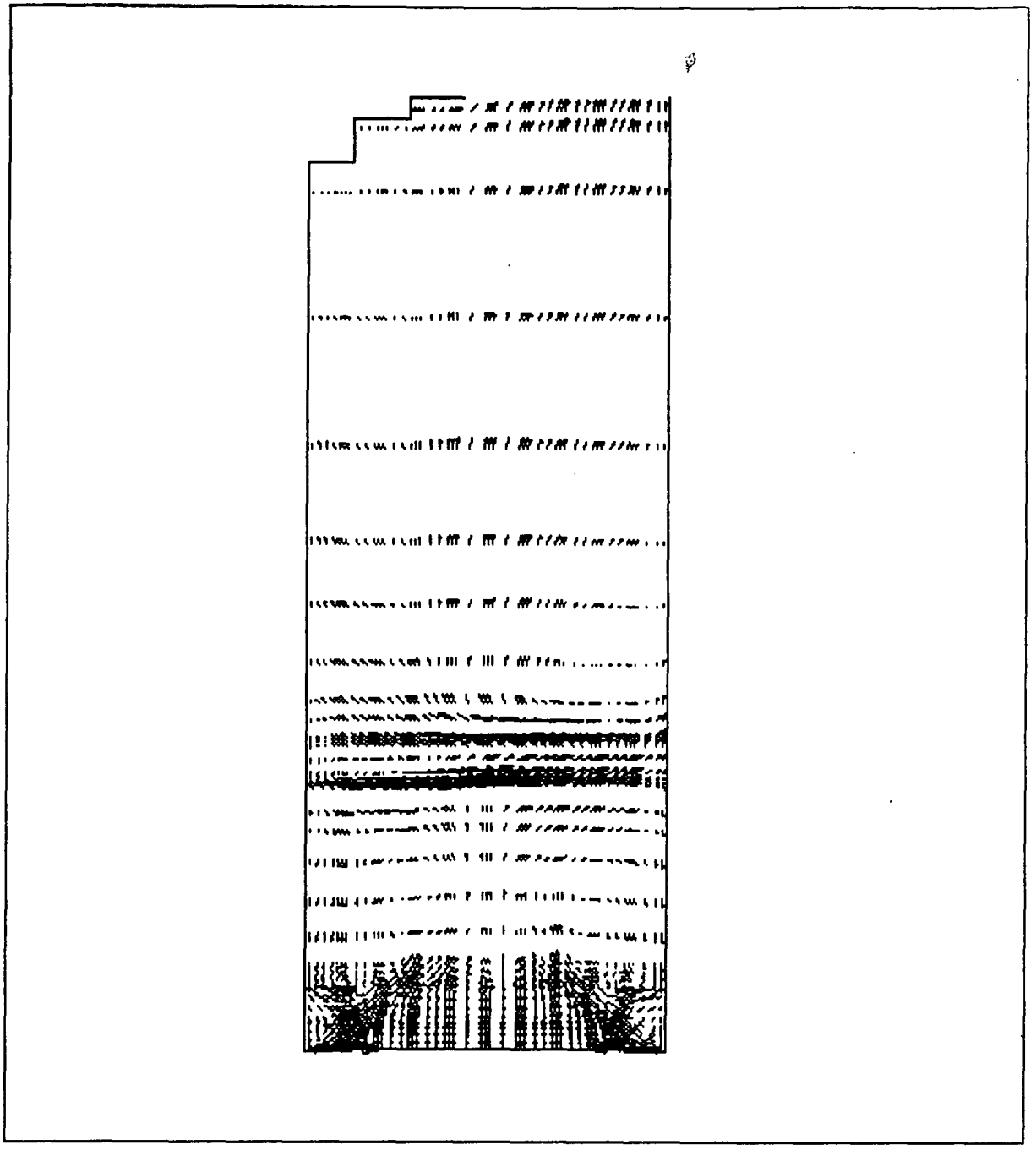

Figure 35 - Vertical Slice of Furnace Near Side Wall

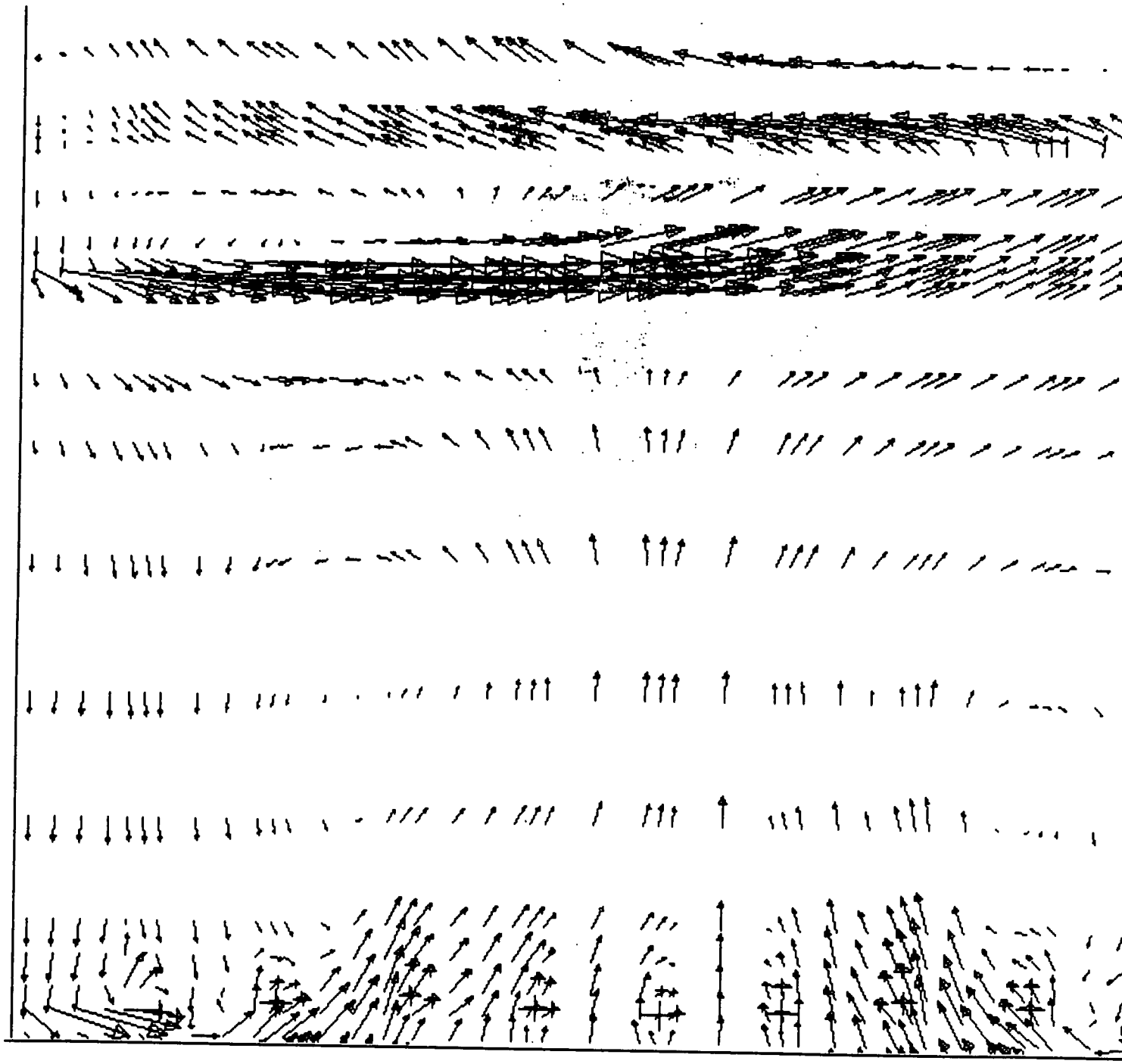

Figure 36 - Zoom of Figure 35 Showing Lower Recirculation Pattern

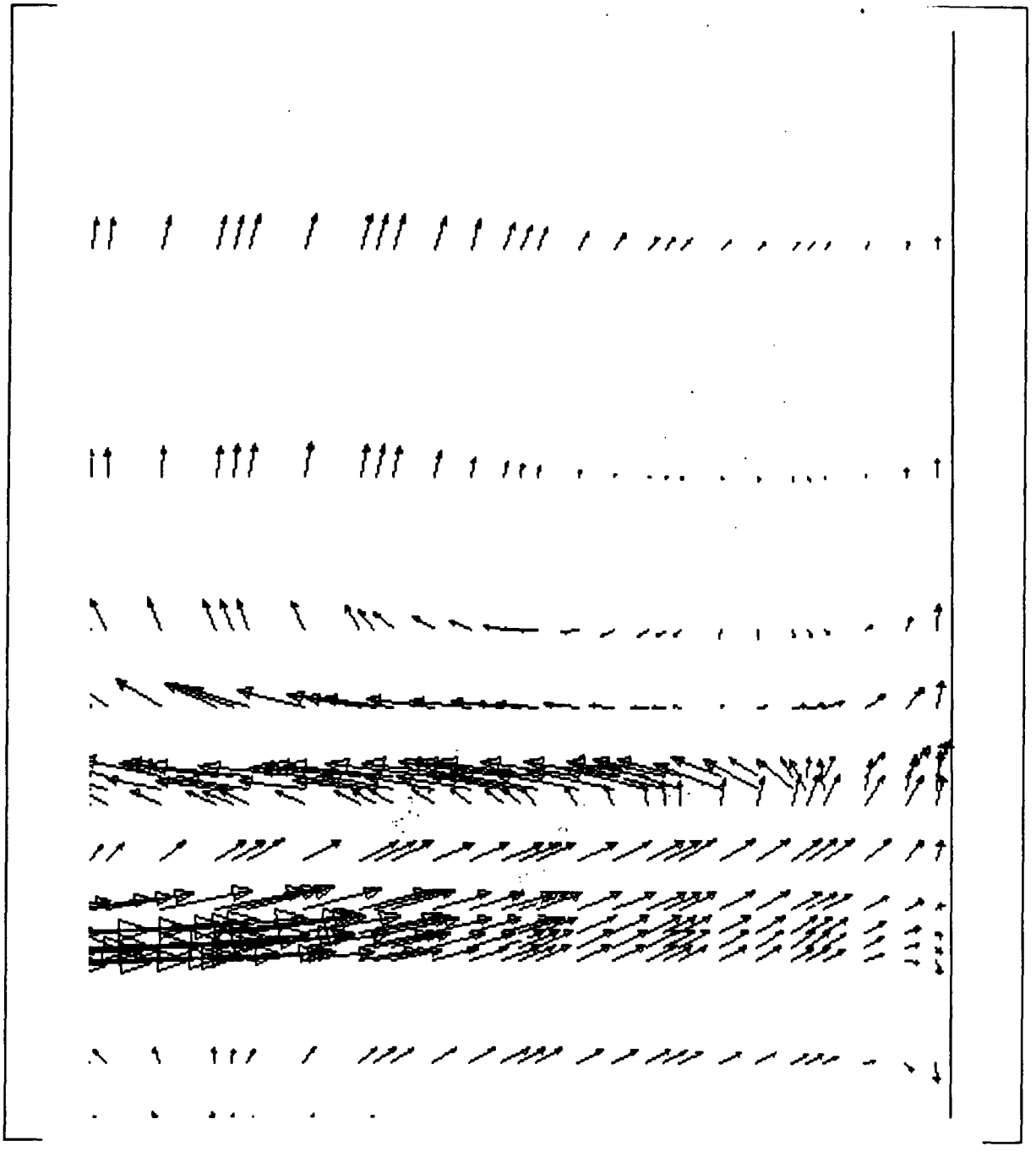

Figure 37 - Zoom of Figure 34 Showing Recirculation Above Tertiary Jets

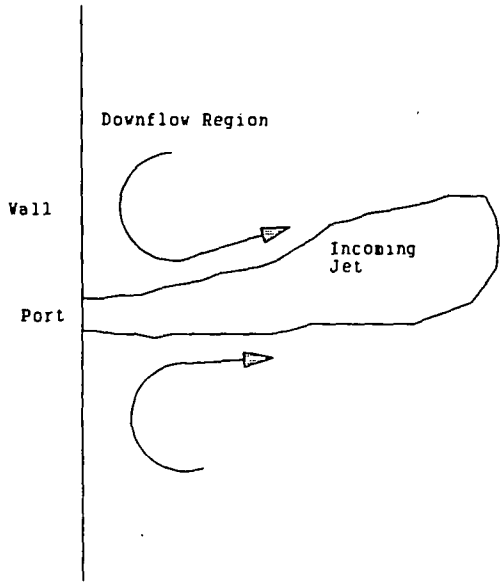

Figure 38 - Entrainment Process

Two questions need to be addressed: "Why does this central core form?", and "Why are the tertiary jets ineffective in breaking it up?". The formation of the central core is easy to explain. When the jets from all four walls meet in the center of the furnace, they have no choice but to bend upward, as the other jets prevent deflection right or left, and the char bed prevents deflection downward, this can be seen in Figures 39 through 41. This behavior could be overcome by the use of two wall interlaced secondaries, and this is being done on many new furnaces, and in retrofits of older furnaces. The secondary jets would not collide in the center of the furnace; instead, they would form an interlaced pattern that would provide good mixing and not promote the formation of the center core. Figure 39 shows the kinetic energy of turbulence of the jets as they enter the furnace, this is convenient for showing velocities in both the x and z directions at the same time. The kinetic energy of the jets on the front and back walls appears slightly lower. This effect seems to be due to downflow induced by the tertiary jets located on the front and back walls.

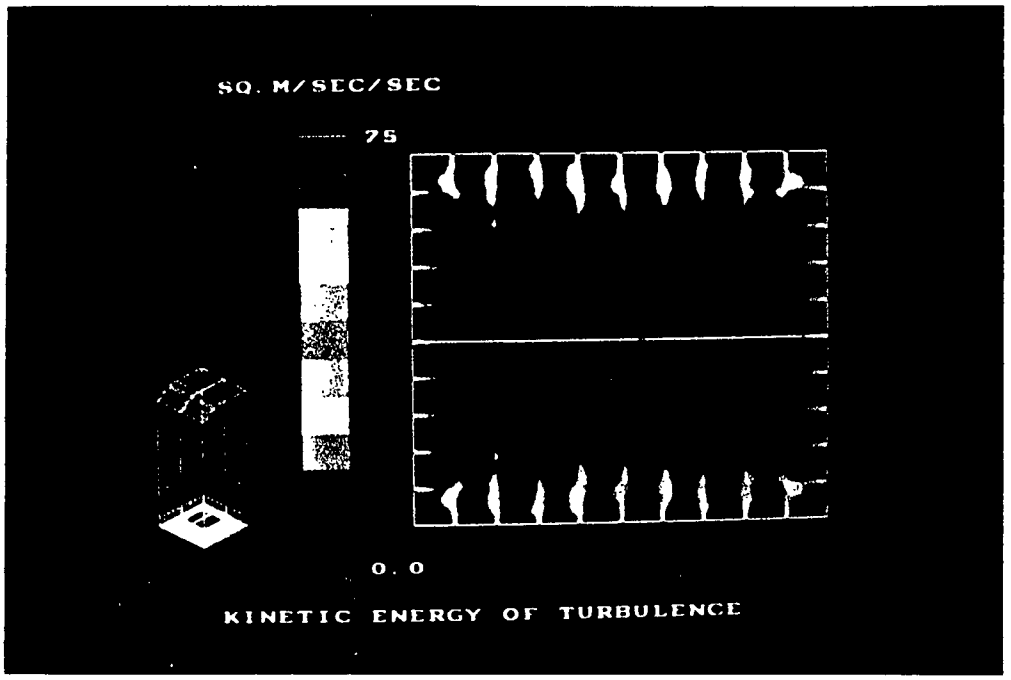

Figure 39 - Penetration of Secondary Jets at Centerline of Secondary Inlet

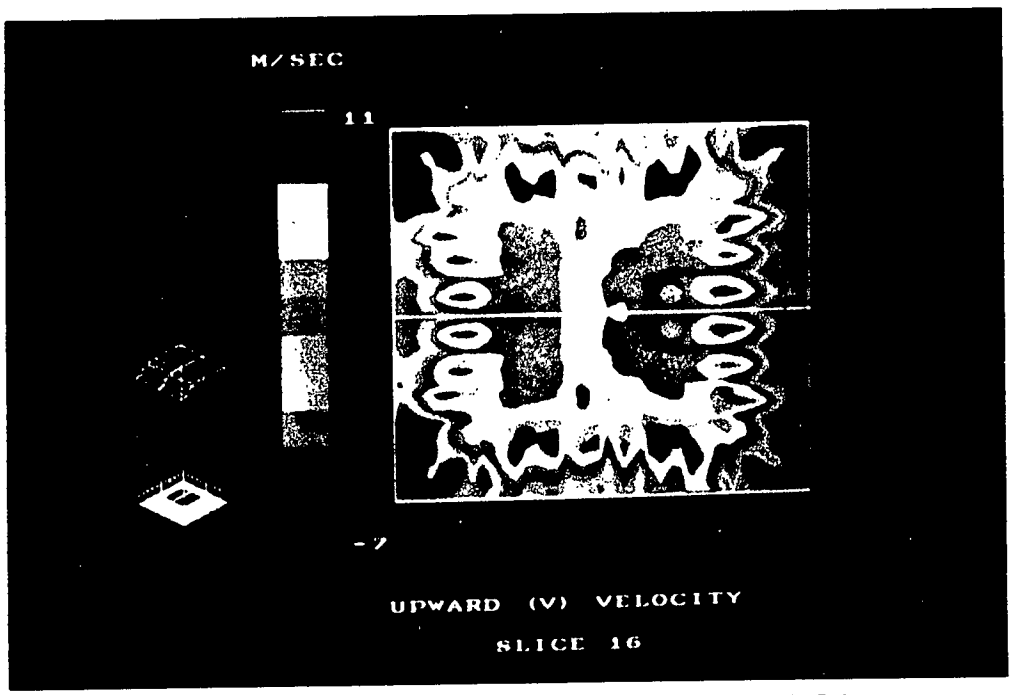

Figure 40 - Upward Flow One Meter Above Secondary Air Inlet

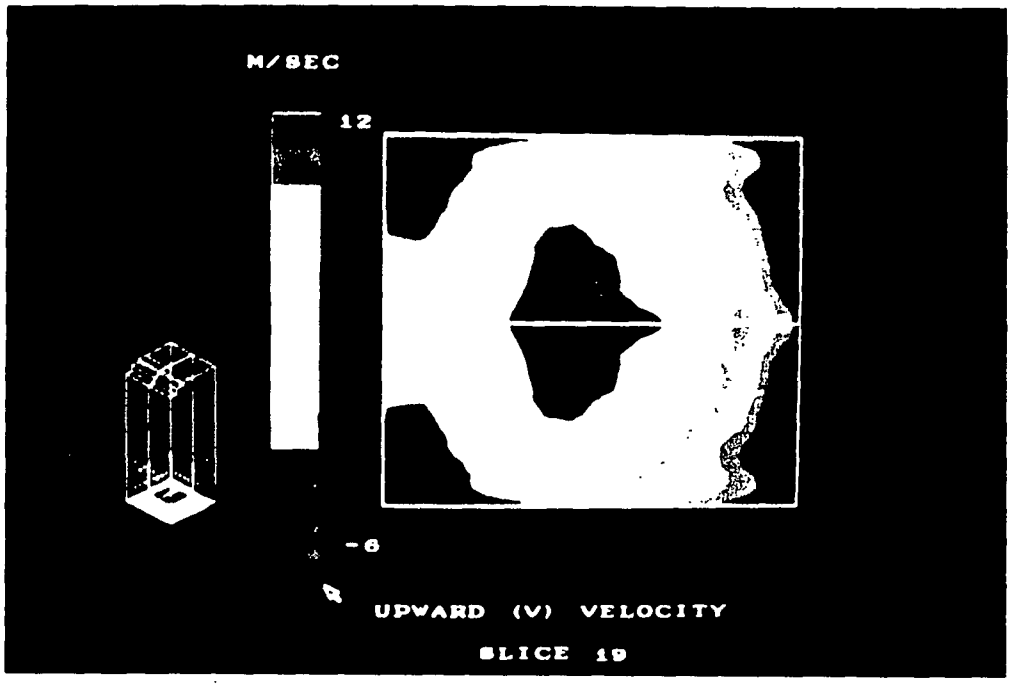

Figure 41 - Upward Flow at Black Liquor Gun Level

The reasons for the tertiary jets being ineffective in breaking up this center core are harder to determine, especially considering the results of the cold flow modelling presented earlier, where the center core was broken up. A likely reason for the core being more persistent is the lower height of the bed in the Base Case, as compared to the bed used in the cold flow case. The lower bed did not extend above the level of the secondary jets, permitting a greater fraction of the secondary air to meet in the center and enhancing the formation of the center core.

The tertiary jets used in the case are meant to be interlaced, when in fact considerable collision occurs between the jets as they reach the center of the furnace; this is shown in Figures 28, 29 and 30. An illustration of what is happening is shown in Figure 42. The jets spread as the enter the furnace and collide, this makes the jets less effective in breaking up they center core, as the collisions of the individual jets tends to create upflow.

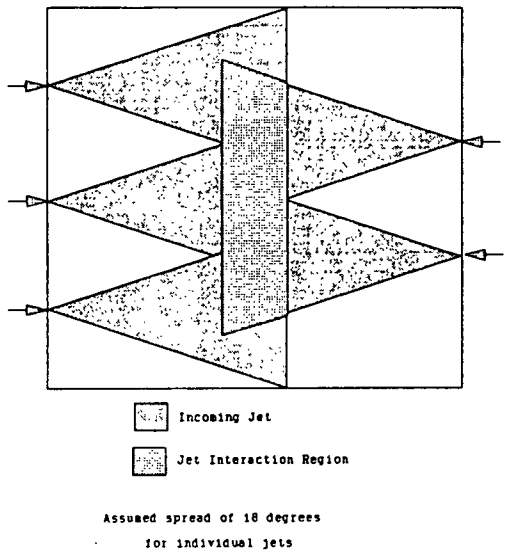

Figure 42 - Collision of "Interlaced" Jets

Corrosion

Corrosion can be severe on a wall surface that has a high incident heat flux and high concentrations of oxygen.[35] Potential problem spots on the furnace wall can be determined by simultaneously viewing the radiative heat flux and the oxygen mass fraction in those cells immediately adjacent to the wall; this is shown in Figures 43, 44, and 45.

The worst combination of high heat flux and oxygen concentration occurs immediately above the primary air ports on all four walls, a typical site for corrosion in operating recovery furnaces.

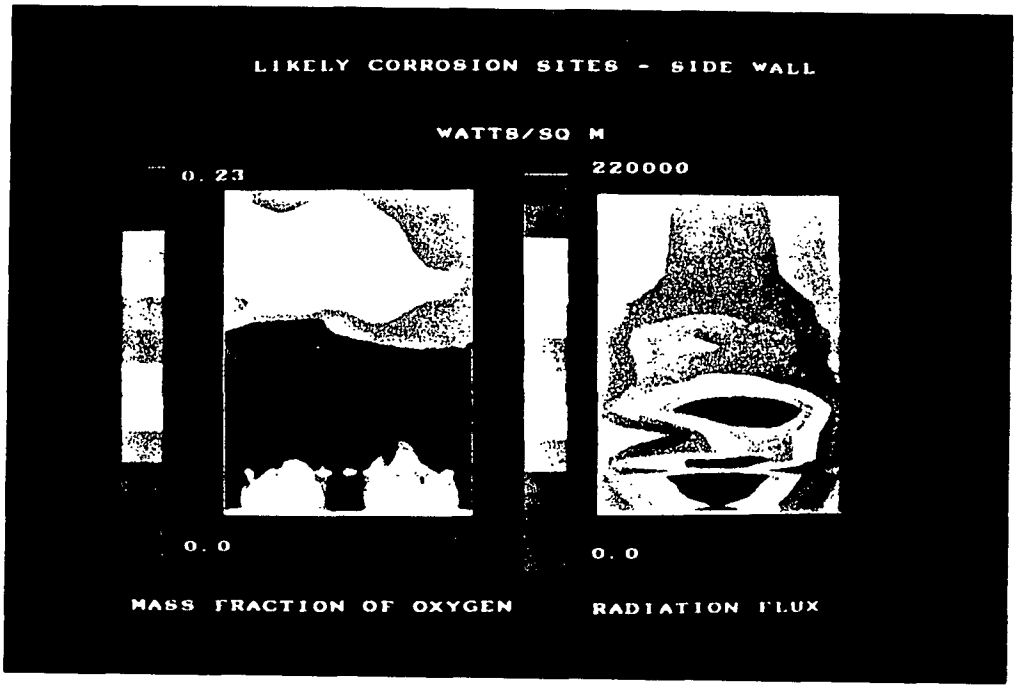

Figure 43 - Heat Flux and O_2 Mass Fraction Adjacent to Side Wall

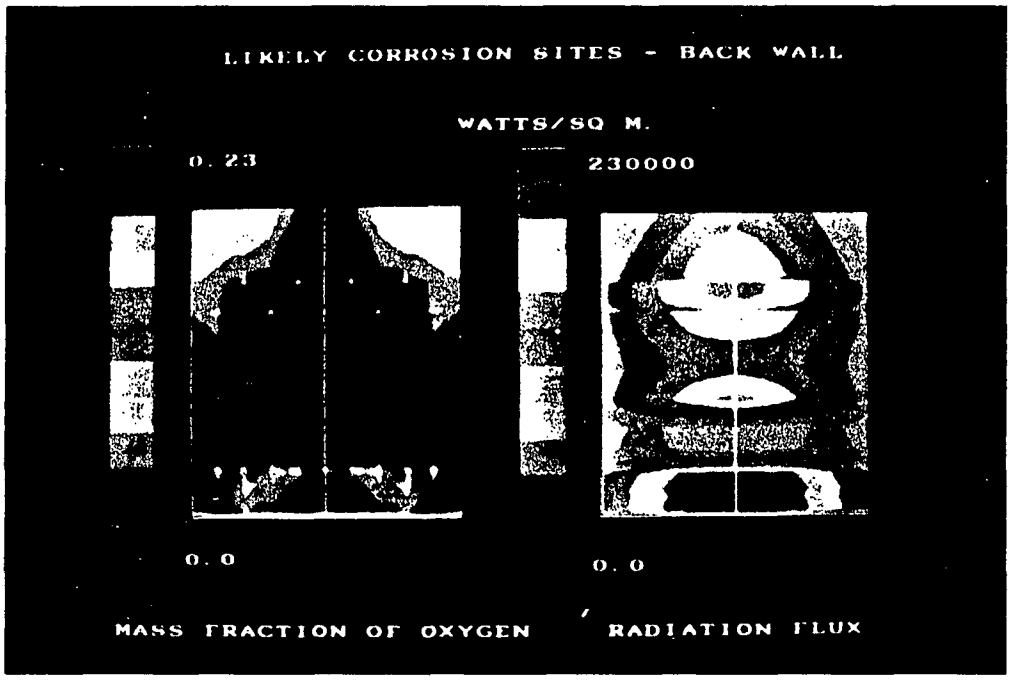

Figure 44 - Heat Flux and O_2 Mass Fraction Adjacent to Sites on Back Wall

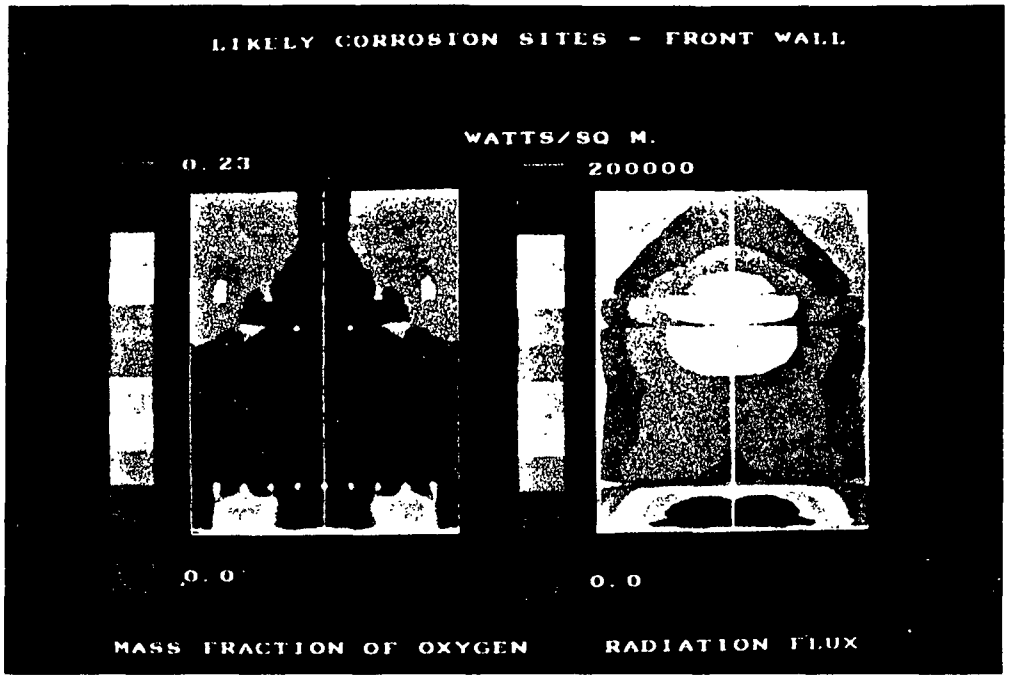

Figure 45 - Heat Flux and O_2 Mass Fraction Adjacent to Front Wall

Species Mass Fractions at the Exit

Exit mass fractions of oxygen, carbon monoxide and fuel will be examined in this section. The average oxygen mass fraction at the exit is 4.2%, which is within the observed range in operating recovery furnaces.

An operational problem discussed earlier was emissions, usually the species of concern are SO_2, CO, and reduced sulfur compounds. Only CO emissions can be evaluated as sulfur species are not determined by the version of FLUENT/RFM used in this thesis. Emissions of CO can be determined by plotting CO mass fraction as the gases pass through the exit plane. With the present version of FLUENT/RFM it is not possible to track sulfur species. Figure 46 shows the mass fraction of CO over the exit plane of the furnace.

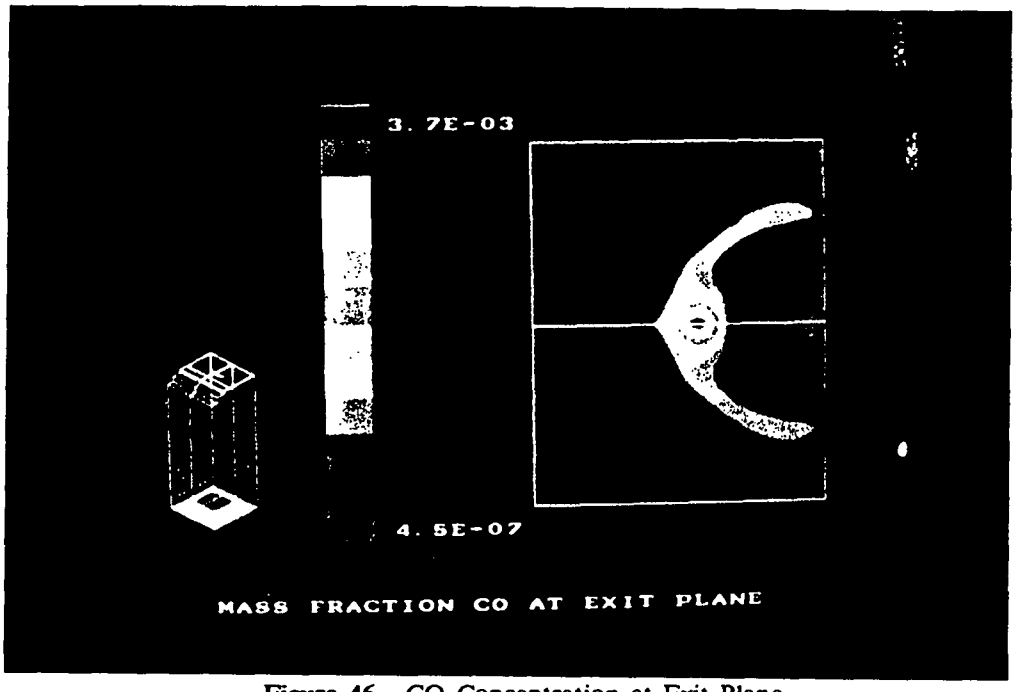

Figure 46 - CO Concentration at Exit Plane

The average CO concentration over the exit plane is 425ppm, which is within the range of observed values (200-2000ppm).[36,37]

The results presented in Figure 46 show that the highest mass fractions of carbon monoxide are found in the center of the furnace. The center core discussed earlier is deficient in oxygen. The uncombusted or partially combusted species in this center core do not mix with the combustion air and do react to completion (i.e. form H_2O and CO_2). The lack of oxygen in this area of high CO concentration at the outlet is shown in Figure 47.

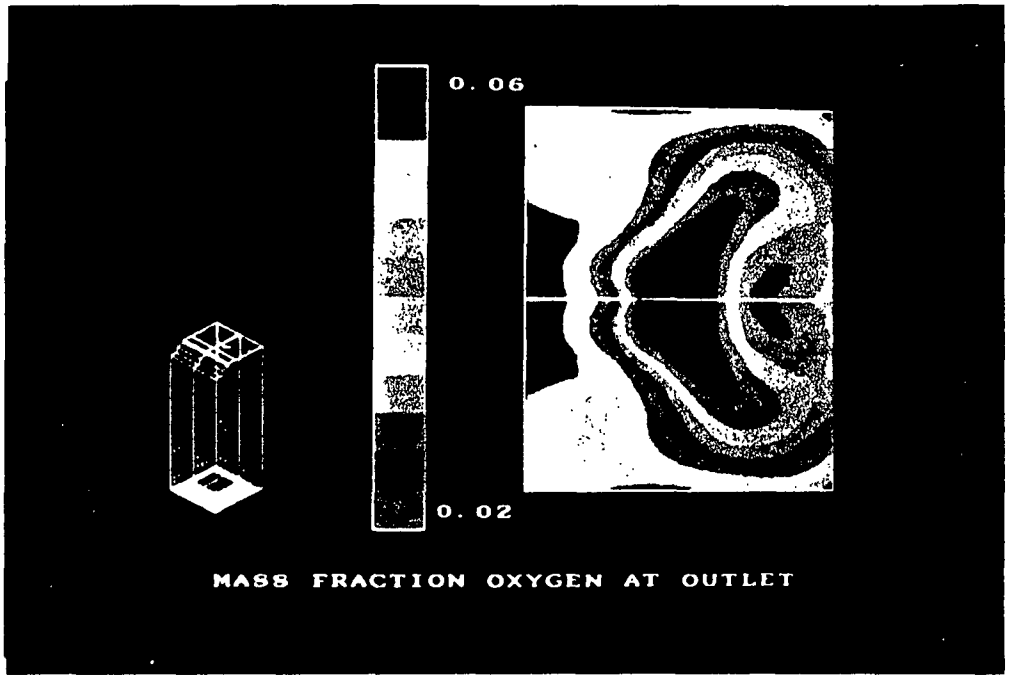

Figure 47 - Oxygen Concentration at Outlet

Temperature Distributions

The temperature distributions in the Base Case are presented in two forms: as average temperatures over cross-sectional slices of the furnace, and as detailed plots of the temperature over the cross-sectional slices. The dominant feature of the temperature distribution is once again the center core, although the effects of liquor and bed burning create local temperature peaks.

Figure 48 shows the average temperature as a function of height above the bed; this shows that the temperature passes through a maximum above the bed and then drops as the gas travels up and out of the furnace cavity. The exit temperature is 750 C, lower than what is normally seen. The lower exit temperature can be attributed to the lack of bed burning taking place in this simulation. The bed burning model used in FLUENT/RFM predicted a net bed growth of 2 kg/sec. Bed growth reduces the exit temperature by diminishing the total heat release. The reduced char combustion also means that excessive amounts of combustion air have been added to the furnace, causing a reduction in the exit temperature due to the dilution effects of these incoming gases.

The general shape of the temperature vs furnace height curve agrees with experimental results.[38] The peak in temperature occurs slightly above the surface of the char bed, where large amounts of CO and pyrolysis gas are present, the secondary jets provide the combustion air.

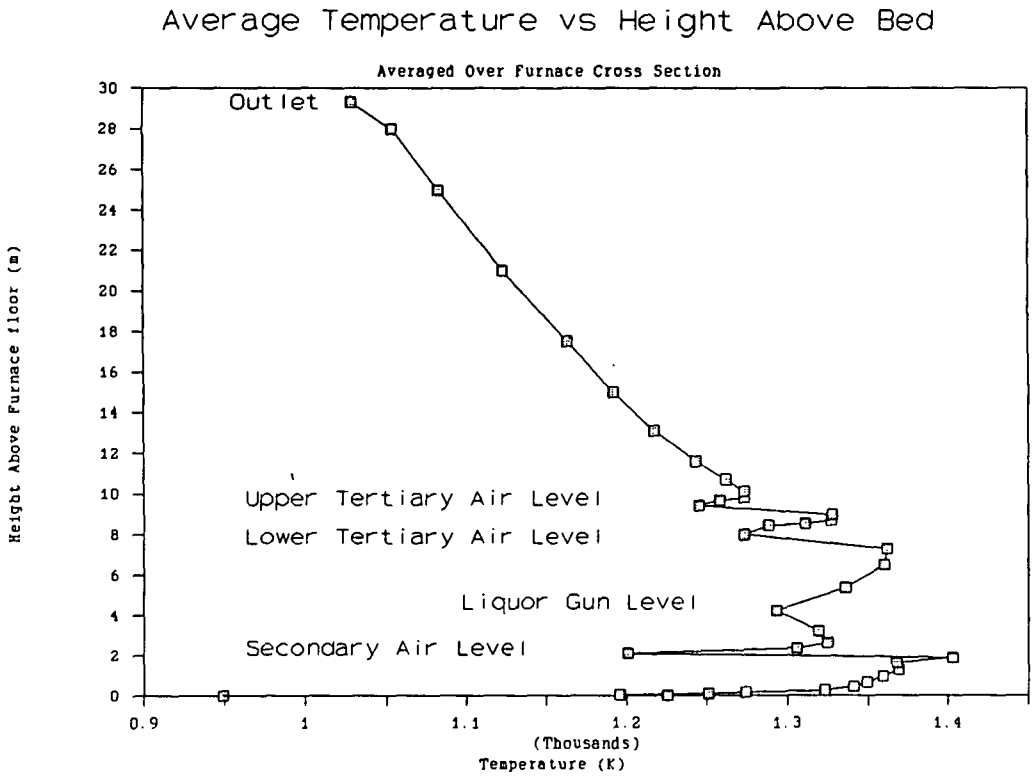

Figure 48 - Temperature as a Function of Furnace Height

The three-dimensional distribution is complex, this complexity usually cannot be determined experimentally, leading to plots of average temperature as a function of height. Figures 48 through 51 show the three-dimensional nature of temperature.

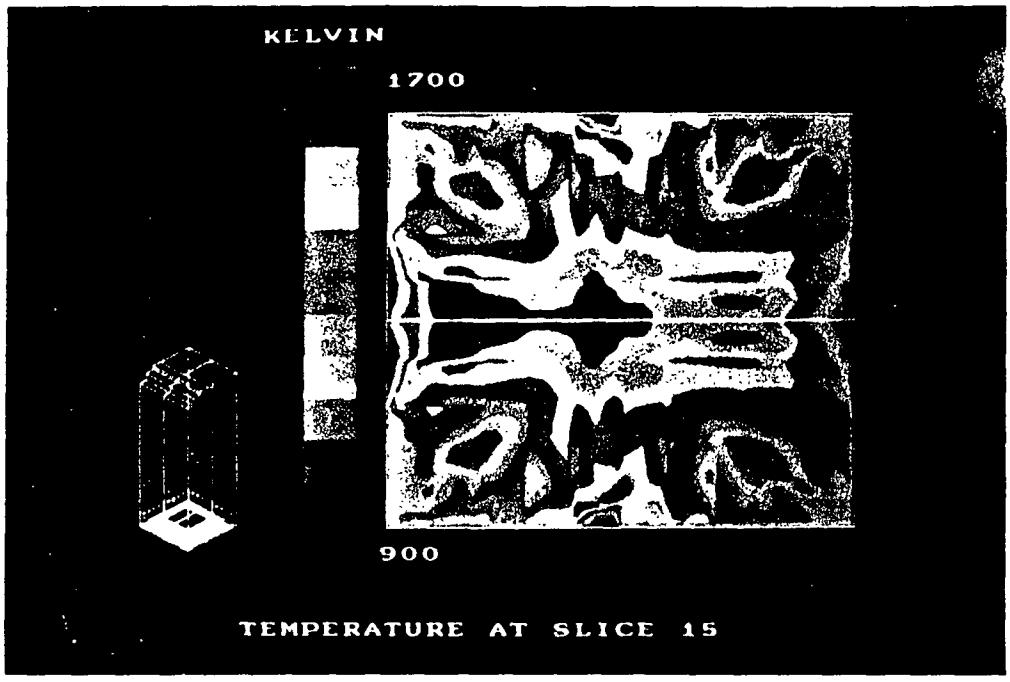

Figure 49 - Temperature Immediately Above Secondary Air Level

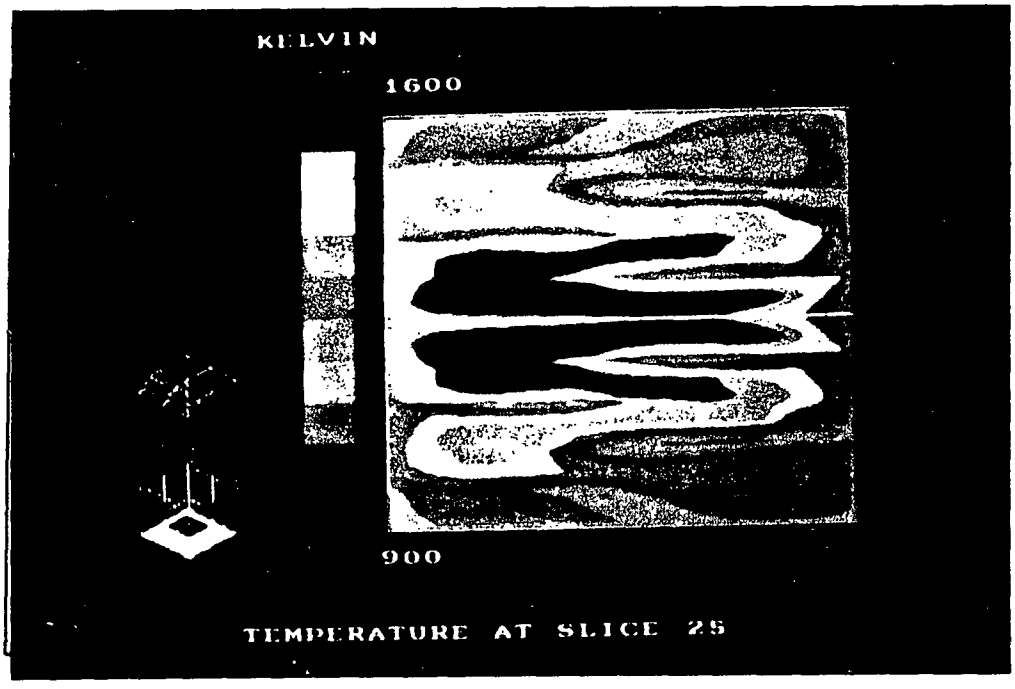

Figure 50 - Temperature at Tertiary Air Level

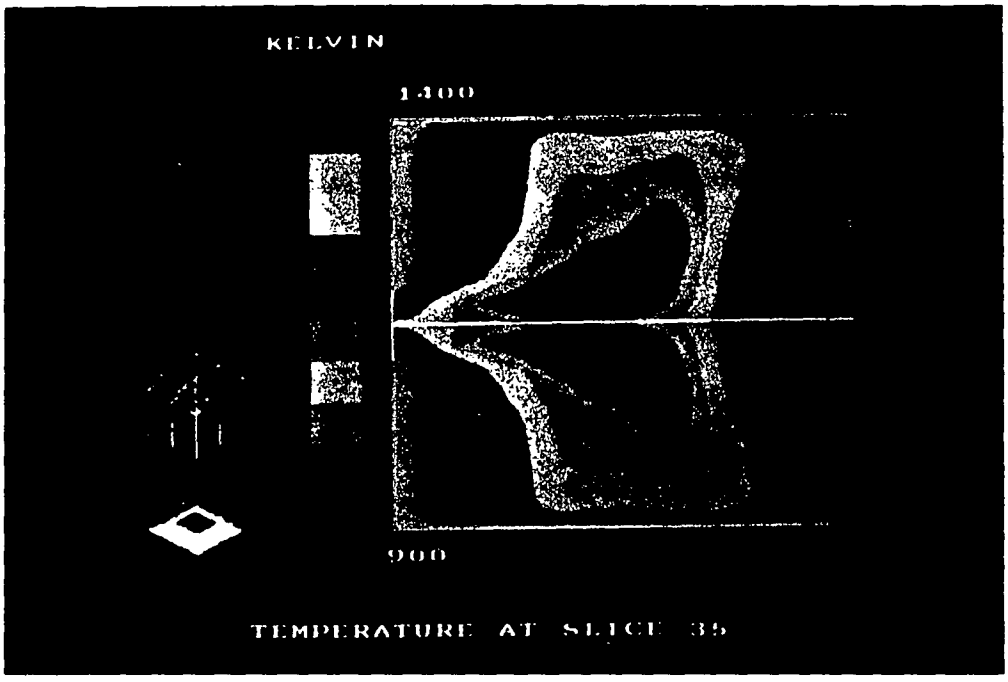

Figure 51 - Temperature Midway Between Tertiary Air Level and Outlet

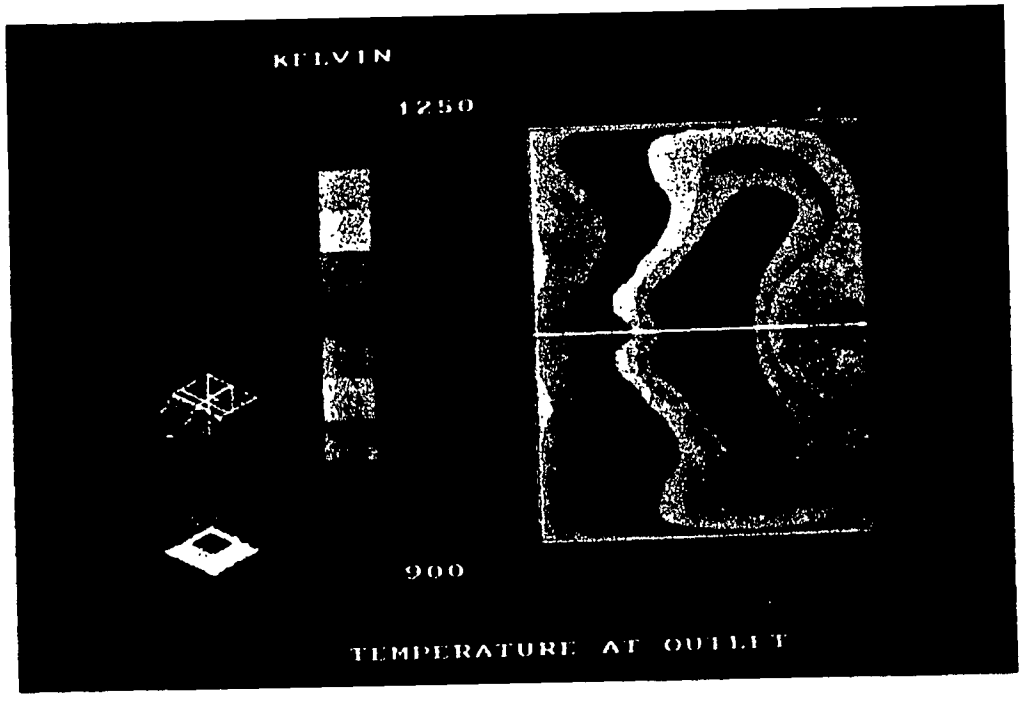

Figure 52 - Temperature at the Outlet

Carryover

The carryover is measured by the amount of black liquor that passes through the exit plane of the furnace. The black liquor is in the char burning or burnt-out stages by the time it reaches the exit. In the base case approximately 0.3 kg/sec of char is exiting the furnace as carryover; this is 2.0% of the total black liquor entering the furnace, and 6.4% of the total inorganic entering the furnace. The amount of carryover is a function of furnace gas velocity, oxygen concentration, and temperature, as shown by Walsh in his PhD thesis.[30] The center core discussed previously is hot, low in oxygen, and has a high upward velocity, all of which promote carryover.

The Energy Balance

A few aspects of the energy balance can be compared against existing data. The work of Lavery examined the heat fluxes incident on furnace walls during oil burning.[39] The total heat input was 108.1 MW; the heat flow to the walls was 40.7 MW or 37.7% of the input, while the heat flow out the furnace exit was 62.3 MW or 57.6% of the total input. The casing losses and the error in the energy balance accounted for the remaining heat. The base case had a total heat input of 118.3 MW; the heat flow to the walls was 48.5 MW, or 41.0% of the total heat input, and the heat flow out the furnace exit was 55.7 MW or 47.1% of the total heat input. The Base Case has a number of sinks of enthalpy, including the enthalpy of the carryover; the enthalpy of inorganic material that accumulates on the bed; and the unrealized combustion of fuel, carbon monoxide, and char carbon as it exits the bounds of the furnace.

The ratio of heat to the walls and enthalpy of exit gases is 0.65 in the experimental case and 0.87 in the Base Case. The fraction of heat transferred to the walls in the Base Case is higher than that seen experimentally. The main reason for this discrepancy is the differences in geometry. The experimental work had the majority of the heat release at the top of the furnace, as this was where the oil burners were located. The lower walls of the furnace received low heat fluxes. In the Base Case all of the wall

surface area is used; this results in a greater transfer of heat to the walls, and less enthalpy in the exit gases.

Heat flux measurements on a recovery furnace during black liquor firing should result in a better comparison. In addition, experimental work would permit a determination of the effective wall emissivity, the absorption coefficient of the furnace gas, and the scattering coefficient of the gas. Currently the numbers used in the model are estimates.

Conclusions

The conclusions that can be drawn from the Base Case simulation:

1. A recovery furnace simulation using all the available flow variables in FLUENT/RFM can be converged;

2. The dominant characteristic of the flow is the large center core that forms in the center of the furnace, opposing secondaries on all four walls (or primaries in a CE unit) create this central core, the tertiary jet arrangement used in the Base Case was unable to break up this central core;

3. The operational problems of corrosion, emission of carbon monoxide, and carryover were examined by use of FLUENT/RFM. Many more aspects of recovery furnace behavior can be examined if they can be related to the three-dimensional distribution of temperature, gas velocities, species concentration, black liquor behavior, and bed burning. Emissions of sulfur species is not possible with this version of FLUENT/RFM;

4. A limited amount of comparison can be made between the Base Case and experimental data due to the minimal amount of experimental data available. The comparison performed generally were favorable, including overall flow patterns, carbon monoxide, oxygen. Discrepancies were found in the heat balance and the exit temperature; although partial explanations of these differences were given.

THE SIMULATION OF THE BASE CASE WITH A UNIFORM TEMPERATURE

The use of scale modelling of recovery furnaces in order to examine the effects of furnace geometry, port geometry, and air distributions, hinges on one basic assumption: that the "cold flows" are a good approximation to the flows in an operating recovery furnace. The cold flow work assumes that the effects of black liquor can be approximated by a use of a temperature of the furnace gases equal to the average temperature in an operating furnace. The effects such as temperature distributions, drop-gas interactions, and bed burning are neglected. Using FLUENT/RFM it was possible to examine the validity of this assumption.

Description of the Case

The simulation used in this investigation had a gas density of 0.235 kg/m^3, which assumes that the gas temperature is 1300K, a typical average temperature for the gases in the kraft recovery furnace. It was necessary to increase the velocity of the incoming jets in order to maintain the same momentum as in the Base Case, as the lower density used resulted in lower mass flow rates through the air ports. Momentum is equal to mass times velocity. If the density of the gas is assumed to be 0.235 kg/m^3 everywhere, including the inlets, then the velocity at the inlets must be increased. The ratio used equals the density of air at 400K (a typical entering temperature) divided by the density used. The geometry used was identical to the Base Case, as was the distribution of mass between the three levels of air. The viscosity of the gas used was that of air at 1300K.

Results

This section will compare the gas flows obtained in the Base Case with those found in the simulation of the Base Case with a uniform temperature. Only the upward velocities will be considered. The comparison was made between the general flow patterns and not the actual velocities. This was necessary as the adjustment made to the incoming velocities makes it impossible to compare absolute velocities as the higher inlet velocities create higher velocities througout the furnace. Figures

53-58 show upward velocity of both cases over a series of cross-sectional slices of the furnace. Figures 59 and 60 show a surface of constant upward velocity for each case.

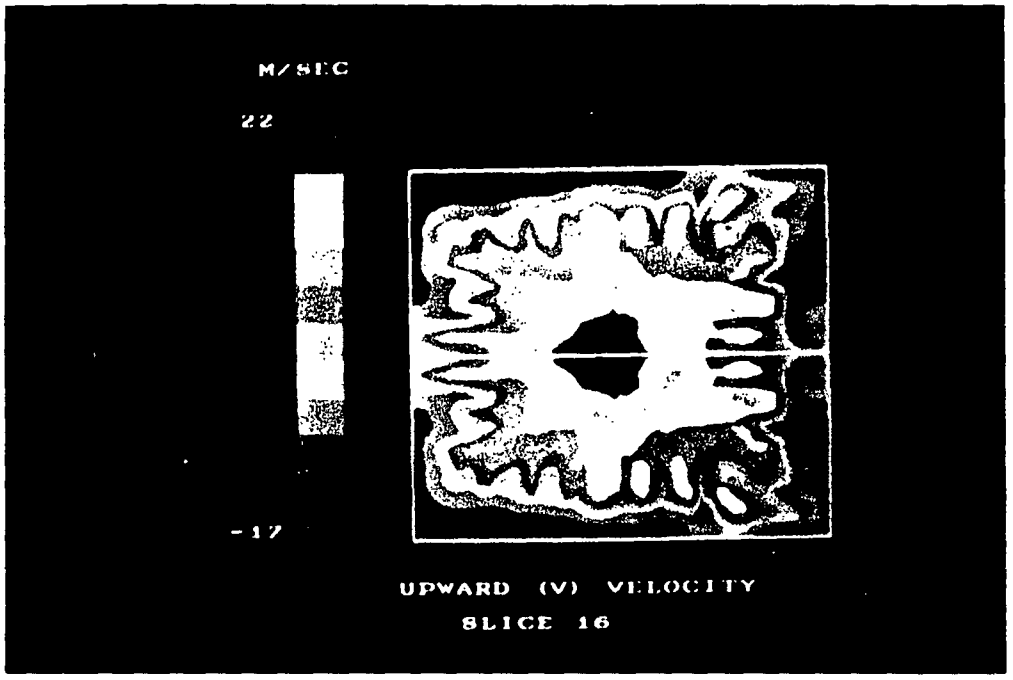

Figure 53 - Upward Velocity Immediately Above Secondary Air Level
Average Temperature Case

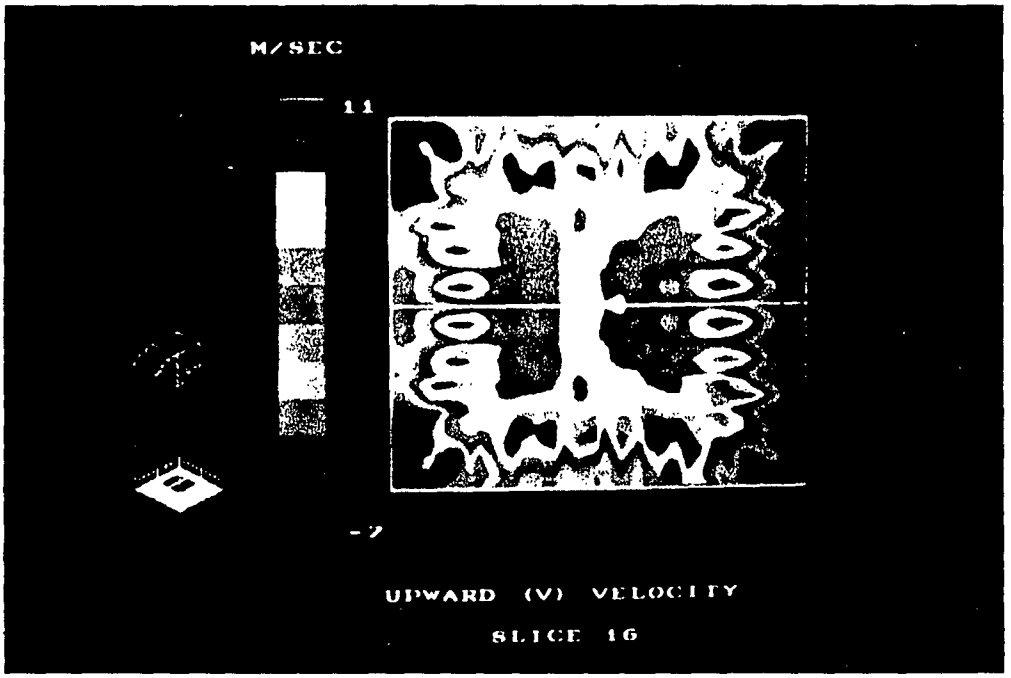

Figure 54 - Upward Velocity Immediately Above Secondary Air Level
Base Case

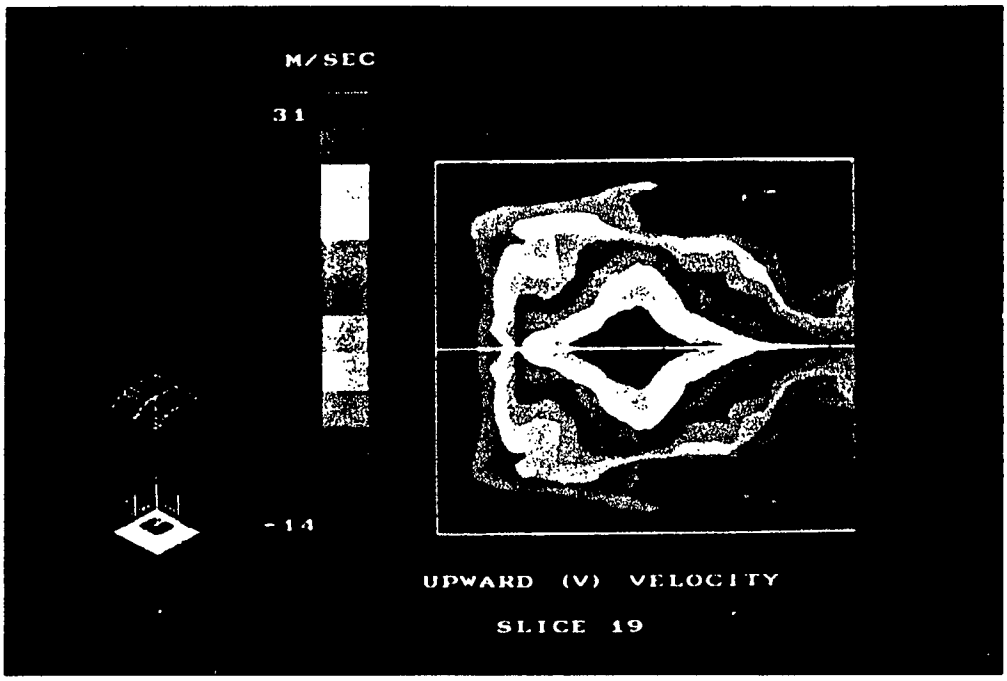

Figure 55 - Upward Velocity at Level of Liquor Guns
Average Temperature Case

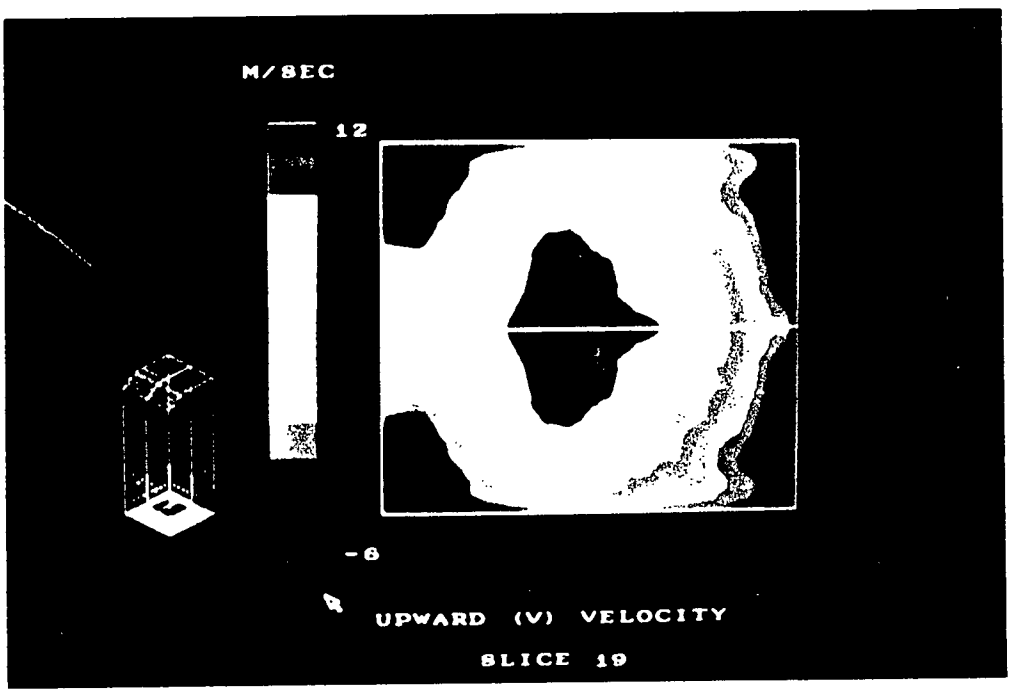

Figure 56 - Upward Velocity at Level of Liquor Guns
Base Case

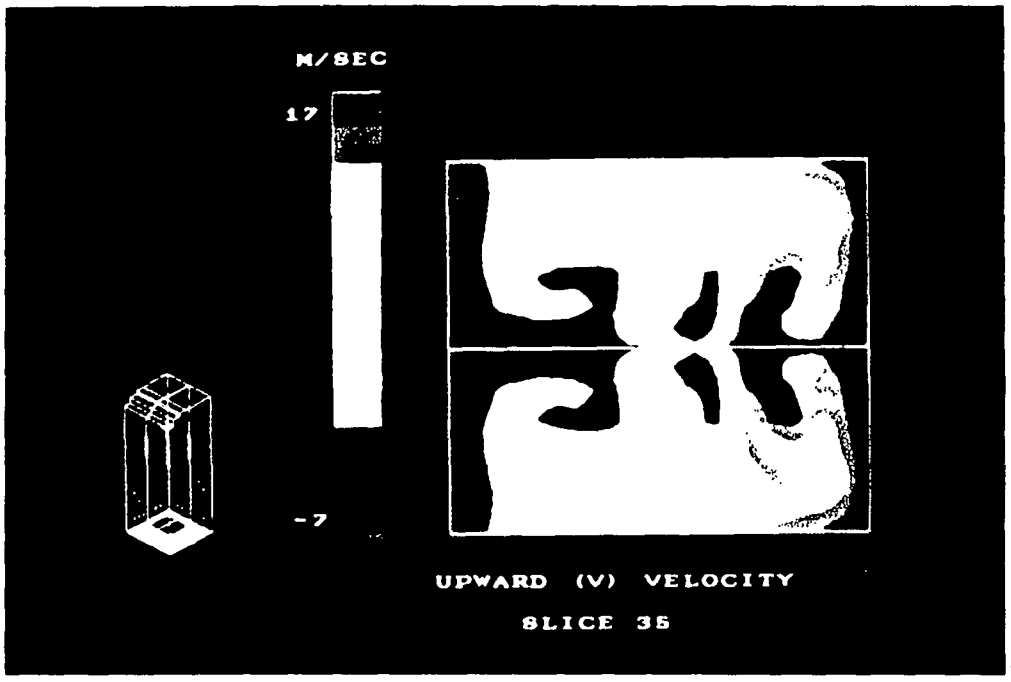

Figure 57 - Upward Velocity Midway Between Tertiary Level and Exit
Average Temperature Case

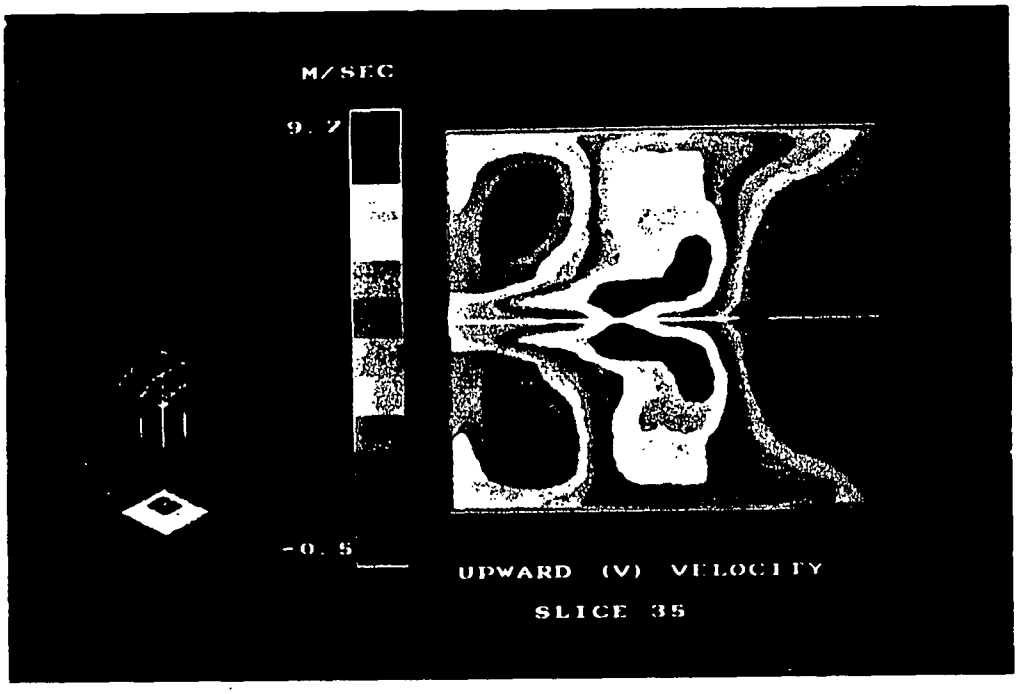

Figure 58 - Upward Velocity Midway Between Tertiary Air Level and Exit
Base Case

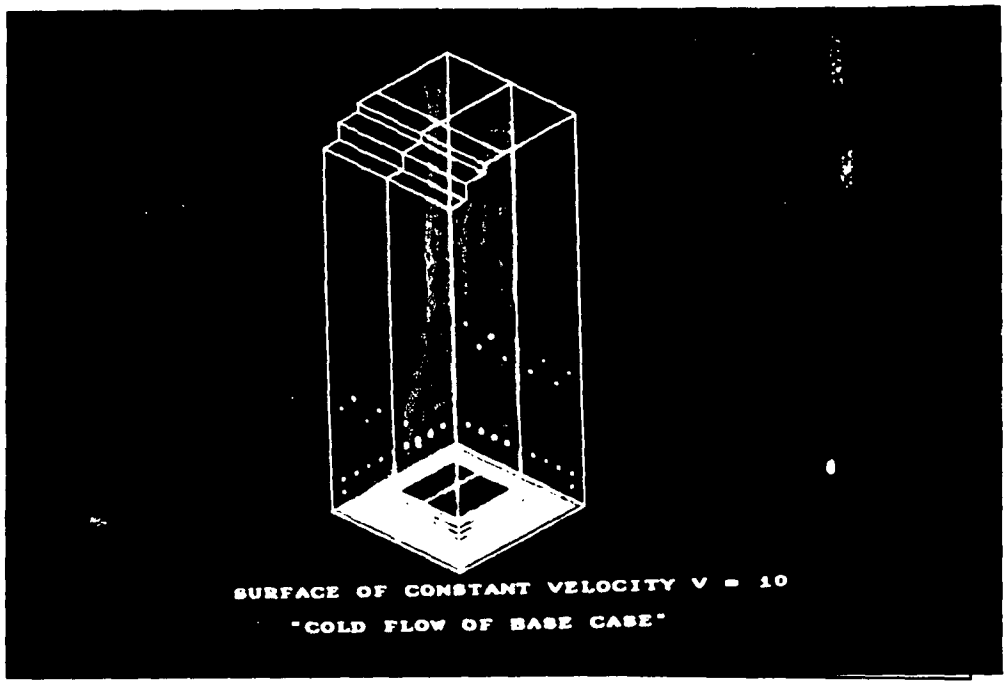

Figure 59 - Surface of Constant Upward Velocity
Average Temperature Case

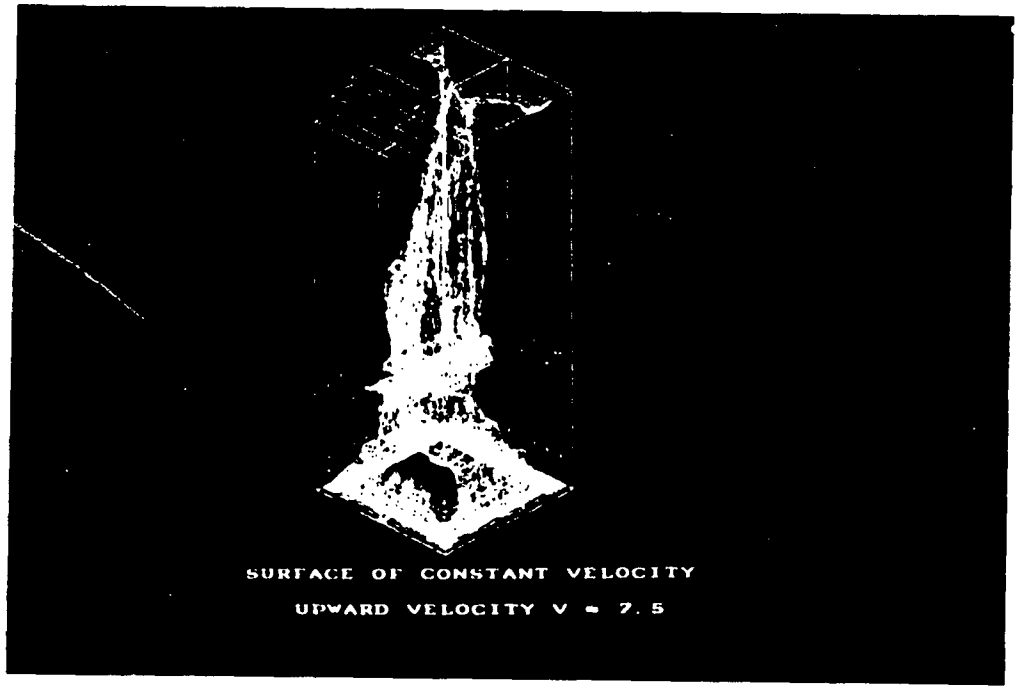

Figure 60 - Surface of Constant Upward Velocity
Base Case

A comparison of the preceding Figures demonstrates that the flow patterns in both of these case are similar. Areas of upflow and downflow are seen in the same parts of the furnace. The major difference is seen in Figures 53 and 54. The center core forms lower in the furnace in the cold flow case, the hot bed in the Base Case may generate enough convective flow that it serves to direct the secondary jets up slightly above the surface of the bed. Based on this investigation it appears that cold flow models of the recovery furnace reproduce the gas flows found in operating furnaces.

CONCLUSIONS

The following conclusions can be drawn as a result of this thesis:

1. It is possible to construct and run a recovery furnace model which incorporates all key process elements (three-dimensional geometry, turbulent gas flow, radiative heat transfer, char bed behavior and geometry, detailed air port geometry and air entry conditions, black liquor spray characteristics, and combustion of pyrolysis gas). A converged simulation can be obtained, albeit with considerable effort (4 months on a MicroVAX II), and the results are logical and consistent with expectation;

2. A large center core of high upward-velocity gas is developed as a consequence of the analytical solution of the Base Case. This central core, which is a dominant feature of the flow, is formed by the collision of the primary and secondary air jets in the center of the furnace. The center core is not effectively broken up by the tertiary jets;

3. Full validation of the FLUENT/RFM code was not possible because detailed data on flow variables in actual recovery furnaces were not available. However, the basic FLUENT code was validated by comparing the results of a cold flow simulation with experimental flow data from recovery furnace scale models. The results of simulations using the full FLUENT/RFM code are reasonable, internally consistent and in qualitative agreement with experience;

4. The gas flow patterns in the Base Case simulation were similar to the patterns in a simulation using the same furnace geometry and a uniform temperature comparable to the bulk average temperature from the Base Case, but without combustion. This suggests that gas flows in recovery furnaces act like driven flows and are primarily a function of furnace geometry and the details of air introduction and are only weakly affected by the combustion processes. This implies that experimental cold flow testing of scale model furnaces can provide useful information for furnace design and/or troubleshooting;

5. The stability of the center core of high upward velocity gas is a strong function of conditions in the lower furnace as well as the momentum in the tertiary air jets. The center core persisted through the furnace in the Base Case simulation and in a simulation using the identical geometry with a uniform temperature compariable to that in the Base Case, but with no combustion. The tertiary air jets were unable to break up the center core in either of these cases. In contrast, the tertiary air was able to break up the core in another "cold flow" simulation in which the only difference in geometry was that the bed extended above the level of the secondary air inlets. In this case the high bed deflected the secondary air upward before it reached the center of the furnace and reduced the intensity of the center core. The vastly different results obtained in these two cases suggest the need for caution in making general statements about the behavior of the recovery furnace based on a few simulations.

RECOMMENDATIONS

Future efforts in the simulation of the kraft recovery furnace should involve the solution of additional cases, the improvement of the FLUENT/RFM code, and the use of larger, faster computers. These three recommendations are discussed in detail below:

1. The improvement of the FLUENT/RFM code should include the addition of more species, specifically H_2, H_2S, and SO_2. It may be possible to calculate the sulfur species concentration in a converged case, in essence freezing the gas flow patterns and oxygen concentrations and adding the reduced sulfur species as the fuel. The phenomenon of fuming should be included along with fume reactions; once again, this could be done using a converged case. The wall drying and pyrolysis model in FLUENT/RFM should be improved when experimental data becomes available. Information on black liquor behavior should be added as experimental results become available. Long term code developments include the inclusion of a dynamic model of bed growth and the use of body fitted coordinates, which will provide a better description of curved surfaces (e.g. the bed surface).

2. The hardware limitations that existed during this stage of the modelling work prevented this author and his colleagues from converging additional simulations. In order to overcome this problem a larger and faster computer is necessary. About 250,000 nodes are necessary in order to eliminate the plane of symmetry and to insure optimal placement of nodes around the bed and air ports. Currently the code requires about 2.5 Megabytes of RAM for every 10,000 nodes, with the addition of more species and the use of 250,000 nodes a computer with in excess of 75 Megabytes of RAM will be needed. In order to get convergence times down to a week and to handle 250,000 nodes along with the additional species a machine that is 50 times faster than the MicroVAX used in this work is necessary.

3. Additional simulations should be performed in order to determine is conclusions number one and two can be made more general. Specifically addressing conclusion one: do four wall secondaries always create the center core of high upward-velocity gas seen in the Base Case, and is the use of two-wall interlaced secondaries a way to overcome this problem ? Conclusion two could be generalized by performing the same two simulations as were done with the Base Case with a number of furnace geometries.

4. An effort must be made to obtain experimental data on operating furnaces and to then simulate the furnace using FLUENT/RFM; important flow properties are temperature, species concentration, and three dimensional velocity distributions. The best place to obtain this data would be at the furnace exit plane. In addition, parametric studies of a base case must be performed in order to find the input parameters which most influence the final flow; this would help in the identification of important research topics;

5. The convergence time of a simulation can be reduced by rewriting the code so that it can best make use of parallel processors. A parallel processor permits the simultaneous execution of computational tasks, rather than one step at a time.

ACKNOWLEDGEMENTS

I would like to thank Dr. Thomas Grace for his direction and insight, which was invaluable to the completion of this research. Thanks to the members of the my advisory committee, Drs. David Clay, Ted Farrington, John Cameron, Hugh Lavery, and Peter Parker. A special thanks to Ted for obtaining FLUENT, an essential component of the FLUENT/RFM model. Craig Brown and Weyerhauser graciously provided one of the MicroVAX computers that were used in the recovery boiler simulations.

Thanks to my wife, Paddy, for providing the love and support essential for my well-being, and thanks to the Institute and its member companies for providing the financial support enabling me to complete my doctoral thesis.

NOMENCLATURE

Variable	Explanation	Units
a_i	the finite difference coefficient Eq. [15]	dimensionless
A	a constant (= 4) Eq. [12]	dimensionless
$A(\lvert P_e \rvert)$	a coefficient that is a function of Peclet Number Eq. [20]	dimensionless
A_f	area of cell face perpendicular to flow Eq. [17]	m^2
A_i	the constant portion of the linearized C_p-T relationship Eq. [25]	kJ/(kg•K)
B_i	the slope of the C_p-T relationship Eq. [25]	kJ/(kg•K^2)
C_p	specific heat capacity (constant pressure) Eq. [8]	kJ/(kg•K)
C_1	constant in k-ε model (= 1.44) Eq. [4]	dimensionless
C_2	constant in k-ε model (= 1.92) Eq. [4]	dimensionless
C_μ	constant in k-ε model (= 0.09) Eq. [6]	dimensionless
d_m	effective diameter of char Eq. [27]	m
D_i	diffusion portion of P_e number Eq. [17]	kg/sec
E	black body emissive power Eq. [9]	kJ/(m_2•sec)
f	mass fraction of a chemical species Eq. [11]	dimensionless
F	convective portion of P_e number Eq. [17]	kg/sec
F_{CO}	mass fraction of CO as a product of fuel combustion Eq. [23]	dimensionless
F_{CO2}	mass fraction of CO_2 as a product of fuel combustion Eq. [23]	dimensionless
F_{H2O}	mass fraction of H_2O as a product of fuel combustion Eq. [23]	dimensionless
F_j	momentum exchange from second phase Eq. [2]	kg/(m^2•sec^2)
g_j	body force (i.e. gravity) Eq. [2]	m/sec^2
G_k	generation term of kinetic energy of turbulence Eq. [5]	kg/(m•sec^3)
h	enthalpy Eq. [8]	kJ/kg
I_{bal}	inert balance Eq. [26]	dimensionless
I_{out}	inert exiting the furnace Eq. [26]	kg
I_{in}	inert entering the furnace Eq. [26]	kg
k	kinetic energy of turbulence Eq. [3]	m^2/sec^2
k_t	total mass transfer coefficient O_2 to the bed Eq. [27]	kg/(m^2•sec•[O_2])
k_m	mass transfer coefficient O_2 to bed	kg/(m^2•sec)
k_r	reaction rate O_2 with C in bed	kg/(m^2•sec)
L	the distance between a central node and its neighbor Eq. [16]	m
m_f	mass fraction of fuel Eq. [12]	dimensionless
m_o	mass fraction of oxygen Eq. [12]	dimensionless
m_{prod}	mass fraction of combustion products Eq. [12]	dimensionless
M_j	molecular weight of species j Eq. [13]	kg/mole
p	pressure Eq. [13]	N/m^2
P_e	Peclet Number Eq. [16]	dimensionless

Q	stoichiometric requirement of O_2 (Co combustion) Eq. [24]	dimensionless
R	gas constant Eq. [13]	kJ/(mole•K)
Re	Reynolds number Eq. [27]	dimensionless
R_f	mass rate of depletion of a chemical species f Eq. [11]	kg/sec
R_i	radiation flux in direction i Eq. [9]	kJ/(m^2•sec)
s	scattering coefficient Eq. [9]	dimensionless
S	stoichiometric requirement of O_2 (Fuel Combustion) Eq. [25]	dimensionless
Sc	Schmidt number Eq. [27]	dimensionless
S_c	constant portion of linearized source term Eq. [15]	variable
S_f	mass rate of transfer from the second phase Eq. [11]	kg/sec
S_h	source term of enthalpy Eq. [7]	kJ/sec
S_{O2}	sink of O_2 for bed	kg/sec
S_p	linear portion of linearized source term Eq. [15]	variable
S^{rad}	enthalpy source due to radiation Eq. [10]	kJ/(m^2•sec)
$S\phi$	general source term Eq. [14]	variable
T	temperature Eq. [8]	K
u_i	velocity in direction i Eq. [1]	m/sec
x_i	distance in direction i Eq [1]	m

Greek

α	absorption coefficient Eq. [9]	dimensionless
Γ_ϕ	general diffusion coefficient Eq. [14]	variable
δx	distance between adjacent nodes Eq. [17]	m
ε	dissipation rate Eq. [3]	m/sec^3
μ	viscosity Eq. [2]	kg/(m•sec)
ρ	density of gas Eq. [1]	kg/m^3
σ_k	constant in k.e. of turbulence equation (=1.0) [3]	dimensionless
σ_ε	constant in dissipation rate equation (=1.3) [4]	dimensionless
σ_h	turbulent Prandtl number for enthalpy Eq. [7]	dimensionless
ϕ	general variable Eq. [14]	variable

LITERATURE CITED

1. Hough G. Chemical Recovery in the Alkaline Pulping Process, TAPPI Press, (1985)

2. Hupa M., Solin P. Combustion Behavior of Black Liquor Drop. 1985 International Chemical Recovery Conference, New Orleans, 335-344.

3. Grace T. M., Cameron J. H., Clay D. T. Role of the Sulfate/Sulphide Cycle in Char Burning - Experimental Results and Implications. 1985 International Chemical Recovery Conference, New Orleans.

4. Moskal M. D., Corrosion of High Pressure Kraft Recovery Boilers. Kraft Recovery Operations Seminar, Orlando, 285-291, (1988).

5. Tran H., How Does a Kraft Recovery Boiler Become Plugged? Kraft Recovery Operations Seminar, Orlando, 175-184, (1988).

6. Grace T. M., Recovery Boiler Explosions. Kraft Recovery Operations Seminar. Orlando, 191-193, (1988).

7. Regan J., Morris K., LeFebvre B., Design Changes to C-E's Kraft Recovery Unit For Performance and Reliability. 1985 International Chemical Recovery Conference, 55-63.

8. FLUENT Users Manual, CREARE Inc. (1987).

9. PHOENICS Users Manual, PHOENICS Inc. (1986).

10. NEKTON Users Guide (1988).

11. FIDAP Users Manual (1988).

12. Bhada R. K., Lange H. B., Markant H. P. Air Pollution from Kraft Recovery Units. TAPPI Environmental Conference, 5-16, (1972).

13. Williams, T.J., Galtung, F.L. A Mathematical Model of a Recovery Furnace, Modeling and Control of Kraft Production, Proceedings ISA/75 Industry Oriented Conference & Exhibit, Milwaukee, 102-130, (1975).

14. Merriam, R.L. Kraft, Version 2.0 - Computer Model of a Kraft Recovery Furnace, Cambridge MA, Arthur D. Little Inc. (1980).

15. Shiang, N. T., Edwards, L. L. Kraft Recovery Furnace Capacity and Efficiency Improvement, 1985 International Chemical Recovery Conference, 145-151.

16. Shick P. E. Predictive Simulation of Recovery Furnace Processes on a Microcomputer, 1986 Kraft Recovery Operations Seminar, Orlando FL, 121-133.

17. Smith, P. J., Smoot, L. D. One Dimensional Model for Pulverized Coal Combustion and Gasification, Combustion Science and Technology, Vol. 23, 17-31, (1980).

18. Smith, P. J., Fletcher, T. H., Smoot L. D. PCGC-2 - Prediction and Measurement of Entrained Flow Coal Gasification Processes, DOE/MC/16518, (1985).

19. Crowe, C. T., Sharma, M. P. The Particle-Source-In Cell (PSI-CELL) Model for Gas Droplet Flows, Journal of Fluids Engineering, Vol 99, 325-332, (1977).

20. Maraktos, N. C., Moult, A. The Computation of Steady and Unsteady, Turbulent, Chemically Reacting Flows in Axi-Symmetrical Domains, Trans IChemE, Vol 57, 156-162, (1979).

21. Hjertager, B. H., Magnussen, B. F. Computer Simulation of Flow, Heat Transfer, and Combustion in Three-Dimensional Furnaces, PCH PhysioChemical Hydrodynamics, Vol 3(3/4), 231-250, (1982).

22. Siddala, R. G., Selcuk, N. Evaluation of a New Six-Flux Model for Radiative Transfer in Rectangular Enclosures, Trans IChemE, Vol. 57, 163-169, (1979).

23. Pratt, D. T., Wormeck, J. J. CREK, A Computer Program for Calculation of Combustion Reaction Equilibrium and Kinetics in Laminar or Turbulent Flows, Thermal Energy Laboratory, Washington State University, Pullman WA, (1976).

24. Gordon, S., McBride, B. Computer Program for Calculation of Complex Chemical Equilibrium Compositions, NASA SP-273 (1971).

25. Selph, C. Generalized Thermochemical Equilibrium Program for Complex Mixtures, Rocket Propulsion Laboratory, Edwards Air Force Base, CA (1965).

26. Eriksson, G., Rosen, E. Thermodynamic Studies of High Temperature Equilibrium, Chemical Scripta, Vol 4, (1973).

27. Patankar, S. V. Numerical Heat Transfer and Fluid Flow, McGraw-Hill, (1980).

28. Numerical Simulation of Flow and Combustion Phenomena in a Power Plant Boiler.

29. Spray Combustor Modelling.

30. Numerical Correlation of Gas Turbine Combustor Ignition.

31. Walsh, A. Doctoral Thesis, The Institute of Paper Chemistry, (1988).

32. Sumnicht, D. Doctoral Thesis in Progress, The Institute of Paper Chemistry, (1988).

33. Adams, T. Air Jets and Mixing in Kraft Recovery Boilers, 1988 Kraft Recovery Operations Seminar, Orlando FL, 201-209 (1988).

34. Dykshoorn, P. Process Recovery Boiler Flow Model Tests, Babcock & Wilcox, RDD:87:6940-01-01:01, (1986).

35. Odelstam T. BLRB Composite Tubes - 15 Years of Experience, 1988 Kraft Recovery Operations Seminar, 303-314, (1988).

36. Sandquist K. Operational Experience with Single Drum Recovery Boilers in North America, 1988 Kraft Recovery Operations Seminar, 245-256 (1988)

37. Fridely, M. V. Upgrading a 1956 Vintage Recovery Steam Generator - II, 1988 TAPPI Engineering Conference, 377-388, (1988).

38. Haddock, C. Stationary Firing at Alabama River Pulp Company, Inc., 1985 Chemical Recovery Operations, 167-171, (1988).

39. Lavery, H. P., Raymond, D. R. Approach for Measuring Heat and Material Balances in Recovery Furnaces, TAPPI Journal, 70-72, (August, 1984).

40. Schneider, S. H. Climate Modelling, Scientific America - Trends in Computing, 132-139, (1988)

41. Nallasamy, M. Turbulence Models And Their Applications To The Prediction Of Internal Flows: A Review. Computers & Fluids Vol. 15, No. 2, 151-194, (February 1987).

42. Miller, P. T., Clay D. The Influence of Composition of Kraft Black Liquor During Pyrolysis, TAPPI Engineering Conference, Seattle Wa, (1986).

43. Launder, B. E., Spaulding, D. B. The Numerical Computation of Turbulent Flows. Computer Methods of Applied Mechanical Engineering No. 3, 269-289 (1974).

APPENDIX 1 - COLD FLOW MODELLING - A COMPARISON OF COMPUTATIONAL AND EXPERIMENTAL METHODS FOR DETERMINING THE GAS FLOW PATTERNS IN THE KRAFT RECOVERY BOILER

A. K. Jones, and T. M. Grace The Institute of Paper Chemistry

Appleton, Wisconsin 54912

J.E. Monacelli Babcock & Wilcox Power Generation Group

Barberton, Ohio 44203

ABSTRACT

Computational fluid dynamics was applied to the problem of gas flow in a kraft recovery furnace. For simplicity, the case chosen to be modelled is the "cold flow case" (the gas flow pattern that derives directly from the method of air introduction and furnace geometry, without complications from combustion, temperature distributions, and liquor spray interactions). The framework for the computational model was FLUENT (a commercially available, finite difference, computational fluid flow program). A three-dimensional description of the recovery furnace with 50,000 computational cells was used. Bilateral symmetry of the furnace was assumed to reduce the computational effort by a factor of two. The results of the computational model are compared with experimental cold flow data obtained on a 1/8th scale model of a recovery furnace. The analytical model corresponded closely with the experimental cold flow data.

INTRODUCTION

This paper describes the first stage in the development of a three-dimensional recovery furnace model, namely, the simulation of cold flow in an existing furnace design. In a cold flow model only the

geometry and method of introduction of the air are assumed to be important. Neglected are the effects of temperature, combustion, and in this case the interaction between the black liquor spray and the gas phase. A particular B&W furnace, located in DeRidder L.A. was simulated as data was available for comparison (1). B&W measured the velocity profiles in a 1/8th scale replica of this furnace design, under a number of flow conditions. This paper examines two computationally developed flow patterns in this recovery furnace, obtained by using FLUENT (a commercially available computational fluid flow program), and compares them with two experimentally determined flow patterns.

The computational flow field is found by use of an analytical cold flow model of the DeRidder unit at 273K. The experimental flow field was developed in an 1/8th scale model this same recovery furnace. The B&W report then provides scaling constants for converting the velocities up to the full sized furnace at 477K. These velocities are then corrected to 273K in order to make a comparison to the computational work.

A DESCRIPTION OF FLUENT

The main tool used in the computational simulation was FLUENT, a finite difference program for the modelling of fluid flows. FLUENT is flexible and comprehensive, permitting its use in a wide variety of flow situations, including two or three dimensional flows, laminar or turbulent flows, and swirling flows. Additional features of FLUENT include a six-flux radiation model, the PSI-CELL model for two-phase flow (2), a combustion model, a number of turbulence models, and a porous flow model.

The variables that are solved for in the simplest three-dimensional case are u-velocity, v-velocity, w-velocity and pressure. If temperature effects are added, the enthalpy and the radiative heat fluxes are also determined. If the K-ε turbulence model is used, then the kinetic energy of turbulence and the

dissipation rate are found. If combustion is included the mole fractions of combustibles (F), oxygen (O), and products (C), must be calculated in each cell. The maximum number of finite element cells that can be solved for in the version of FLUENT used (version 2.8) is 50,000.

The attractive features of FLUENT are 1/ interactive input; 2/ flexibility -almost any type of flow can be modelled; 3/ internally generated relaxation coefficients, which usually result in stable iterations; and 4/ excellent graphics for viewing the results.

The process of setting up a fluid flow simulation is straightforward, as the description of a flow is menu driven. Cartesian or cylindrical regions can be described. In a cartesian description the cells are rectangular parallelpipeds that can be different lengths in each coordinate direction. A number of different cell types can be specified. Typically five different types are used: 1/ live cells - the variables in these cells are solved for at each iteration; 2/ inlet cells - the values of the flow variables are specified for these cells and remain the same throughout the calculation; 3/ wall cells - these cells act as barriers to the flow and are used to describe the flow geometry; 4/ outlet cells - the value of the flow variables are solved for, but these cells are placed on boundaries of the flow; 5/ symmetry cells - they define lines or planes of symmetry in the flow, which reduces the number of cells necessary to describe a given flow geometry.

In addition to a description of the flow geometry, it is necessary to specify the physical properties of the fluid and the boundary conditions in the wall and inlet cells. The mass flow rates in the inlet cells are controlled by varying the gas velocity or the distance between adjacent nodes.

THE COLD FLOW SIMULATION

The analytical "cold flow" model was setup with physical dimensions as close as possible to those of the full-sized furnace, in order to justify comparison between the experimental and analytical cases. The

upper limit of 50,000 nodes makes it necessary to use some approximations. An isoparametric view of the furnace is shown in Figures 1 and 2. Due to the symmetry involved, it is only necessary to describe half of the furnace. The flow patterns in the other half of the furnace will be a mirror image of the area of the furnace modelled. The symmetry plane is parallel to the side walls and cuts the bullnose and bed in half.

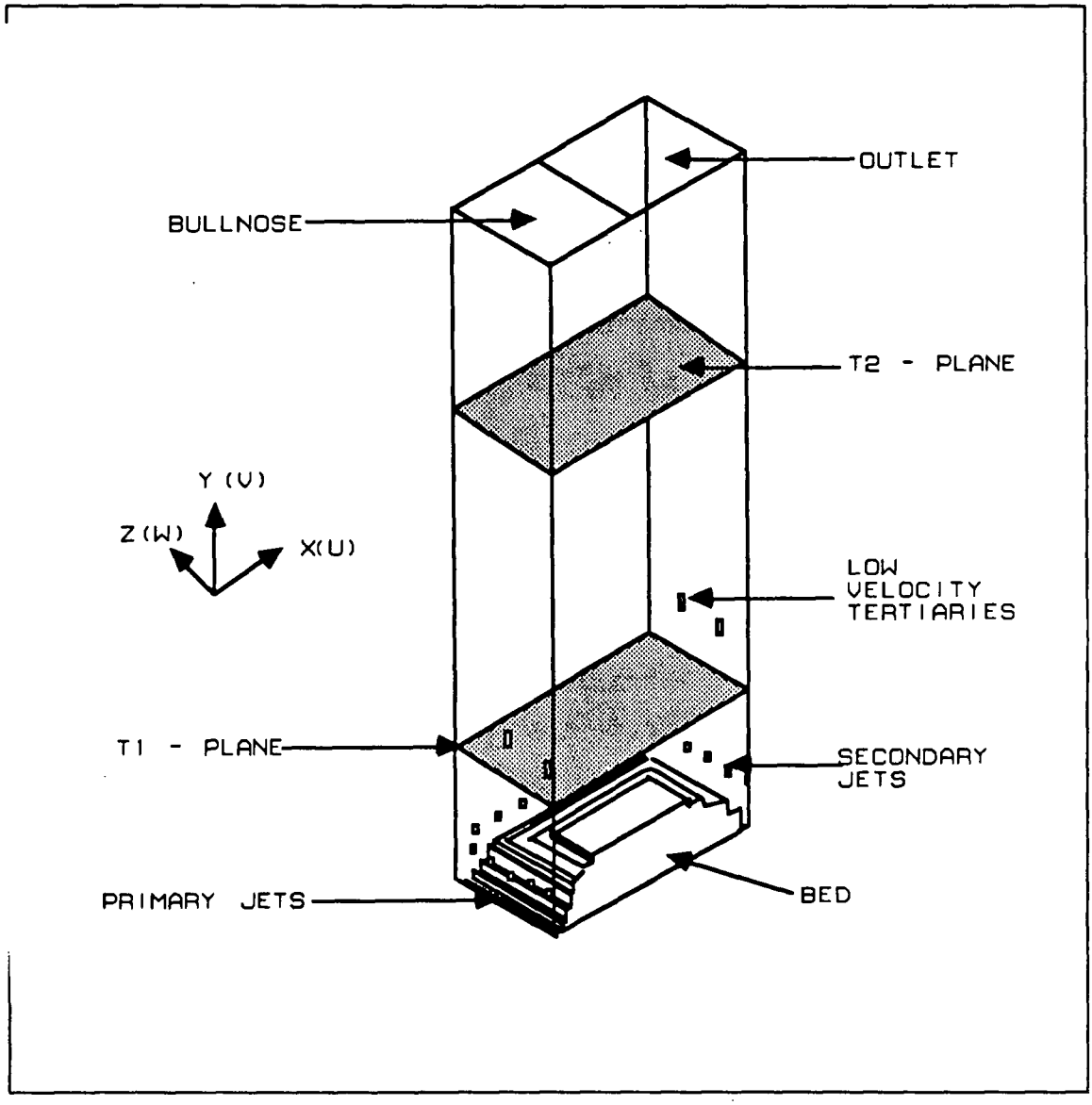

Figure 1 - Illustration of Furnace Geometry - Low Velocity Tertiaries

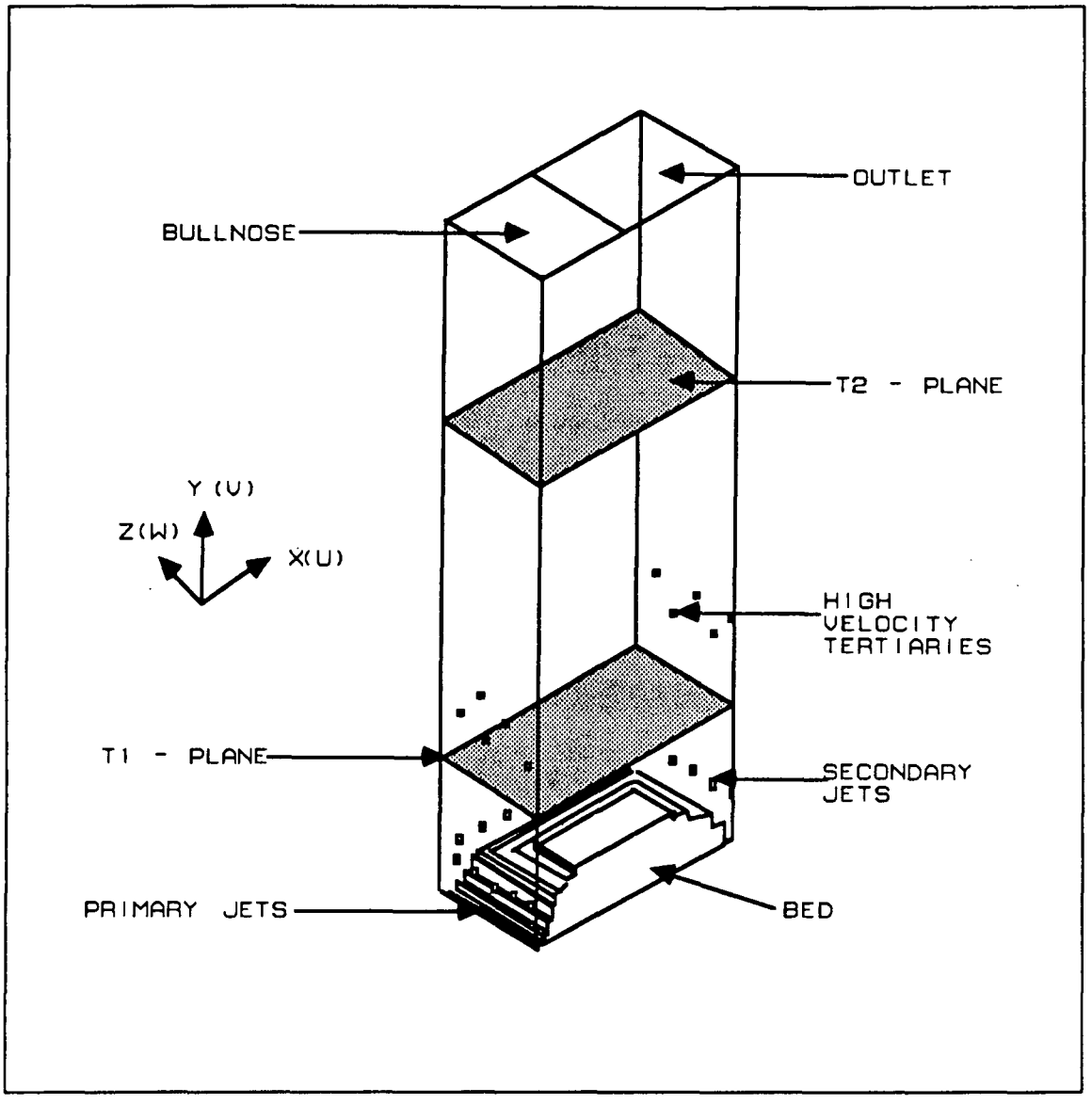

Figure 2 - Illustration of Furnace Geometry - High Velocity Tertiaries

The full sized furnace is 9.6 meters by 10.6 meters in cross section and 27.0 meters high (to the bullnose). The FLUENT model is 10.0 meters by 5.0 meters (due to symmetry) and 30.0 meters high. The bullnose extends 5 meters across the top of the furnace in both cases. The bullnose slopes slightly downward to the back of the furnace, but this was ignored in the computational model in order to reduce the number of nodes used. The resulting effect on the gas flow patterns should be negligible, and the slope is minimal.

The air inlets were modelled in the following manner:

Primary air

A row of nodes along the walls were designated as inlets, the distance between the inlet nodes and the nodes above and below were adjusted in order to satisfy the volumetric flow rates. This treats the primary air as if it was a planar jet completely encircling the furnace. A shortage of nodes made description of individual primary ports impractical. The primary air was injected 1 meter above the furnace floor at a velocity of 40 meters/sec.

Secondary air

Individual air ports of approximately the same dimensions as the ports in the actual furnace were used for the secondary air. The dimensions of the ports in the full-sized furnace were 7.6 cm by 35.5 cm in the model they were 11.4 cm by 23.7 cm. The areas were the same, the individual dimensions had to be adjusted, this approximation was necessary due to computer hardware limitations that restricted the total number of cells that could be used. The width of the secondary and tertiary air ports (11.4 cm), was an average of the actual widths. The half of the furnace modelled had 16 secondary ports, each with an inlet velocity of 36 meters/sec (identical to the prototype furnace). The injection level was 3 meters above the furnace floor.

Tertiary air

Separate air ports on the walls were used, with approximately the same shape as those in the actual furnace. Two configurations were examined. In the first configuration 4 ports at 10 meters above the

furnace floor were used, two on each the front and back walls, with an inlet velocity of 10 meters/sec, (identical to the prototype furnace), as shown in Figure 3. The port sizes were 11.4 cm by 1.02 m, the same area as the actual ports which were 15.2 cm by 76.2 cm. In the second configuration, 8 smaller ports with an inlet

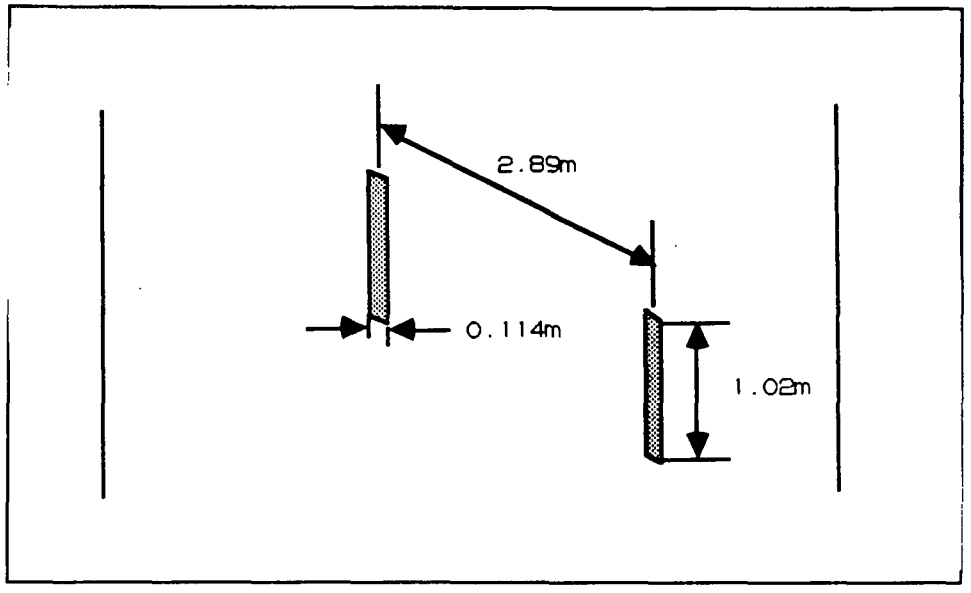

Figure 3 - Low Velocity Tertiaries

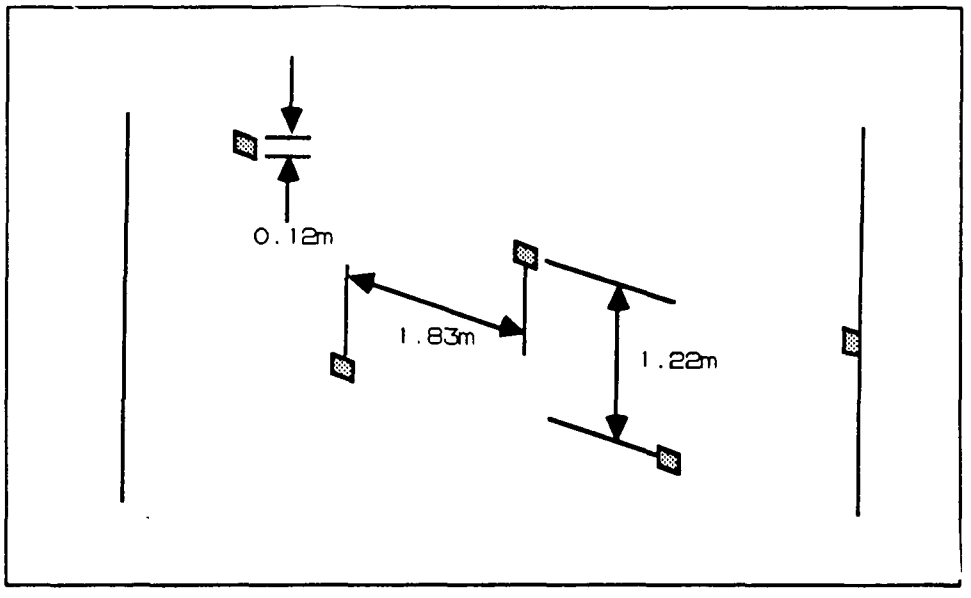

Figure 4 - High Velocity Tertiaries

velocity of 77 meters/sec were used, four on each the front and back walls. Two closely spaced levels of tertiary air were used (at 9.5 and 10.5 meters above the floor of the furnace), this is shown in Figure 4. The port sizes in this case were 11.4 cm square, as opposed to the 12.7 cm ID circular ports used in the actual furnace.

Two computational cases were examined: the first corresponds to experimental case 1, with the low velocity tertiaries; the second to experimental case 2, with the high velocity tertiaries. The computational cases were setup so that they corresponded as closely as possible to the two experimental cases.

The bed shape used (Figure 5) corresponded as closely as possible to the one used in the experimental work (Figure 6); with the top of the bed extended slightly above the secondary air ports. The use of body fitted coordinates would eliminate the staggered bed shape and the resulting numerical problems, leading to a more accurate description of the flow around the bed, but this is not yet available as part of FLUENT.

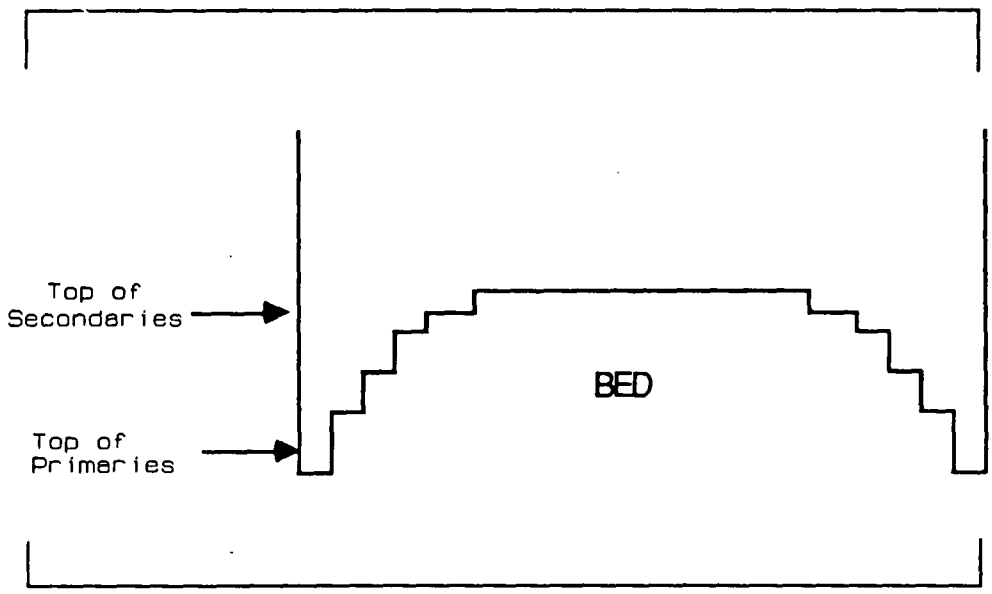

Figure 5 - Outline of Computational Bed Model

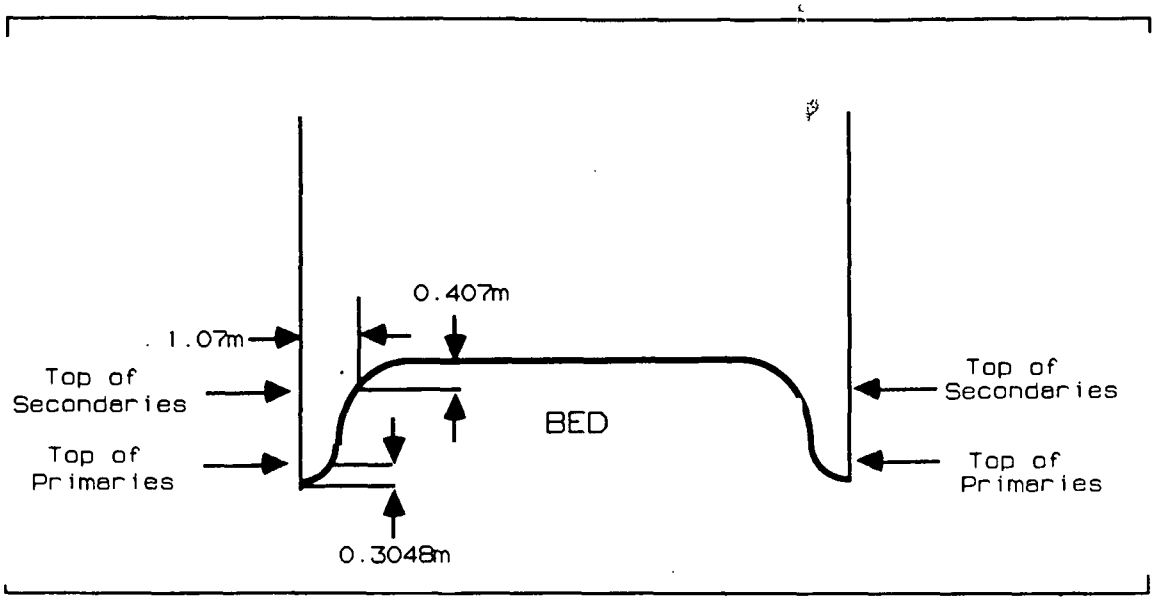

Figure 6 - Dimensions of Experimental Bed

The mass flow rates in the FLUENT models were the same as the full-sized B&W furnace; the total flow rate for the half of the furnace modelled was 48 kg/sec (380,000 lbs/hr). In case 1 the flow was split into 50% primary, 40% secondary and 10% tertiary air. In case 2 the flow was split into 46% primary, 36% secondary and 18% tertiary air.

EXPERIMENTAL DATA

The data used to test the analytical cold flow models is part of a B&W investigation (1). The furnace examined was the Boise Cascade Process Recovery Boiler, located in DeRidder, LA. This furnace was experiencing excessive particulate carryover. The problem was believed to be due to insufficient breakup of a high velocity core of gas by the existing tertiary air jets.

A number of changes in the tertiary air system were considered. These changes were evaluated by constructing an 1/8th scale replica of the DeRidder recovery furnace, and conducting cold flow

measurements in this replica. The velocities within the scaled-down furnace were measured with a hot film anemometer at two traverse planes, T1 located halfway between the secondary and tertiary air ports, and T2 located about halfway between the tertiary air ports and the bullnose. Isovelocity plots were constructed using these data.

The two cases that were simulated will be designated case 1 and case 2. In both cases a bed was included in the bottom of the furnace; The shape of this bed is shown in Figure 6.

RESULTS - A COMPARISON BETWEEN THE EXPERIMENTAL AND COMPUTATIONAL CASES

This section will describe in detail the results of modelling with FLUENT the two cases described earlier and compare these results with the experimental cases. The contour plots will be compared on the basis of average upward velocity at 273K, and on the general flow pattern.

In order to make a comparison of the experimental and computational cases it is first necessary to put them on an equal basis. In the experimental work the average upward velocity is calculated by adding together all the positive velocities and dividing by the number of these positive velocities. The average upward velocity in the prototype (full-size furnace at 400^Xo^XF) can then be calculated based on scaling criteria. In case 1 the scaling factor is 218, in case 2 it is 295. This results in a average velocity in feet/min which can then be converted to m/sec. Finally a temperature correction is applied converting the experimental results to 273K. The results obtained computationally are already in m/sec, at the cold flow temperature of 273K.

Case 1 - T1 Traverse

The T1 traverse is a horizontal slice located above the bed as show in Figure 1. Contours of the upward velocity (V-velocity) are shown in Figures 7 and 8 (experimental and computational results).

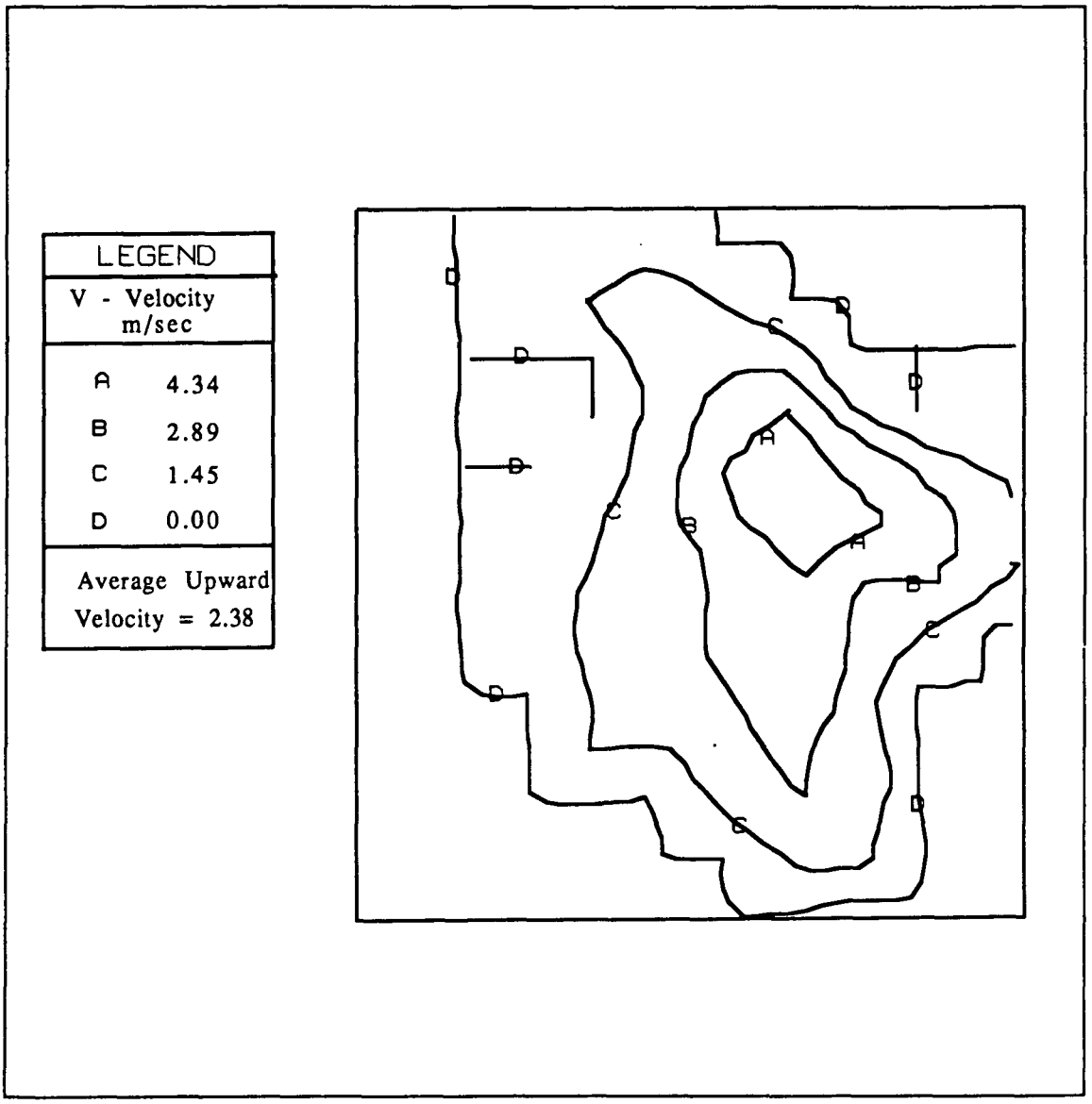

Figure 7 - Low Velocity Tertiaries - T1 Slice Experimental Results

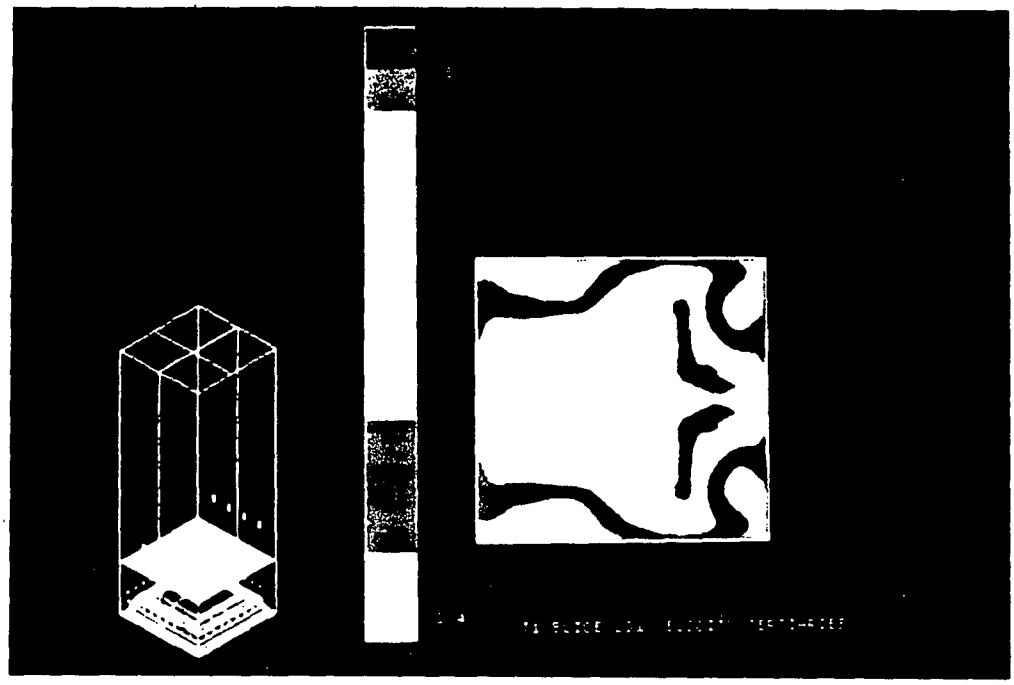

Average Upward Velocity = 1.8

Figure 8 - Low Velocity Tertiaries - T1 Slice

The main features of these contour plots are the upflow region in the center of the furnace and the downflow regions around the outside. The computational T1 traverse for case 1 shows good agreement with the experimental results with respect to the general flow patterns, with the location of downflow regions and the maximum upward velocity corresponding to the experimental results. The average upward velocity is about 30% higher in the experimental case than in the computational case (1.80 m/sec vs 2.40 m/sec). This is due to the use of a staggered bed, the air jets tend to be deflected upwards rather than following the surface of the bed. This reduces the intensity of the central core, as some of the gas is deflected upwards before it reaches the center of the furnace.

The velocities are highest in the center as all the secondary jets meet at this point and are forced to move upwards. The downflow regions around the perimeter of the furnace are created due to entrainment of gas by the secondary jets.

Case 1 - T2 Traverse

At the T2 traverse, a horizontal slice located above the tertiary jets (see Figure 1), the velocity contours obtained experimentally have taken on a much different appearance, this is shown in Figure 9. At the back of the furnace a region of recirculation is present. At the front of the furnace the upward velocities are large. The back of the furnace is a large stagnant region, resulting in poor use of the furnace volume for combustion of the flue gases.

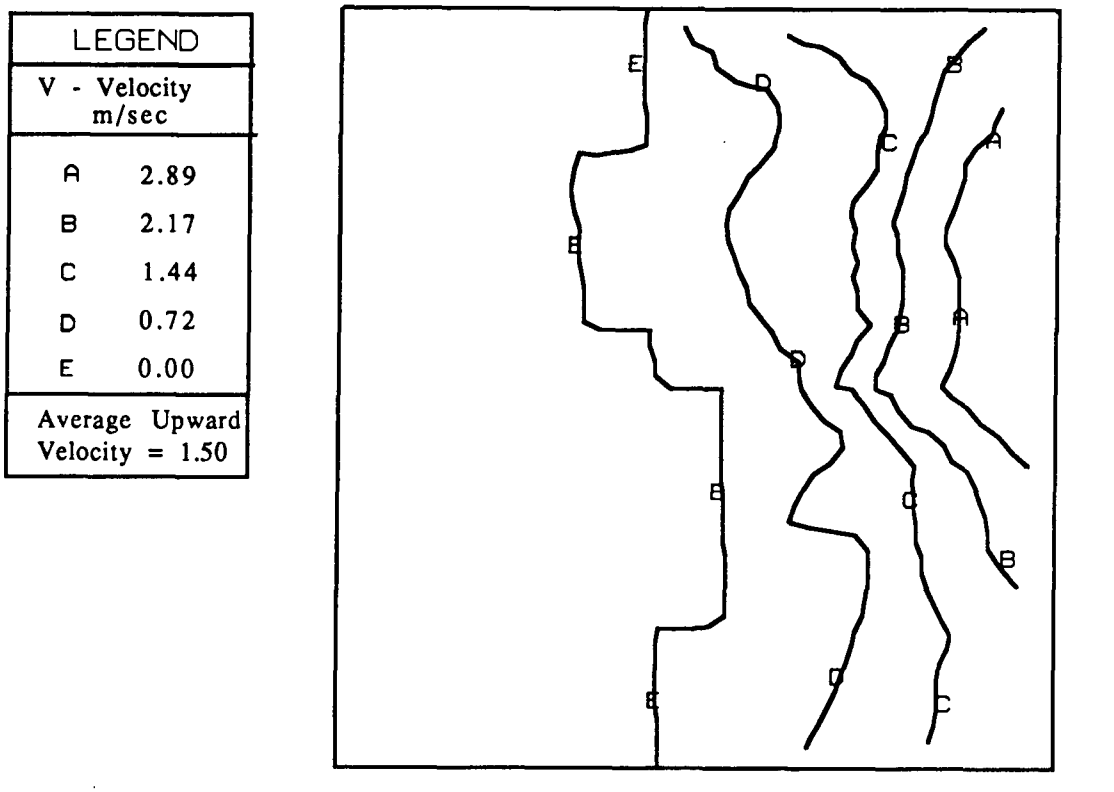

Figure 9 - Low Velocity Tertiaries - T2 Slice Experimental Results

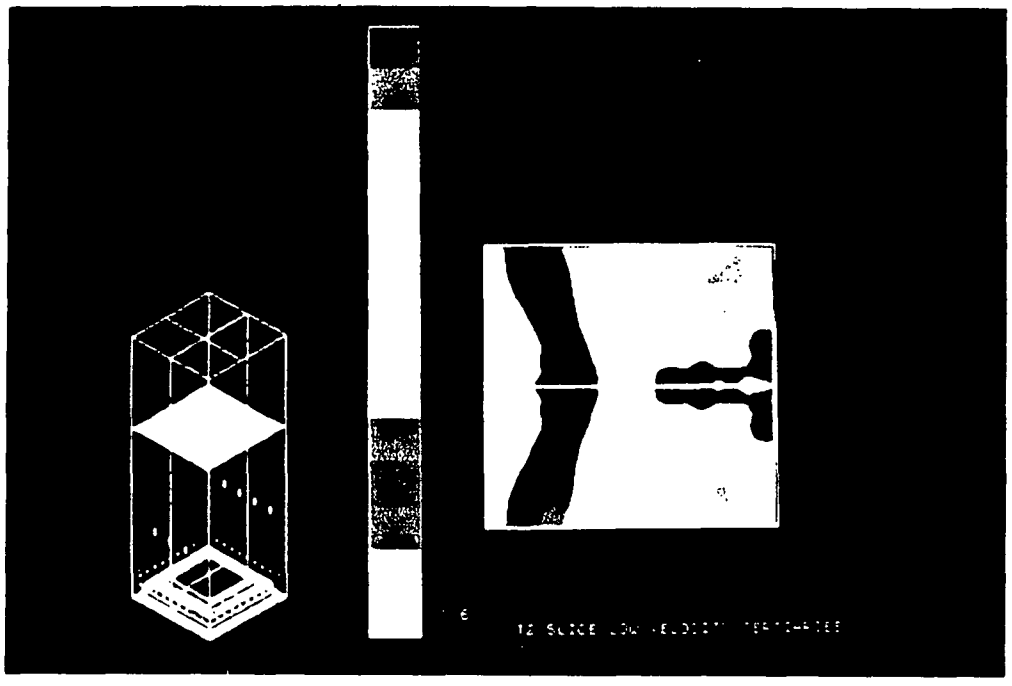

Average Upward Velocity = 0.83

Figure 10 - Low Velocity Tertiaries - T2 Slice

At the T2 traverse in case 1 the existence of a the large stagnant region seen experimentally is confirmed using FLUENT (Figure 10). The location of the maximum upward velocity is at the front wall in both cases. The average upward velocity in the experimental case is 1.50 m/sec, compared to 0.83 m/sec in the computational case. This is once again due to the numerical problems discussed earlier, persisting up to the T2 traverse.

Case 2 - T1 Traverse

The comparison at the T1 traverse for case 2 is essentially the same as for case 1, except that the discrepancy in the average upward velocity is higher (1.60 vs 2.94 m/sec) (Figures 11 and 12).

Case 2 - T2 Traverse

Case 2 has much higher velocity tertiaries, this results in a better utilization of the furnace volume, as shown in Figure 13. The stagnant region at the back of the furnace has been eliminated.

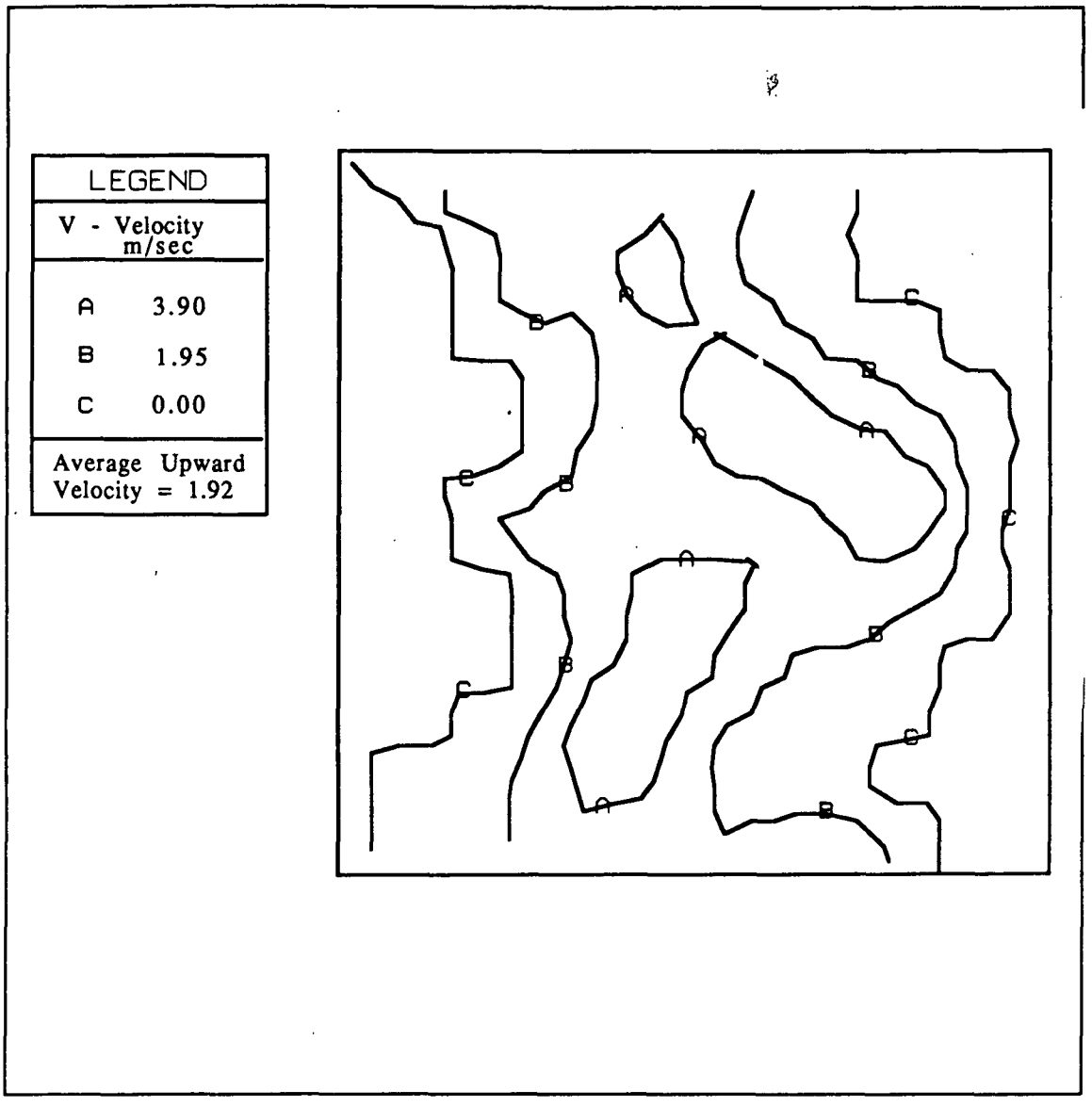

Figure 11 - High Velocity Tertiaries - T1 Slice
Experimental Results

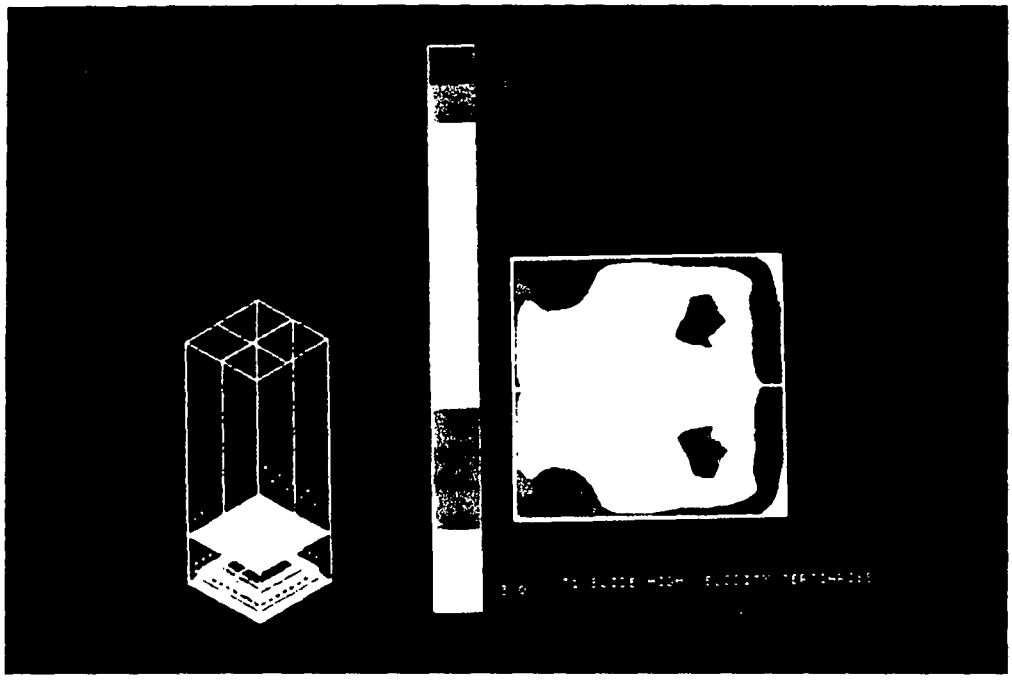

Average Upward Velocity = 1.60

Figure 12 - High Velocity Tertiaries - T1 Slice

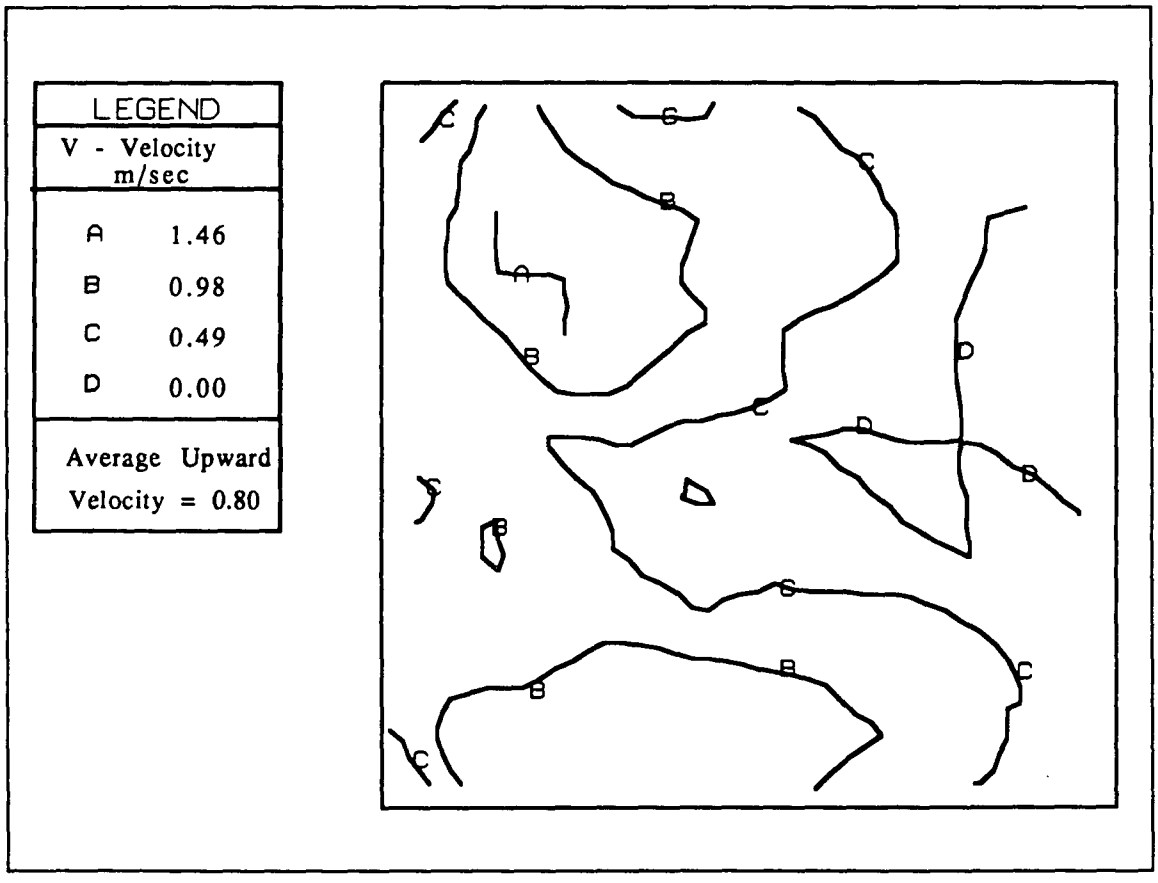

Figure 13 - High Velocity Tertiaries - T2 Slice
Experimental Results

The experimental T2 traverse in case 2 has no downflow, the computational results have only small areas of downflow against the side walls (Figure 14). The average upward velocity found experimentally and computationally are both 0.80 m/sec. The numerical problems are no longer a factor as the center core has been almost completely eliminated in both cases, and the average upward velocity should be just the total mass flow rate divided by, the cross sectional area times the density; which is the same in both cases.

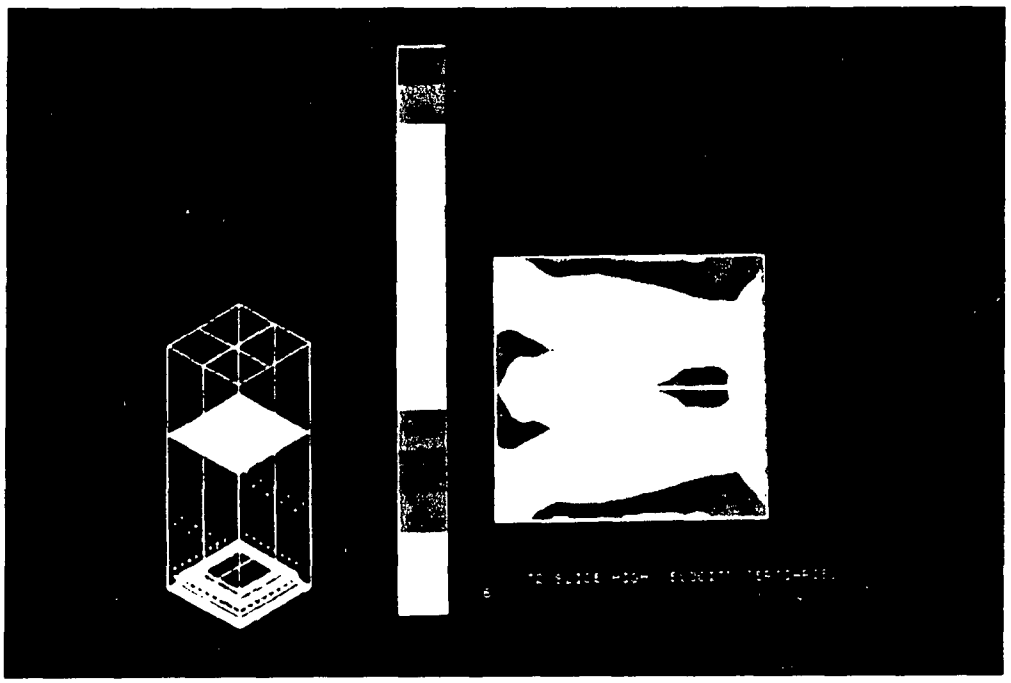

Average Upward Velocity = 0.80

Figure 14 - High Velocity Tertiaries - T2 Slice

The reason for the elimination of the stagnant region can be seen by comparing Figures 15 and 16. Contours of the U-velocities are shown on a horizontal slice that cuts through the midpoint of the tertiary jets. Immediately apparent is the difference in penetration distance between the two cases. This increased penetration allows breakup of the core of high velocity gas created in the lower furnace.

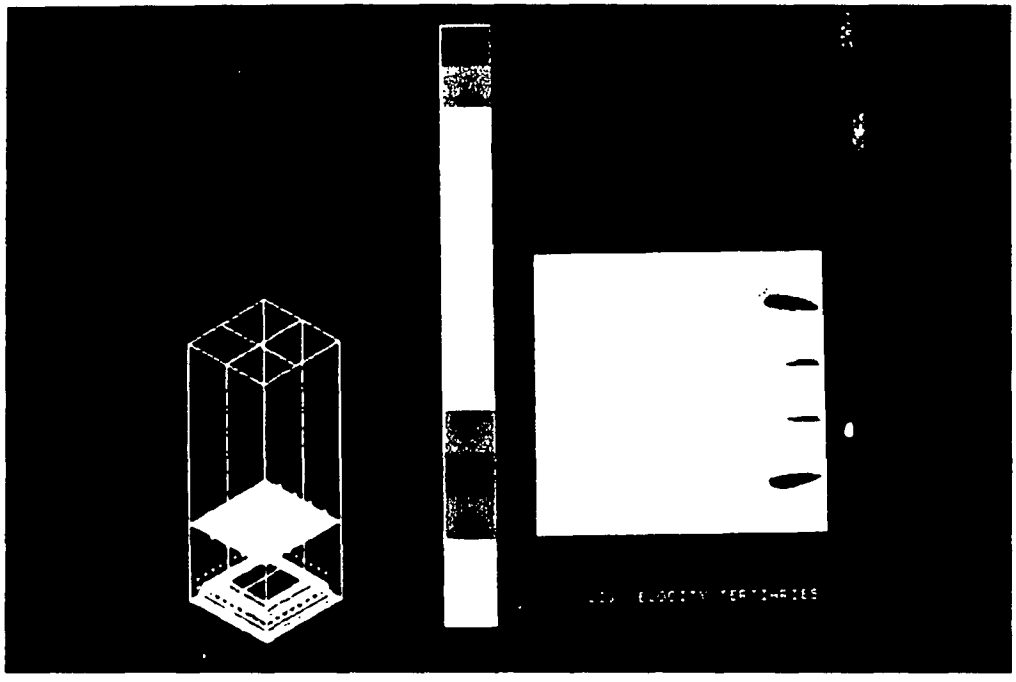

Figure 15 - Low Velocity Tertiaries - Tertiary Jets

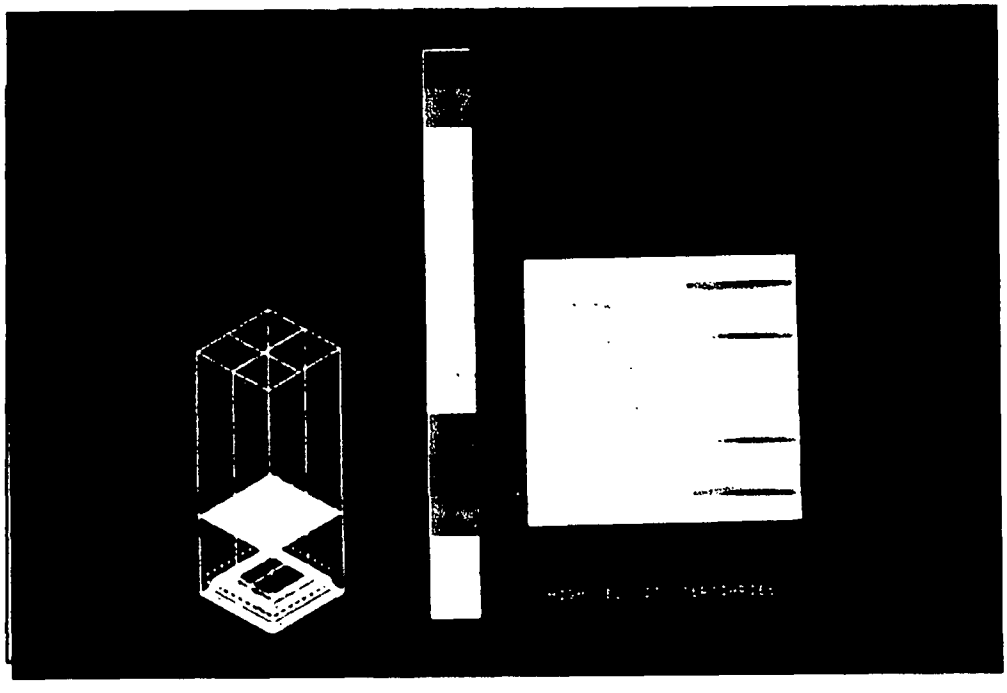

Figure 16 - High Velocity Tertiaries - Tertiary Jets

LIMITATIONS OF MODELLING TECHNIQUES

Both numerical and experimental scale modelling have inherent drawbacks. Both can be effective if the limitations of these techniques are kept in mind.

The main limitations of computational modelling are: 1/ the need to use staggered nodes to describe a diagonal surface (i.e. bed surface); 2/ the empiricism of built-in turbulence models; 3/ the large amount of computer time required to converge complex problems, (a typical problem takes about 7 days of CPU time to converge on a MicroVax); 4/ the difficulty in deciding when a flow pattern has converged; and 5/ the limitation in the number of nodes, making it impossible to describe fine details of the flow around the bed and in jets.

Experimental scale modelling of gas flows has the following limitations: 1/ once a scale model has been constructed only minor changes can be made in the geometry; 2/ it is difficult or impossible to satisfy all the scaling criteria; 3/ it is very difficult to measure large numbers of velocities within the model, and these velocities may be altered by the act of measuring them; 4/ temperature effect cannot be easily added.

CONCLUSIONS

The main conclusions that can be drawn from the modelling effort thus far are:

1/ FLUENT can be used effectively to simulate the flow patterns in the kraft recovery boiler;

2/ The benefit of modifying the tertiary jets in the B&W furnace can be observed by the use of FLUENT, in agreement with experimental results;

3/ Numerical problems are created due to the primary and secondary air jets impacting on the staggered bed, in future modelling work the bed will not extend above the level of the secondaries, this should result in a more realistic flow pattern.

LITERATURE CITED

1. Dykshoorn, P.; Process Recovery Boiler Flow Model Tests; RDD:87:6940-01-01:01, (July 1986)

2. Crowe, C.T., Sharma, M.P.; The Particle-Source-In-Cell (PSI - CELL) Model for Gas-Droplet Flows; Journal of Fluids Engineering, Vol 99 (July 1977); pp. 325 - 332

APPENDIX 2 - CONVERGENCE QUESTIONS

The purpose of this section is to address three important aspects of convergence, namely 1. The method for converging a complex simulation of the kraft recovery boiler; 2. The determination of when a case is converged; and 3. Ways in which convergence can be hastened in the future.

CONVERGENCE OF A RECOVERY FURNACE SIMULATION

The convergence of a kraft recovery boiler simulation involves a number of stages of solution, along with careful manipulation of the underrelaxation parameters. All the variables cannot be turned on at once with any hope of getting a converged or even a stable result. The best method found for convergence of a simulation is as follows:

1. Start with a solution of just the pressure and the three velocities, all other variables are turned off. The default underrelaxation parameters of 0.2 for the velocities and 0.5 for the pressure appear to be the largest value that can be used. Perform about 25 to 30 iterations;

2. Next turn on the calculation of k and ϵ with the default underrelaxation of 0.2 for both, ensuring that the turbulent boundary conditions have been set. Perform an additional 150-200 iterations, until the normalized residuals for U, V, and W are below about 0.05. This should establish a velocity field;

3. The next step is to turn on the enthalpy calculations (H); the underrelaxation parameter for all variables should be turned down to 0.01, with the exception of pressure which should be set at 0.025, and temperature which can be set at 0.05. Ensure that all properties for the walls have been set (temperature and emissivity), patch in a temperature of 1250K everywhere (the

term patching refers to the technique of specifying the value of a variable, rather than calculating its value, and is accomplished using the PA option in the main menu of FLUENT/RFM), an additional 20 to 30 iterations should now be executed;

4. Black liquor firing can now begin; check to ensure that the black liquor properties and the spray properties have been specified. Patch in an oxygen mass fraction of 0.04 everywhere in the furnace, One exception is those cells below the primary air jets and around the perimeter of the bed (J=2); the oxygen mass fraction should be patched in at a very small amount (1E-04 works). Problems occur in these cells due to the presence of oxygen, carbon monoxide (from the bed), and high turbulence levels; this creates excessive amounts of CO_2, unless low oxygen levels are used. In addition, values for C and Q must be patched; a mass fraction of 0.01 for both is appropriate. Set the underrelaxation parameter for the drop equal to 0.2, and perform a C2 calculation for every ten C1 calculations. The first C1 iteration following the first C2 calculation may result in the message "Rapid Divergence - Abort" being printed, ignore this message and continue with another C1 calculation, it shouldn't happen again. Keep the underrelaxation coefficients at the same level for the next 50 iterations, then slowly increase them.

The underrelaxation parameters should never be increased above 0.2 for U, V, W, H, D, E and viscosity. The maximum value used for pressure is 0.5, for the species F, O, C, B, and Q, a value of 0.4 has been successfully used. A value of 0.3 for the particle droplet calculation should be used, as any larger value results in unstable bed growth and carryover. The sweep direction can be specified, either direction 1 or 2 works, while direction 3 does not. It may be best to alternate between direction 1 and 2, although this has not been determined. The number of sweeps can also be specified, the best results found were using 10 sweeps for pressure and 5 sweeps for all the other variables, except for radiation which should be kept at the default as it is calculated differently.

Observations:

1. It appears that a temperature field cannot be patched in without inducing unstable behavior of the simulation; after patching a temperature field very low values of the relaxation coefficients must be used;

2. Increasing the underrelaxation parameters above the recommended level causes rapid divergence;

3. Make frequent backups of your data file, so that if a simulation begins to diverge you can back up and start again;

4. Do not change the ratio of the pressure and the velocity underrelaxation parameters; a ratio of 2.5 : 1 seems to work best.

DETERMINATION OF CONVERGENCE

Convergence of a simulation can be determined by a number of methods, the most dependable appears to be average temperature. The average temperature is determined in the "heat flux by zone" calculation, by typing VA N HZ when in the main FLUENT/RFM menu. Once the temperature remains steady over about 100 calculations then you can be reasonable sure that the simulation is converged. Other ways of determining convergence include the closure of the inert mass balance, which approaches 100% from above, and the energy balance, which approaches 100%. The normalized residuals of a simulation can be used as another means of determining convergence, although numerical

problems with the simulation restrict how low these residuals can go. The final method is by observing some characteristics of the flow (i.e. an isovelocity plot) before and after a reasonable number of iterations (50-100); if no significant changes occur, then convergence is likely.

MEANS OF IMPROVING CONVERGENCE

The rate and extent of convergence should be enhanced in future versions of the FLUENT code. One method for improved convergence rates is to use a whole field solver. A whole field solver determines the values of the flow variables without the use of sweeps; it permits more rapid convergence but requires the solution of a N x N matrix where N is the number of nodes. The memory requirements for large cases become astronomical as N^2 memory locations must be defined. The use of sparse matrix techniques reduces the magnitude of this task in some cases.

The extent of convergence of a recovery furnace model would be enhanced if more nodes could be used; this would come at the expense of the rate of convergence as each iteration would take longer. Ideally about 250,000 nodes would be required to model the recovery furnace; this is due to the wide variation in dimensions which exist.

Optimization of the underrelaxation parameters would help in improving the convergence rate; this requires experience in the behavior of a recovery boiler simulation, and experimentation with the model. At the present time, the underrelaxation parameters that work are known, but these are not necessarily the optimum values.

APPENDIX 3 - ORIGINAL SUBROUTINES WRITTEN FOR FLUENT/RFM

```
      SUBROUTINE ENBAL
CCCCCCCCCCCCCCCCCCCCCCCCCCCCCCCCCCCCCCCCCCCCCCCCCCCCCCCCCCCCCCCCCCCC
C                                                                     C
C     ENTHALPY OF INCOMING AIR + ENTHALPY OF INCOMING BLACK           C
C     LIQUOR + HEATING VALUE OF BLACK LIQUOR =  HEAT TO WALLS         C
C     + HEAT OUT WITH FLUE GASES + HEAT OUT WITH CARRYOVER            C
C     + UNREALIZED COMBUSTION                                         C
C                                                                     C
C     ALL ENTHALPIES EXPRESSED AS JOULES                              C
C                                                                     C
C     WRITTEN BY ANDREW JONES JUNE 1988                               C
C                                                                     C
CCCCCCCCCCCCCCCCCCCCCCCCCCCCCCCCCCCCCCCCCCCCCCCCCCCCCCCCCCCCCCCCCCCC
      INCLUDE 'COMMON.FOR'
      WRITE(IO,*)'STARTING ENERGY BALANCE'
      ENTHIN = 0
      ENTOUT = 0
C     ENTHALPY OF INCOMING AIR
      HINFLO = 0
      DO 1 K = 1,NK
      DO 1 J = 1,NJ
      DO 1 I = 1,NI
      L = LINDEX(I,J,K)
      CALL FFARNB
      IF(LC.LT.ICI) GOTO 1
      IF(LCXP.EQ.ICL) HINFLO = HINFLO +
     + SY(J)*SZ(K)*R(J)*DEN(L)*U(LXP)*CCPG(L)*(T(L)-273)
      IF(LCXM.EQ.ICL) HINFLO = HINFLO -
     - SY(J)*SZ(K)*R(J)*DEN(L)*U(L)*CCPG(L)*(T(L)-273)
      IF(LCYP.EQ.ICL) HINFLO = HINFLO +
     + SX(I)*SZ(K)*RM(J+1)*DEN(L)*V(LYP)*CCPG(L)*(T(L)-273)
      IF(LCYM.EQ.ICL) HINFLO = HINFLO -
     - SX(I)*SZ(K)*RP(J-1)*DEN(L)*V(L)*CCPG(L)*(T(L)-273)
      IF(NK.EQ.1) GOTO 1
      IF(LCZP.EQ.ICL) HINFLO = HINFLO +
     + SX(I)*SY(J)*DEN(L)*W(LZP)*CCPG(L)*(T(L)-273)
      IF(LCZM.EQ.ICL) HINFLO = HINFLO -
     - SX(I)*SY(J)*DEN(L)*W(L)*CCPG(L)*(T(L)-273)
1     CONTINUE
      WRITE(IO,*)'ENTHALPY OF INCOMING AIR = ',HINFLO
      ENTHIN = ENTHIN + HINFLO
C     ENTHALPY OF INCOMING BLACK LIQUOR
      BLIN = PFTOT*1255.2*(400-273)
      ENTHIN = ENTHIN + BLIN
      WRITE(IO,*)'ENTHALPY OF INCOMING BLACK LIQUOR = ',BLIN
C     HEATING VALUE OF BLACK LIQUOR
C     ENTHALPY LOST DUE TO VAPORIZATION OF WATER
      ENWBL = -(1-SOLIDS)*PFTOT*DELTAH
      WRITE(IO,*)'HEATING VALUE OF WATER IN BL = ',ENWBL
      ENTL = ENWBL
C     ENTHALPY OF VOLATILES BURNING
      ENVO = FVOLAT*SOLIDS*HREACT*PFTOT
     1       +FVOLAT*SOLIDS*QFRAC*HREACO*PFTOT
      WRITE(IO,*)'HEATING VALUE OF VOLATILES IN BL = ',ENVO
      ENTL = ENTL + ENVO
C     ENTHALPY OF CARBON BURNING
      ENC = FCHAR*SOLIDS*COHREA*PFTOT
      WRITE(IO,*)'HEATING VALUE OF CARBON IN BL = ',ENC
      ENTL = ENTL + ENC
C     ENTHALPY OF SMELT MELTING
```

```
      ENSM =  -(1-FCHAR-FVOLAT)*3.16E+05*SOLIDS*PFTOT
      WRITE(IO,*)'HEATING VALUE OF SMELT MELTING = ',ENSM
      ENTL = ENTL + ENSM
      WRITE(IO,*)'HEATING VALUE OF BLACK LIQUOR = ',ENTL
      ENTHIN = ENTHIN + ENTL
C     HEAT TRANSFERRED TO WALLS
C     FIND HEAT TRANSFER COEFFICIENT FOR EACH WALL CELL....
C
      TQ = 0
      DO 330 K = 1,NK
      DO 330 J = 1,NJ
      DO 330 I = 1,NI
        L = LINDEX(I,J,K)
        IF(ICELL(L).GT.ICW) GOTO 330
        CALL NEIGHB
        QCELL  = 0.0
C       SKIP IF LINK CUT AND FLUX IS ZERO....
        IF(LINKH(LC).EQ.1.AND.HFLUX(LC).EQ.0.0) GOTO 320
C       DO EACH CELL FACE IN TURN....
        IF(LCXP.NE.ICL) GOTO 310
          HPRLOC = CCPG(LXP)*DEPEND(T(LXP),VISL,NVISL)
     *             / AMAX1(DEPEND(T(LXP),CTCG,NTCG),1.0E-15)
          XAREA  = SY(J)*SZ(K)*R(J)
          QCELL  = QCELL  +  (H(L)-H(LXP))*XAREA *
     *             HGAMEX(SXU(I+1)*0.5,E(LXP),DEN(LXP),HPRND,HPRLOC)
          ETERM = 2.0*(RBOUND(ICELL(L))/(2.0-RBOUND(ICELL(L))))*
     1            (STEFAN*T(L)**4-RAX(LXP))*XAREA
        QCELL = QCELL + ETERM
310     IF(LCXM.NE.ICL) GOTO 311
          HPRLOC = CCPG(LXM) * DEPEND(T(LXM),VISL,NVISL)
     A             / AMAX1(DEPEND(T(LXM),CTCG,NTCG),1.0E-15)
          XAREA  = SY(J)*SZ(K)*R(J)
          QCELL  = QCELL  +  (H(L)-H(LXM))*XAREA *
     *             HGAMEX(SXU(I  )*0.5,E(LXM),DEN(LXM),HPRND,HPRLOC)
          ETERM = 2.0*(RBOUND(ICELL(L))/(2.0-RBOUND(ICELL(L))))*
     1            (STEFAN*T(L)**4-RAX(LXM))*XAREA
        QCELL = QCELL + ETERM
311     IF(LCYP.NE.ICL) GOTO 312
          HPRLOC = CCPG(LYP) * DEPEND(T(LYP),VISL,NVISL)
     A             / AMAX1(DEPEND(T(LYP),CTCG,NTCG),1.0E-15)
          YPAREA = SX(I)*SZ(K)*RP(J)
          QCELL  = QCELL  +  (H(L)-H(LYP))*YPAREA*
     *             HGAMEX(SYV(J+1)*0.5,E(LYP),DEN(LYP),HPRND,HPRLOC)
          ETERM = 2.0*(RBOUND(ICELL(L))/(2.0-RBOUND(ICELL(L))))*
     1            (STEFAN*T(L)**4-RAY(LYP))*YPAREA
        QCELL = QCELL + ETERM
312     IF(LCYM.NE.ICL) GOTO 313
          HPRLOC = CCPG(LYM) * DEPEND(T(LYM),VISL,NVISL)
     A             / AMAX1(DEPEND(T(LYM),CTCG,NTCG),1.0E-15)
          YMAREA = SX(I)*SZ(K)*RM(J)
          QCELL  = QCELL  +  (H(L)-H(LYM))*YMAREA*
     *             HGAMEX(SYV(J  )*0.5,E(LYM),DEN(LYM),HPRND,HPRLOC)
          ETERM = 2.0*(RBOUND(ICELL(L))/(2.0-RBOUND(ICELL(L))))*
     1            (STEFAN*T(L)**4-RAY(LYM))*YMAREA
        QCELL = QCELL + ETERM
313     IF(NK.LT.3) GOTO 320
          ZAREA  = SX(I)*SY(J)
          IF(LCZP.NE.ICL) GOTO 314
            HPRLOC = CCPG(LZP) * DEPEND(T(LZP),VISL,NVISL)
     A               / AMAX1(DEPEND(T(LZP),CTCG,NTCG),1.0E-15)
```

```
          QCELL  = QCELL  +  (H(L)-H(LZP))*ZAREA *
     *               HGAMEX(SZW(K+1)*0.5,E(LZP),DEN(LZP),HPRND,HPRLOC)
          ETERM = 2.0*(RBOUND(ICELL(L))/(2.0-RBOUND(ICELL(L))))*
     1            (STEFAN*T(L)**4-RAZ(LZP))*ZAREA
        QCELL = QCELL + ETERM
314       IF(LCZM.NE.ICL) GOTO 320
            HPRLOC = CCPG(LZM) * DEPEND(T(LZM),VISL,NVISL)
     A               / AMAX1(DEPEND(T(LZM),CTCG,NTCG),1.0E-15)
            QCELL  = QCELL  +  (H(L)-H(LZM))*ZAREA *
     *               HGAMEX(SZW(K  )*0.5,E(LZM),DEN(LZM),HPRND,HPRLOC)
          ETERM = 2.0*(RBOUND(ICELL(L))/(2.0-RBOUND(ICELL(L))))*
     1            (STEFAN*T(L)**4-RAZ(LZM))*ZAREA
        QCELL = QCELL + ETERM
320     CONTINUE
        TQ  = TQ   + QCELL
330   CONTINUE
      EVAPWB = WALLEN + BEDEN
      WRITE(IO,*)'HEAT FROM WALLS FOR EVAPORATION = ',EVAPWB
      WRITE(IO,*)'HEAT TO WALLS (CONVECTION AND RADIATION) = ',-TQ
      WRITE(IO,*)'TOTAL HEAT TO WALLS = ',-(EVAPWB+TQ)
      ENTOUT = ENTOUT - TQ - EVAPWB
C     HEAT OUT WITH FLUE GASES
      J = NJ
      K = 1
      I = 1
      TTOT = 0
      HOUT = 0
      NCELL = 0
      RADO = 0
      DO 11 K = 1,NK
      DO 11 I = 1,NI
      CALL FFARNB
      IF(LC.NE.ICO) GOTO 11
      YPAREA = SX(I)*SZ(K)*RP(J)
      RADO = RADO + RAY(L)*YPAREA
      TTOT = TTOT + T(L)
      NCELL = NCELL + 1
      ATD = SX(I)*SZ(K)*RM(J-1)*DEN(L)*CCPG(L)*(T(L)-273)
      HOUT = HOUT + ATD*V(L)
11    CONTINUE
      WRITE(IO,*)'ENTHALPY OF FLUE GASES LEAVING = ',HOUT
      WRITE(IO,*)'RADIATION OUT OF EXIT PLANE = ',RADO
      ENTOUT = ENTOUT + HOUT + RADO
C     HEAT OUT WITH CARRYOVER
      TAVE = TTOT/NCELL
      CAROV = (CIOUT+CCOUT)*1255.2*(TAVE-273)
      WRITE(IO,*)'ENTHALPY OF CARRYOVER = ',CAROV
      ENTOUT = ENTOUT + CAROV
C     UNREALIZED COMBUSTION DUE TO FUEL AND CO IN EXIT FLUE GAS
C     GROWTH OF BED AND CARBON IN CARRYOVER
      J = NJ
      K = 1
      I = 1
      FOUT = 0
      QOUT = 0
      DO 21 K = 1,NK
      DO 21 I = 1,NI
      CALL FFARNB
      IF(LC.NE.ICO) GOTO 21
      FOUT = FOUT + SX(I)*SZ(K)*DEN(L)*V(L)*F(L)
```

```
      QOUT = QOUT + SX(I)*SZ(K)*DEN(L)*V(L)*Q(L)
21    CONTINUE
      FUNR = FOUT*HREACT + FOUT*HREACO*QFRAC
      QUNR = QOUT*HREACO
      CUNR = 0
      CEX = 0
      BEDIO = 0
      DO 25 K = 1,NK
      DO 25 J = 1,NJ
      DO 25 I = 1,NI
      L = LINDEX(I,J,K)
      IF(ICELL(L).NE.10)GOTO 25
C     REMOVE SENSIBLE HEAT AND HEAT OF REACTION DUE
C     TO ALL CARBON LANDING ON THE BED
      CUNR = CUNR + BEDCEL(L+2*NI)*1255.2*(T(L)-273)
      CUNR = CUNR + BEDCEL(L+2*NI)*COHREA
C     HEAT OUT WITH INORGANICS TO BED
      BEDIO = BEDIO + BEDCEL(L+3*NI)*1255.2*(T(L)-273)
C     IF SHRINKING CONSIDER CHAR TO ENTER CONTROL VOLUME
      IF(BEDCEL(L+4*NI).LT.0) THEN
      CEX = CEX + 1255.2*(T(L)-273)*BEDCEL(L+4*NI)
      CEX = CEX + BEDCEL(L+4*NI)*COHREA*24/94.7
      ENDIF
25    CONTINUE
      WRITE(IO,*)'ENTHALPY OUT WITH INORGANICS ON BED = ',BEDIO
      WRITE(IO,*)'UNREALIZED COMBUSTION FOR CO = ',QUNR
      WRITE(IO,*)'UNREALIZED COMBUSTION FOR FUEL = ',FUNR
      WRITE(IO,*)'UNREALIZED COMBUSTION FOR CARBON = ',CUNR
C     INCREMENT UNREALIZED CARBON COMBUSTION DUE TO CARRYOVER
      CCUN = COHREA*CCOUT
      WRITE(IO,*)'UNREALIZED COMBUSTION FOR CARRYOVER',CCUN
      CUNR = CUNR + CCUN
      TOTUN = CUNR + QUNR + FUNR
      ENTOUT = ENTOUT + TOTUN + BEDIO
      WRITE(IO,*)'TOTAL UNREALIZED COMBUSTION = ',TOTUN
C     ENTHALPY OF CARBON SOURCE DUE TO BED SHRINKAGE
      WRITE(IO,*)'ENTHALPY ADDED DUE TO BED SHRINKAGE = ',-CEX
      ENTHIN = ENTHIN - CEX
C     OVERALL BALANCE
      WRITE(IO,*)'TOTAL ENTHALPY IN = ',ENTHIN
      WRITE(IO,*)'TOTAL ENTHALPY OUT = ',ENTOUT
      ENTDIF = ENTOUT - ENTHIN
      IF(ENTDIF.GT.0)
     1 WRITE(IO,*)'CURRENTLY CREATING ',ENTDIF,' KJ OF ENERGY'
      IF(ENTDIF.LT.0)
     1 WRITE(IO,*)'CURRENTLY DESTROYING ',-ENTDIF,' KJ OF ENERGY'
      IF(ENTDIF.EQ.0) WRITE(IO,*)'COMPLETELY BALANCED!!!'
      ENCLO = 100*ENTOUT/ENTHIN
      WRITE(IO,*)'ENERGY BALANCE IS ',ENCLO,' % CLOSED'
      RETURN
      END
```

```
      SUBROUTINE MASBAL
CCCCCCCCCCCCCCCCCCCCCCCCCCCCCCCCCCCCCCCCCCCCCCCCCCCCCCCCCCCCCCCCCCCC
C                                                                     C
C     SHOWS THE MASS BALANCE, INDICATING ALL INLET AND                C
C     OUTLET CELLS                                                    C
C                                                                     C
CCCCCCCCCCCCCCCCCCCCCCCCCCCCCCCCCCCCCCCCCCCCCCCCCCCCCCCCCCCCCCCCCCCC
      INCLUDE 'COMMON.FOR'
      REAL MBI,MBO,MB
      REAL AINFLO,OUTFLO,OUTATD,ATD,TMAS
      MBI = 0.0
      AT = 0.0
      BT = 0.0
      CT = 0.0
      DT = 0.0
      ET = 0.0
      TMAS = 0.0
      MBO = 0.0
      IF ((IOCAL.EQ.0).AND.(ICCAL.EQ.0).AND.(IBCAL.EQ.0).AND.
     1    (IQCAL.EQ.0).AND.(IFCAL.EQ.0)) THEN
      WRITE(IO,*)' CANNOT DO MASS BALANCE WHEN NO SPECIES ARE PRESENT'
      RETURN
      ENDIF
      AINFLO = 0.0
      OUTFLO = 0.0
      OUTATD = 0.0
      XOUT = 0
      DO 1 K = 1,NK
      DO 1 J = 1,NJ
      DO 1 I = 1,NI
      L = LINDEX(I,J,K)
      CALL FFARNB
C
C     DO OUTLET CELLS FIRST....
      IF(LC.NE.ICO) GOTO 16
      IF(J.NE.NJ) GOTO 14
      ATD = SX(I)*SZ(K)*RM(J-1)*DEN(L)
      OUTFLO = OUTFLO + ATD*V(L)
      OUTATD = OUTATD + ATD
      XOUT = XOUT + ATD*V(L)*(1-B(L)-C(L)-F(L)-Q(L)-O(L))
14    CONTINUE
16    CONTINUE
C
C     NOW, THE INPUT CELLS, DOING EACH FACE IN TURN....
      IF(LC.LT.ICI) GOTO 17
      IF(LCXP.EQ.ICL) AINFLO = AINFLO +
     + SY(J)*SZ(K)*R(J)*DEN(L)*U(LXP)
      IF(LCXM.EQ.ICL) AINFLO = AINFLO -
     - SY(J)*SZ(K)*R(J)*DEN(L)*U(L)
      IF(LCYP.EQ.ICL) AINFLO = AINFLO +
     + SX(I)*SZ(K)*RM(J+1)*DEN(L)*V(LYP)
      IF(LCYM.EQ.ICL) AINFLO = AINFLO -
     - SX(I)*SZ(K)*RP(J-1)*DEN(L)*V(L)
      IF(NK.EQ.1) GOTO 17
      IF(LCZP.EQ.ICL) AINFLO = AINFLO +
     + SX(I)*SY(J)*DEN(L)*W(LZP)
      IF(LCZM.EQ.ICL) AINFLO = AINFLO -
     - SX(I)*SY(J)*DEN(L)*W(L)
17    CONTINUE
C
```

```
C       CALCULATE TOTAL MASS ADDITION FROM PHASE 2....
        IF(LC.NE.ICL) GOTO 18
        AT = AT + AMASEX(L)
        BT = BT + BMASEX(L)
        CT = CT + OMASEX(L)
        DT = DT + QMASEX(L)
        ET = ET + WMASEX(L)
        IF(LCYM.EQ.10) THEN
        BT = BT + (1-QBED)*BEDCEL(L+5*NI)
        DT = DT + QBED*BEDCEL(L+5*NI)
        ENDIF
18      CONTINUE
1       CONTINUE
        XIN = (1-0.23)*AINFLO
        TMAS =  AT + BT + CT + DT + ET
        MBI = AINFLO + TMAS
        MBO = OUTFLO
        MB = MBO*100/MBI
        XBAL = XOUT*100/XIN
        WRITE(IO,*)'***********MASS BALANCE SUMMARY****************'
        WRITE(IO,*)'MASS OUT ',MBO
        WRITE(IO,*)'TOTAL MASS IN ',MBI
        WRITE(IO,*)'THE MASS BALANCE IS ',MB,'% CLOSED'
        WRITE(IO,*)'MASS IN THROUGH PORTS ',AINFLO
        WRITE(IO,*)'TOTAL MASS EXCHANGED PHASE 2 TO PHASE 1 ',TMAS
        WRITE(IO,*)'CARBON EXCHANGED TO CO2 ',BT
        WRITE(IO,*)'CARBON EXCHANGED TO CO ',DT
        WRITE(IO,*)'OXYGEN EXCHANGED ',CT
        WRITE(IO,*)'WATER EXCHANGED ',ET
        WRITE(IO,*)'FUEL EXCHANGED ',AT
        WRITE(IO,*)'NITRGEN INTO FURNACE ',XIN
        WRITE(IO,*)'NITROGEN OUT OF FURNACE ',XOUT
        WRITE(IO,*)'THE INERTS BALANCE IS',XBAL,'% CLOSED'
        RETURN
        END
```

```
      SUBROUTINE BCALC
CCCCCCCCCCCCCCCCCCCCCCCCCCCCCCCCCCCCCCCCCCCCCCCCCCCCCCCCCCCCCCCCCCC
C                                                                     C
C     'BCALC' UPDATES FIELD OF SPECIES B. WATER                       C
C                                                                     C
CCCCCCCCCCCCCCCCCCCCCCCCCCCCCCCCCCCCCCCCCCCCCCCCCCCCCCCCCCCCCCCCCCC
      INCLUDE 'COMMON.FOR'
      REAL SMP,CP,VOLUME,BCREAT,URF,BTERM
      INTEGER N
      RESMAX = 0.0
      BRES = 0.0
      BAPS = 0.0
      URF = UR1B
      IF(NITER.GE.NUR2SW) URF = UR2B
      DO 1 K = 1,NK
      DO 1 J = 1,NJ
      DO 1 I = 1,NI
      CALL FFARNB
C
C     CHECK FOR BOUNDARIES....
      IF(LC.EQ.ICL) GOTO 2
      AP(L) = 0.0
      SU(L) = DBLE(B(L))
      GOTO 1
2     CONTINUE
C
C     CALCULATE F.D. COEFFICIENTS....
      CALL ACOEFF(SMP,CP,BPRND,B,LINKB)
C
C     CALCULATE SOURCE TERMS....
      VOLUME = SX(I)*XAREA
      BCREAT =   PREEXP*DEN(L)*DEN(L)*SQRT(T(L))*F(L)*O(L)*
     * EXP(-ACTIVE/GASCON/1000.0/T(L))*VOLUME*(SRATIO+1.0)*WFRAC
      IF(IECAL.EQ.0) GOTO 5
      IF(E(L).LT.1.0E-15) GOTO 4
      BTERM = AMIN1(F(L),O(L)/SRATIO)
      BCREAT = AMIN1(BCREAT,RAFAC*DEN(L)*D(L)/E(L)*VOLUME*BTERM*
     *         (1+SRATIO)*WFRAC)
      GOTO 5
4     CONTINUE
C     TURBULENCE CONTROLLED BUT E NOT YET KNOWN....
      BCREAT = 0.0
5     CONTINUE
      SU(L)     = SU(L) - DBLE(CP*B(L)+BCREAT+WMASEX(L))
      SP(L)     = SP(L) - CP-BMASEX(L)-AMASEX(L)-WMASEX(L)-OMASEX(L)
     1            - QMASEX(L)
C
C     DO THE BOUNDARIES....
      CALL ALINK(LINKB,B,BPRND)
      CALL AFLUX(BFLUX)
C
C     CALCULATE CENTRE COEFFICIENT ETC....
      CALL ACENTR(B,BRES,BAPS,URF)
1     CONTINUE
      IF(MONITR.EQ.1) WRITE(IO,6) RESMAX,IRMAX,JRMAX,KRMAX
6     FORMAT('    SPECIES B -'/
     1  '  MAXIMUM RESIDUAL = ',1PE10.3,' AT (',I3,',',I3,',',I3,')')
C
C     SOLVE....
      DO 8 N = 1,NCSWP
```

```
      CALL SOLVER(NI,NJ,NK,AZM,AYM,AXM,AP,AXP,AYP,AZP,SU,B,ISWPDR)
8     CONTINUE
      RETURN
      END
      SUBROUTINE QCALC
CCCCCCCCCCCCCCCCCCCCCCCCCCCCCCCCCCCCCCCCCCCCCCCCCCCCCCCCCCCCCCCCCCCC
C                                                                     C
C    'QCALC' UPDATES FIELD OF SPECIES Q.  CARBON MONOXIDE             C
C                                                                     C
CCCCCCCCCCCCCCCCCCCCCCCCCCCCCCCCCCCCCCCCCCCCCCCCCCCCCCCCCCCCCCCCCCCC
      IMPLICIT REAL (P-R)
      INCLUDE 'COMMON.FOR'
      REAL SMP,CP,VOLUME,QCREAT,URF,QTERM
      INTEGER N
      RESMAX = 0.0
      QRES = 0.0
      QAPS = 0.0
      URF = UR1Q
      IF(NITER.GE.NUR2SW) URF = UR2Q
      DO 1 K = 1,NK
      DO 1 J = 1,NJ
      DO 1 I = 1,NI
      CALL FFARNB
C
C     CHECK FOR BOUNDARIES....
      IF(LC.EQ.ICL) GOTO 2
      AP(L) = 0.0
      SU(L) = DBLE(Q(L))
      GOTO 1
2     CONTINUE
C
C     CALCULATE F.D. COEFFICIENTS....
      CALL ACOEFF(SMP,CP,QPRND,Q,LINKQ)
C
C     CALCULATE SOURCE TERMS....
      VOLUME = SX(I)*XAREA
C     CREATION OF Q (CO)
      QCREAT =  PREEXP*DEN(L)*DEN(L)*SQRT(T(L))*F(L)*O(L)*
     * EXP(-ACTIVE/GASCON/1000.0/T(L))*VOLUME*(SRATIO+1.0)*QFRAC
      IF(IECAL.EQ.0) GOTO 5
      IF(E(L).LT.1.0E-15) GOTO 4
      QTERM = AMIN1(F(L),O(L)/SRATIO)
      QCREAT=AMIN1(QCREAT,RAFAC*DEN(L)*D(L)/E(L)*VOLUME*QTERM*
     *       QFRAC*(1+SRATIO))
C     CONSUMPTION OF Q (CO)
5     QDES = -QDEXP*DEN(L)*DEN(L)*SQRT(T(L))*Q(L)*O(L)*
     * EXP(-QDACT/GASCON/1000.0/T(L))*VOLUME*(QRATIO+1.0)
      IF(IECAL.EQ.0)GOTO 55
      IF(E(L).LT.1.0E-15) GOTO 4
      QTERM = AMIN1(Q(L),O(L)/QRATIO)
      QDES = -AMIN1(-QDES,RAFAC*DEN(L)*D(L)/E(L)*VOLUME*QTERM)
      GOTO 55
4     CONTINUE
C     TURBULENCE CONTROLLED BUT E NOT YET KNOWN....
      QDES = 0.0
55    CONTINUE
C     BED BURNING MODEL GOES HERE
      IF(ICELL(LYM).EQ.10.)QCREAT =QCREAT+28./12*BEDCEL(L+5*NI)*QBED
C     DIVIDE QDES BY Q(L) SO THAT IT CAN BE ADDED TO SP(L)
      IF(Q(L).NE.0) QDES = QDES/Q(L)
```

```
      SU(L)     = SU(L) - DBLE(CP*Q(L)+QCREAT+QMASEX(L)*(1.+1.33333))
      SP(L)=SP(L)-CP-AMASEX(L)-BMASEX(L)+QDES-WMASEX(L)-OMASEX(L)
     1       -QMASEX(L)
      IF(ICELL(LYM).EQ.10)SP(L)=SP(L)-QBED*BEDCEL(L+5*NI)
C
C     DO THE BOUNDARIES....
      CALL ALINK(LINKQ,Q,QPRND)
      CALL AFLUX(QFLUX)
C
C     CALCULATE CENTRE COEFFICIENT ETC....
      CALL ACENTR(Q,QRES,QAPS,URF)
1     CONTINUE
      IF(MONITR.EQ.1) WRITE(IO,6) RESMAX,IRMAX,JRMAX,KRMAX
6     FORMAT('    SPECIES Q -'/
     1  '  MAXIMUM RESIDUAL = ',1PE10.3,' AT (',I3,',',I3,',',I3,')')
C
C     SOLVE....
      DO 8 N = 1,NCSWP
      CALL SOLVER(NI,NJ,NK,AZM,AYM,AXM,AP,AXP,AYP,AZP,SU,Q,ISWPDR)
8     CONTINUE
      RETURN
      END
```

APPENDIX 4 - USERS MANUAL FOR FLUENT/RFM

This users manual is not a "stand-alone" guide to using FLUENT/RFM. Familiarity with the FLUENT users guide is required before consulting this document. The purpose of this document is give a description of the capabilities of the FLUENT/RFM code, along with a description of the unique aspects of the code concerning case set up and obtaining output. Appendix 1 should be consulted for information concerning the techniques necessary to obtain a converged simulation of the a recovery furnace model.

CAPABILITIES AND LIMITATIONS OF FLUENT/RFM

FLUENT/RFM is specific to the kraft recovery furnace model, although any simulation done with FLUENT can be performed with FLUENT/RFM, with three requirments: 1. Rectangular coordinates must be used; 2. Only black liquor drops can be simulated; and 3. Porous cells cannot be used. These changes were necessary in order to reduce the size of the data files, and due to changes in the S2 calculation method.

FLUENT/RFM can read in FLUENT data and case files but FLUENT/RFM data and case files cannot be read by FLUENT. Currently the maximum number of computational cells is 50,000, and the maximum number of black liquor drops is 10,000. Running a case with the maximum number of drops and cells with a flow variables included requires 24,000 pages of memory (12 megabytes) on the MicroVax; this is as large as can be handled with 16 Megabytes of memory as the operating system needs some memory space. An iteration of the most complex and largest case takes about 55 minutes for calculation of the gas phase, and about 30 minutes for the second phase (this varies somewhat depending on the droplet trajectories). The case file is 1200 blocks (600 Kbytes) and the data file is 12000 blocks (6 Mbytes) for the largest possible case.

FLUENT/RFM solves the steady state flow variables of pressure, u-velocity, v-velocity, w-velocity, enthalpy, kinetic energy of turbulence, dissipation rate, mass fraction of fuel, mass fraction of oxygen, mass fraction of carbon dioxide, mass fraction of steam, and mass fraction of carbon monoxide. The second phase calculation determines the path and fate of the black liquor drop. Two or three dimensional simulations can be performed. Additional flow properties are calculated from those solved for, including temperature, radiation fluxes, exchange terms between the gas and droplet phases, exchange terms between the gas phase and the smelt bed, velocity vectors, and streamlines (in a 2-D simulation).

FLUENT/RFM cannot be used to determine pollutant formation, as microscale turbulence is not modelled.

SETTING UP A CASE

This description will assume that the furnace simulation is oriented so that the height is along the Y axis, the width along the X axis and the depth along the Z axis. Follow this convention when first setting the dimensions of the furnace (S1 option - DD suboption).

The Plane of Symmetry

The first step in setting up a case is to specify the furnace geometry; this starts by specifying the furnace dimensions. It may be necessary to use a plane of symmetry through the center of the furnace, as was done in the Base Case described in this thesis. Using this symmetry plane has advantages and drawbacks as documented in the body of this thesis. A symmetry plane cannot be used if both the secondaries and tertiaries are interlaced as flow though the middle of the furnace cannot be modelled.

If opposing secondaries are used then a symmetry plane may be used that is parallel to the tertiary jets, so interlacing is possible. A symmetry plane should be used if insufficient nodes are available to effectively describe the air ports and the bed. What constitutes insufficient nodes is difficult to define; ideally, enough nodes should be used so that increasing the number of nodes results in no change to the flow variables. This evaluation has yet to be performed for a simulation of the recovery furnace as it requires excessive amounts of computer time. A good rule of thumb is to never increase the spacing between adjacent nodes by more than 50%. For example, suppose node 1 is at 10 meters and node 2 is at 11 meters, then node 3 should be not be further than 1.5 meters from node 2 (i.e 12.5 meters). If the operator finds that this constraint cannot be satisfied throughout the furnace and opposing secondaries are present, then a plane of symmetry should be used.

If a plane of symmetry is used then it should be placed at nodes (X,Y,1), where X and Y imply all values of X and Y. The reason for this becomes apparent when the case is viewed; reflection is performed through Z = 1. Reflection is necessary to show the whole furnace.

Describing the Walls

The walls are described as described in the FLUENT manual, with one exception DO NOT USE W9, as this is a bed cell in FLUENT/RFM. The outlet should be specified at the top of the furnace (i.e. Y = Ylast).

Describing Air Ports

In order to specify an air port it necessary to locate (using the GA option) 6 nodal lines, 3 each in the two directions perpendicular to the inlet direction of the air jet. For example a jet on the back wall (X = 1 in the Base Case), would require moving 3 each of the Y and Z nodal lines. The geometry

of an air port is shown in Figure 1. Note that the boundaries of the port are midway between the nodal lines. The nodal lines X2 and Y2 describe the midpoint of the port, the nodal lines Y1 and Y3 are to Δy above and below nodal line Y2, where Δy is the height of the port. X1 and X3 are moved so that they are Δx to the right and left of X2.

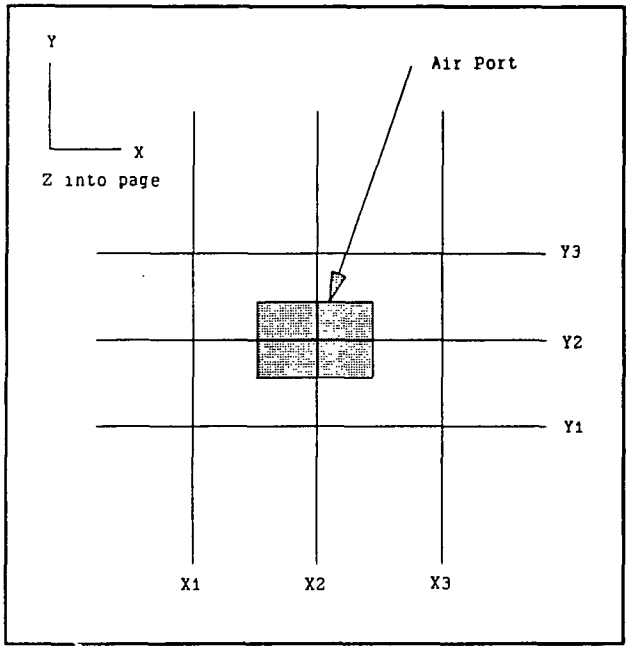

Most furnaces have large numbers of primary ports; it would require an excessive number of nodes to describe each primary port. Instead, a more economical use of nodes can be realized by using a slot jet that extends along the entire length of the wall. The height of the jet can be adjusted so that the mass flow is correct, this is shown in equation [1].

$$H_p = M/(\rho_g \bullet V_p \bullet S) \qquad [1]$$

Where: H_p is the height of the slot;
ρ_g is the density of the incoming gas;
V_p is the velocity of the primary jets;
S_p is the length of the slot jet.

The use of slot jets is an approximation, and could lead to an underestimate of the penetration of the jets, as slot jets have lower penetration distances than square jets with the same momentum. At the primary air level this is not very important, as the jets impact on the bed in a very short distance. The secondary and tertiary jets are usually fewer in number so that individual jets are described.

Describing the Bed

Once the furnace geometry and the ports have been described, it is now time to add the bed to the furnace. Bed calls are W9 cells. The bed should be built like the roof of a LEGO house. Do not start building up the bed right against the wall of the furnace as this does not provide for the primary jets to enter the furnace: instead, start about three or four cells in from the wall. All cells that are exposed to the furnace gases should be designated W9 cells, the internal cells of the bed can be made any type of wall cell, as they will not influence the flow. The entire furnace floor should be made up of W9 cells.

Furnace Gas Properties

The SP (set parameters) option contains many new variables that must be set in a recovery furnace simulation. The suggested values for these variables appear in the last section of this users guide. Remember to activate gravity in the Expert menu, unless you want rather excessive carryover.

Black Liquor

The black liquor spray must be described, this is done by entering the Setup Phase 2 menu (S2) option, and then entering the Set Group (SG) sub-menu. The default sprays can be used or sprays can

be defined by the user. The defaults sprays are shown in Figure 2; they assume a plane of symmetry. The sprays on the plane of symmetry are in fact half sprays as shown in Figure 2. If the user specifies the sprays, then prompts will appear that ask for details about each spray.

The incoming velocity of the droplet is specified in the SG submenu. The velocity components V_v (the vertical velocity) and V_h (the velocity horizontal to the wall on which the nozzle is located) can be independently specified; the third velocity, V_p (the velocity parallel to the spray direction), is thus fully specified as defined by equation [3]. These velocities are shown in Figure 2. Obviously V_h and V_v must be less than V (the total velocity).

$$V_p = SQRT(V^2 - V_v^2 - V_h^2) \qquad [2]$$

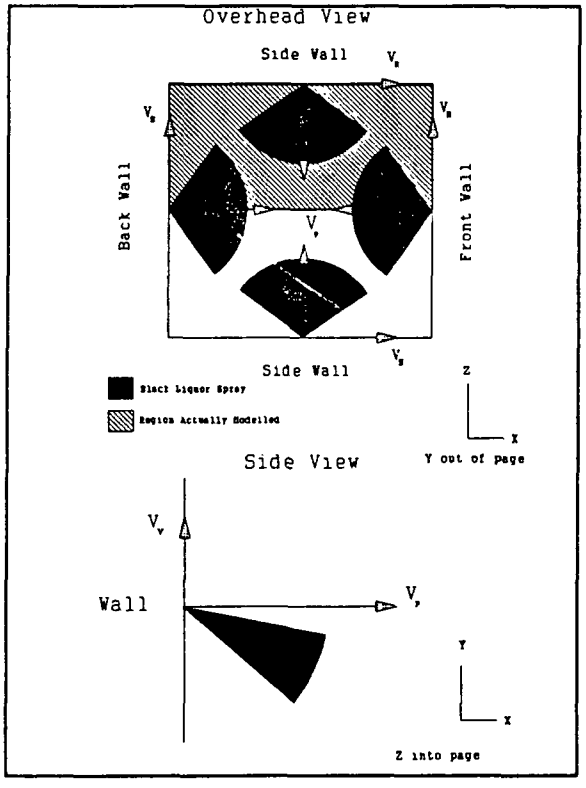

Figure 2 - Incoming Black Liquor Spray

The maximum number of drops is 10,000. The number of drops can be calculated as follows.

$$N_d = \Sigma (N_{dc} \bullet N_{vvc} \bullet N_{wpc}) \qquad [3]$$

Where: N_d is the number of drops;
N_{dc} is the number of diameter classes;
N_{vvc} is the number of vertical velocity classes;
N_{wpc} is the number of wall perpendicular classes;
The summation is over all the nozzles.

The physical constants of the black liquor can be specified by entering the PC section of the S2 menu. The suggested values for the parameters in this section are given in the last section of this users manual.

VIEWING AND OUTPUTTING RESULTS

Outputting the results is similar to the methods used in FLUENT. With a number of exceptions, they are listed here:

1. In order to get profiles of flow variables on the bed (i.e. char burning rate, O_2 concentration, and temperature), it is necessary to turn on the bed profiles option in the SP submenu of the "View Graphic" menu. In addition, bed profiles are plotted on Slice 15 in the Y (or 2) direction. Thus the command "SL 2 Y 15" should be entered before attempting to view the bed profiles.

2. The VA "View Alphanumerics" option in the main menu has been changed. The command sequence to see V velocity on Y plane 3, in the range of x values of 1 to 5, and a range of Z values of 5 to 10 would be, VA N V 2 1 5 5 10. The N is in response to the question "Is This A Repeat of the Same Variable". Specifying Y saves time when you are repeatedly viewing the same variable;

3. Different windows can be used when viewing variables over slices of the furnace, the windows used are 1 to 6, using the CH option in the VU submenu to see these windows. The color scale used can be based on the global values of a variable, the values over the slice being plotted , or over a user specified range (warning: do not specify a range smaller than the range over the slice you are looking at or the program may crash);

4. When taking photos of the screen a number of other option are useful. The ML option in "View Graphics" allows the user to plot a color rainbow that can be used as a legend (LE), it can allow the addition of text in a specified point on the screen (TX), and wipe out parts of the screen (WO). Two warnings: never open two windows (i.e. by performing a CH in the VU suboption with a window open), and never use the ML option without a window open. Windows can be closed by using the EP option in the VG menu. Experience with taking photos suggest that the following settings should be used: Aperture f8 or f5.6, Exposure 1/4 second to 1/16 second, EL 400 ASA film.